BOEING

Solar Power Satellite System Definition Study

SPS SOLID-STATE ANTENNA POWER COMBINER, FINAL REPORT

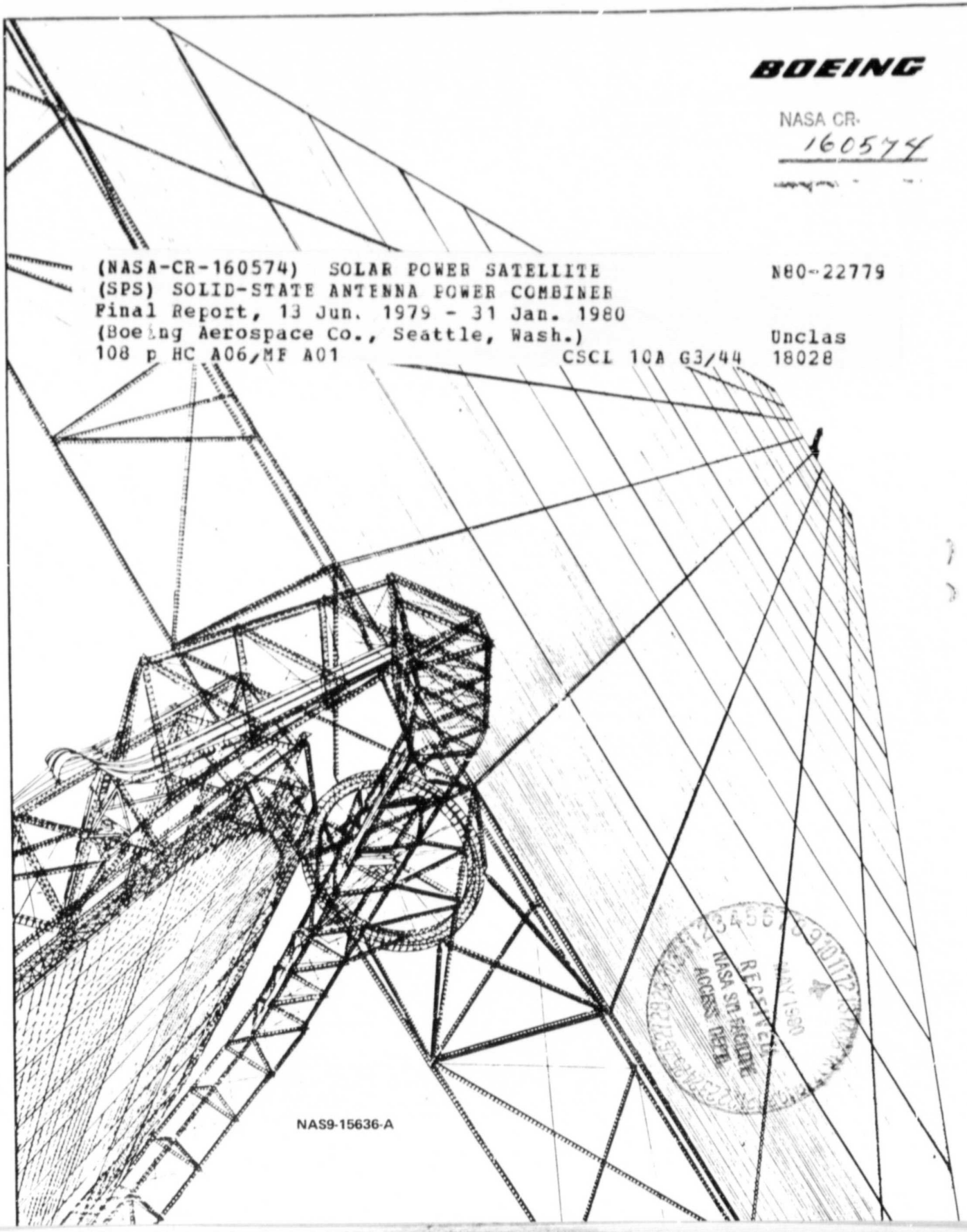

BOEING

NAS9-15636-A

D180-25895-1

SPS SOLID-STATE ANTENNA POWER COMBINER

Prepared For The NASA Lyndon B. Johnson Space Center
Houston, Texas 77058

Under Contract No. NAS9-15636

Final Report for Period of June 13, 1979
to January 31, 1980

Project Monitor: L. Leopold

Project Engineer: G. W. Fitzsimmons 3-3-80

Project Manager: E. J. Nalos 3-4-80

BOEING AEROSPACE COMPANY
P.O. Box 3999, Seattle, Wa. 98124
February 29, 1980

ACKNOWLEDGEMENT

Acknowledgements are extended to Louis Leopold of NASA for his guidance of our efforts prior to and throughout the contract.

Contributors to the document, although not acknowledged esewhere, were Walt Lund and Dr. Jeff White, both at Boeing. Walt was most valuable as a frequent consultant on antenna questions and contributed the theoretical directivity estimate. Jeff developed the Appendix on "Antenna Characterization" and was very helpful on the final three antenna gain measurement and on error calculations.

Credit is also extended to Dave Lunden who performed the preliminary antenna evaluations and last, but not least, to Norman Simmons who fabricated all of the circuit components.

TABLE OF CONTENTS

		PAGE
	ACKNOWLEDGEMENT	i
	TABLE OF CONTENTS	ii
	LIST OF FIGURES	iii
	LIST OF TABLES	iv
	SUMMARY	v
1.0	INTRODUCTION	1
	1.1 BACKGROUND	1
	1.2 TECHNICAL OBJECTIVES	3
	1.3 TASK ORGANIZATION	4
2.0	POWER AMPLIFIERS	9
	2.1 GENERAL DISCUSSION	9
	2.2 SPECIFICATIONS	9
	2.3 AMPLIFIER PERFORMANCE	10
3.0	ANTENNA FEED NETWORK	21
	3.1 0 - 180° HYBRID	21
	3.2 TWO-WAY POWER DIVIDER	22
	3.3 INTEGRATED FEED NETWORK	23
4.0	POWER-COMBINING ANTENNA	42
	4.1 BACKGROUND	42
	4.2 SUBSTRATE MATERIAL	42
	4.3 COUPLING NETWORKS	46
	4.4 ANTENNA DESIGN	50
5.0	ANTENNA RANGE EVALUATION	66
	5.1 ANTENNA RANGE PATTERNS	66
	5.2 ANTENNA GAIN	67
	5.3 ANTENNA DIRECTIVITY	68
	5.4 ANTENNA EFFICIENCY	71
	5.5 AMPLIFIER COMBINING	72
	5.6 ANTENNA EFFICIENCY WITH AMPLIFIERS	73
6.0	CONCLUSIONS AND RECOMMENDATIONS	85
7.0	APPENDIX: ANTENNA CHARACTERIZATION	89

LIST OF FIGURES

FIGURE NO.	TITLE	PAGE
1.1	SOLID-STATE POWER COMBINING MODULE CONCEPT	6
1.2	POWER COMBINING MICROSTRIP SLOTLINE ANTENNA	7
1.3	POWER COMBINING ANTENNA, FEED NETWORK AND POWER AMPLIFIER BLOCK DIAGRAM	8
2.1	COPY OF AMPLIFIER ORDER SPECIFICATION	14
2.2	TRONTECH AMPLIFIER SCHEMATIC DIAGRAM	15
2.3	HIGH POWER INSERTION GAIN AND PHASE AND RETURN LOSS TEST CONFIGURATION BLOCK DIAGRAM	17
2.4	AMPLIFIER TEST SETUP FOR HIGH POWER MEASUREMENTS	18
2.5	AMPLIFIER GAIN AND INSERTION PHASE VERSUS FREQUENCY	19
2.6	AMPLIFIER GAIN AND INSERTION PHASE VERSUS DRIVE POWER	20
	0-180 DEGREE HYBRID	
3.1	INSERTION LOSS	27
3.2	ISOLATION	28
3.3	RETURN LOSS	29
3.4	INSERTION PHASE	30
	TWO-WAY POWER DIVIDER	
3.5	INSERTION LOSS	31
3.6	ISOLATION	32
3.7	RETURN LOSS	33
3.8	RETURN LOSS	34
3.9	RELATIVE INSERTION PHASE	35

LIST OF FIGURES (Continued)

FIGURE NO.	TITLE	PAGE
	INTEGRATED FEED NETWORK	
3.10	INSERTION LOSS	36
3.11	INSERTION PHASE	37
3.12	RETURN LOSS	38
3.13	ISOLATION	39
3.14	PHOTOGRAPH OF THE ANTENNA FEED NETWORK	40
3.15	AUTOMATIC NETWORK ANALYZER	41
4.1	SLOTLINE CHARACTERISTIC IMPEDANCE AND WAVELENGTH	55
4.2	MICROSTRIP-SLOTLINE-MICROSTRIP LINE TEST FIXTURES	56
4.3	SLOTLINE INSERTION LOSS	57
4.4	SLOTLINE RETURN LOSS	58
4.5	SLOTLINE ANTENNA COUPLING METALIZATION PATTERNS	59
4.6	EVALUATION OF A SLOTLINE ANTENNA	60
4.7	COPPER METALIZATION PATTERN FOR FOUR FEED MICROSTRIP ANTENNA	61
4.8	FOUR-WAY POWER-COMBINING MICROSTRIP/SLOTLINE ANTENNA	62
4.9	FOUR-WAY POWER-COMBINING ANTENNA WITH GROUND PLANE	63
4.10	REAR-VIEW SHOWING FEED NETWORK OF ANTENNA AND GROUND PLANE	64
4.11	RETURN LOSS OF COMPLETED FOUR-FEED ANTENNA	65

LIST OF FIGURES (Continued)

FIGURE NO.	TITLE	PAGE
5.1	POWER-COMBINING ANTENNA PATTERN (H CUT COPOLARIZED)	75
5.2	POWER-COMBINING ANTENNA PATTERN (E CUT COPOLARIZED)	76
5.3	POWER-COMBINING ANTENNA PATTERN (H CUT CROSS-POLARIZED)	77
5.4	POWER-COMBINING ANTENNA PATTERN (E CUT CROSS-POLARIZED)	78
5.5	PATTERN OF POWER-COMBINING ANTENNA WITH AMPLIFIERS (H CUT COPOLARIZED)	79
5.6	PATTERN OF POWER-COMBINING ANTENNA WITH AMPLIFIERS (E CUT COPOLARIZED)	80
5.7	PATTERN OF POWER-COMBINING ANTENNA WITH AMPLIFIERS (H CUT CROSS-POLARIZED)	81
5.8	PATTERN OF POWER-COMBINING ANTENNA WITH AMPLIFIERS (E CUT CROSS-POLARIZED)	82
5.9	ANTENNA SY STEM BLOCK DIAGRAM	83
5.10	RANGE INSERTION LOSS WITH AND WITHOUT POWER-COMBINING ANTENNA AMPLIFIERS	84
7.1	ARRANGEMENT OF TEST EQUIPMENT FOR THE MEASUREMENT OF ANTENNA GAIN	98
7.2	OUTDOOR ANTENNA RANGE	99
7.3	DIAGRAM OF THE DIRECTIVITY MEASUREMENT SYSTEM	100

LIST OF TABLES

TABLE NO.	TITLE	PAGE
2.1	TRONTECH AMPLIFIERS PERFORMANCE AFTER REWORK AND TUNING	15
2.2	AMPLIFIERS SPECIFICATION AND LARGE SIGNAL MEASURED VALUES	16
3.1	INTEGRATED FEED NETWORK PERFORMANCE SUMMARY AT 2.45 GHz	25

EXECUTIVE SUMMARY

A low loss power-combining microstrip antenna suitable for solid-state SPS application has been developed. A unique approach for performing both the combining and radiating function in a single cavity-type circuit has been verified, representing substantial refinements over previous demonstration models in terms of detailed geometry to obtain good matching and adequate bandwidth at the design frequency. The combiner circuit was designed, built and tested in the Boeing Microwave Circuit Laboratory and the overall results support the view that the solid-state power-combining antenna approach is a viable candidate for a solid-state SPS antenna building block.

In order to verify the low loss combining concept, standard state-of-the-art antenna measurement techniques were utilized, compatible with the present scope of the six-month program. These limit the precision of measurement and suggest that more precise (calorimetric) techniques be used in future work. The antenna efficiency is measured as the ratio of the measured gain and the antenna directivity, both of which have inherent errors associated with their measurements. These are discussed in detail in the body of the report. Part of the losses are attributed to the developmental nature of the antenna which utilized a section of microstrip line, a non-optimum dielectric substrate and silver conducting epoxy in its fabrication. Accounting for these losses, which would not exist in an optimized combiner design, and for the measured cross-polarized component of radiation ($\sim$1%), the combining loss, to within the measurement accuracy of $\pm$ .33 dB, is negligible.

Significant additional information on the performance of the combiner-radiator module was obtained by the incorporation of four carefully matched low cost silicon bipolar transistor amplifiers. A precision hybrid feed network was constructed as part of this program to assure properly phased inputs to the amplifiers. When the four solid-state power amplifiers yielding a combined output power of 1/2 watt were added to the antenna, the output power was summed perfectly in the antenna beam without any measurable added

loss over that obtained without the amplifiers. This confirms the principal contention that all losses associated with the power-combining process are insignificant to within current measurement errors. The regularity of the measured E and H antenna patterns with and without the amplifiers also indicate that all the amplifiers are combining properly, with the added gain on the antenna range corresponding to the bench measured amplifier gain to within 0.1 dB. Specific recommendations are included identifying further steps in the development of the solid-state power-combining modularized concept.

1.0 INTRODUCTION

The results described here represent a logical second step of an experimental verification program to adapt a modular solid-stage concept previously developed and reduced to practice by Boeing to generate, combine and radiate rf power. This concept is particularly applicable to the space-tenna design for a Solar Power Satellite (SPS).

1.1 BACKGROUND

If solid-state printed circuit modularized transmitters are used in place of tubes and waveguide, the Solar Power Satellite (SPS) launch mass may be reduced, the operating reliability may be enhanced and it, therefore, should cost less. To implement this approach it is essential that means be found to sum the power of many relatively low power solid-state sources in a low-loss manner. Also, that means be provided to properly control the phase of the outputs of the large number of solid-state sources required.

To avoid the power combining losses associated with circuit hybrids it was proposed that the power from multiple solid-state amplifiers be combined by direct coupling of each amplifier's output to the radiating antenna structure. The resulting savings in transmitter efficiency ranges from 4% to 10% depending upon the configurations being compared. The selected power-combining antenna consists of a unique printed (metalized) microstrip circuit on a ceramic type dielectric substrate which is backed by a shallow light-weight aluminum cavity which sums the power of four microwave sources. The antenna behaves like two one-half wavelength slotline antennas coupled together via their common cavity structure. A significant feature of the antenna configuration selected is that the radiated energy is summed to yield a single radiated output phase which represents the average insertion phase of the four power amplifiers. This energy may be sampled and by comparison with the input signal one can phase error correctly to maintain the insertion phase of all solid-state power combining modules at exactly the same value. This insures that the insertion phase of each SPS power combining antenna

module is identical even though the power amplifiers are fabricated to relatively loose (low cost) insertion phase requirements.

A sketch of how this concept might appear is illustrated in Figure 1.1. Two solid-state power amplifier modules with two rf outputs each at 5 watts are shown delivering power to the antenna. The power amplifiers derive their input from an integrated circuit which performs the function of phase error correction so that each antenna module (each with two power amplifier modules) has the same insertion phase. The phase error correction circuit does this by sampling the radiated power from the antenna module using two probes and comparing the phase of it with that of the module input. To help dissipate the heat of the power amplifiers via radiation a ceramic substrate is proposed. The high thermal conductivity of the ceramic substrate and of the aluminum cavity and ground plane will spread the heat so that all surfaces will participate in the cooling process.

Figure 1.2 contains a sketch of the power combining microstrip antenna proposed to be evaluated under the program. This antenna contains improvements which should widen the bandwidth over the original model developed previously by Boeing. It will be noted that the dielectric substrate is metalized on both sides. The underside, within the cavity, contains the four microstrip feed lines which are coupled to the two radiating slots on the top side via two narrow slotlines. In order to feed the antenna properly two of the rf inputs are required to be 180° out-of-phase with the remaining two (as noted in Figure 1.2). Thus, to test the antenna, an antenna feed network is required which will provide the four 0° - 180° equal amplitude outputs.

The material that follows describes a program to verify the suitability of this concept for SPS. An appropriate microstrip antenna was developed and was evaluated when driven from four solid-state power amplifiers.

1.2 TECHNICAL OBJECTIVES

The objective of the program is to demonstrate the suitability of a 2.45 GHz power combining microstrip slotline antenna when fed by four solid-state amplifiers to the needs of a solar power satellite. The program entails the design and fabrication of a four feed microstrip antenna and a stripline antenna phasing network which will be integrated with four transistor amplifiers to demonstrate that the total solid-state module (amplifiers plus antenna) will operate as an efficient power combining-radiating system. The antenna developed will be evaluated for gain, pattern and efficiency on the antenna range with and without the amplifiers. The amplifiers will be connected directly to the antenna without benefit of isolators so that their interaction via the antenna will be unimpeded. The combined output power of the amplifiers will be approximately 1/2 watt.

For completeness the program "Statement of Work" is reproduced below for reference.

> The contractor shall demonstrate the suitability of a 2.45 GHz power combining microstrip slot-line antenna when fed by four solid-state amplifiers to the needs of a solar power satellite. The following work shall be performed by the contractor for this task:
>
> a) Specify, purchase and bench test four solid-state power amplifiers for adequate phase and amplitude response to verify suitability for power combiner module test.
>
> b) Incorporate four power amplifiers into a four-feed combiner module. Refine the four-feed combining antenna design in terms of substrate size, cavity size, slot width, slot spacing and slot feed mechanism to properly match the amplifiers to the module. The designed minimum combined power output will be one-half watt.

c) Demonstrate via antenna range measurement the efficiency of the power combining antenna utilizing an 0° - 180° feed system. Demonstrate via antenna range measurement the efficiency of the power combining antenna driven by the four solid-state amplifiers. Range of accuracies of approximately ± .5 dB will be applied.

d) Prepare monthly progress letter reports and a final report for submittal to NASA. The test solid-state antenna power combiner shall be shipped to JSC in an "as is" condition following completion of contractor tests.

1.3 TASK ORGANIZATION

The block diagram, shown in Figure 1.3, illustrates the components developed for the program prior to a final measurement effort on the antenna range. The block diagram illustrates the manner in which the antenna feed network, the power amplifiers and the microstrip antenna are connected. The four cables connecting the amplifiers and the antenna are required to have equal electrical lengths. So, also, are the cables connecting the antenna feed network and the amplifiers. This is necessary to retain the proper phasing of the antenna. Not shown in Figure 1.3 are four equal length cables to be substituted for the amplifiers when the antenna is to be evaluated alone.

The program was accomplished by breaking the effort into four separate tasks. They are:

1. Power Amplifiers Specification and Verification.

2. Antenna Feed Network Design Development and Evaluation.

3. Power Combining Antenna Design Development and Evaluation.

4. Antenna Range Evaluation of the Completed System.

The organization of the report that follows is arranged in this same order.

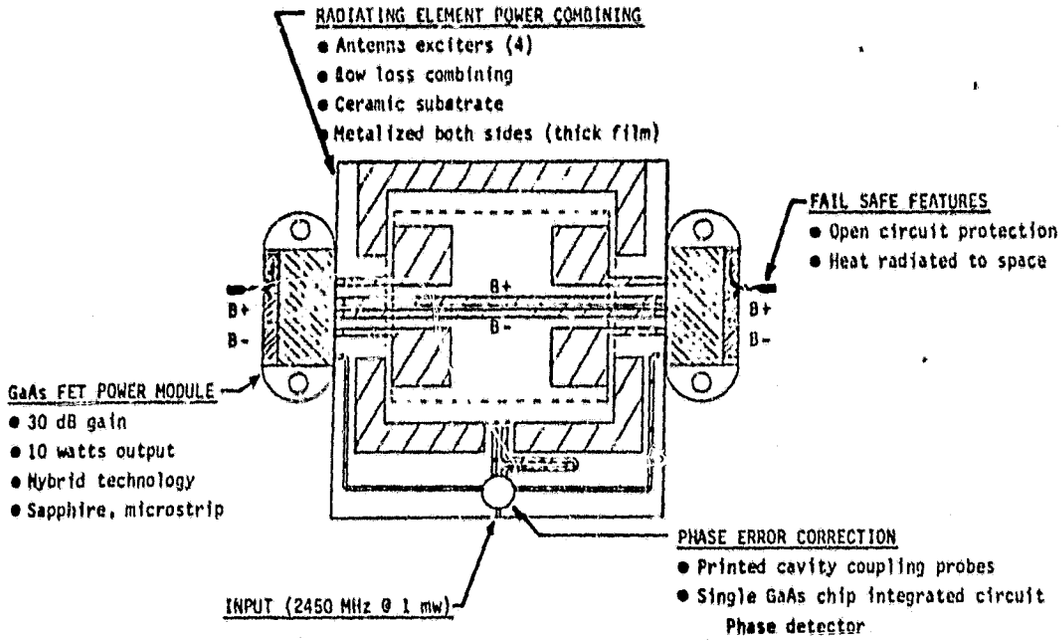

(a) PLAN VIEW

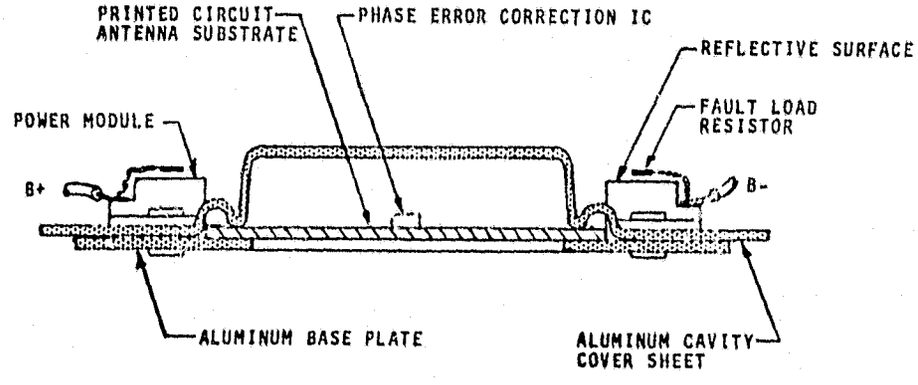

(b) CROSS SECTION

FIGURE 1.1 SOLID STATE POWER COMBINING MODULE CONCEPT (20 WATTS)

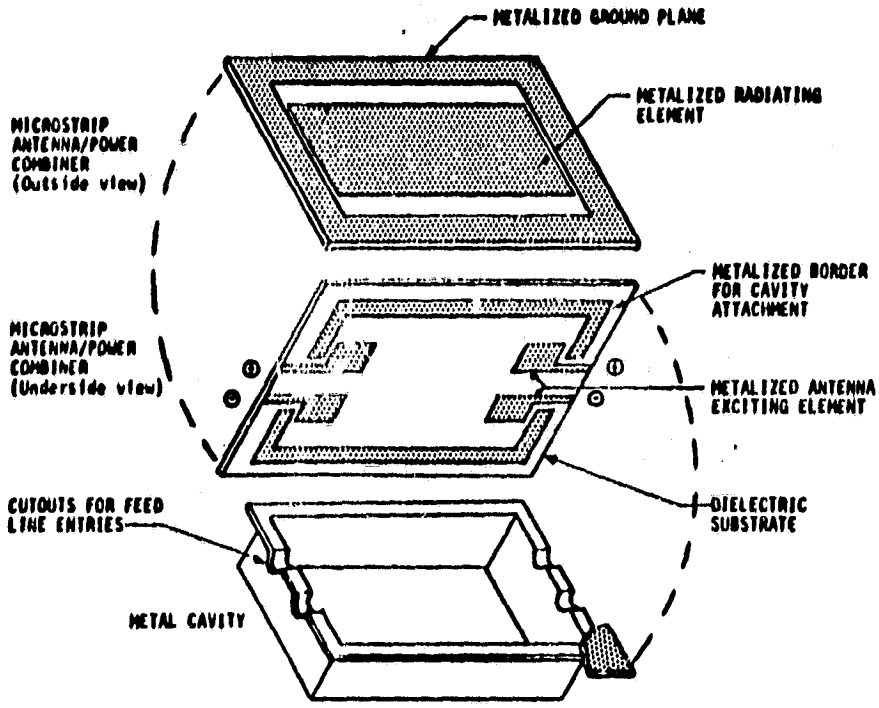

(a) BREAK-A-WAY VIEW

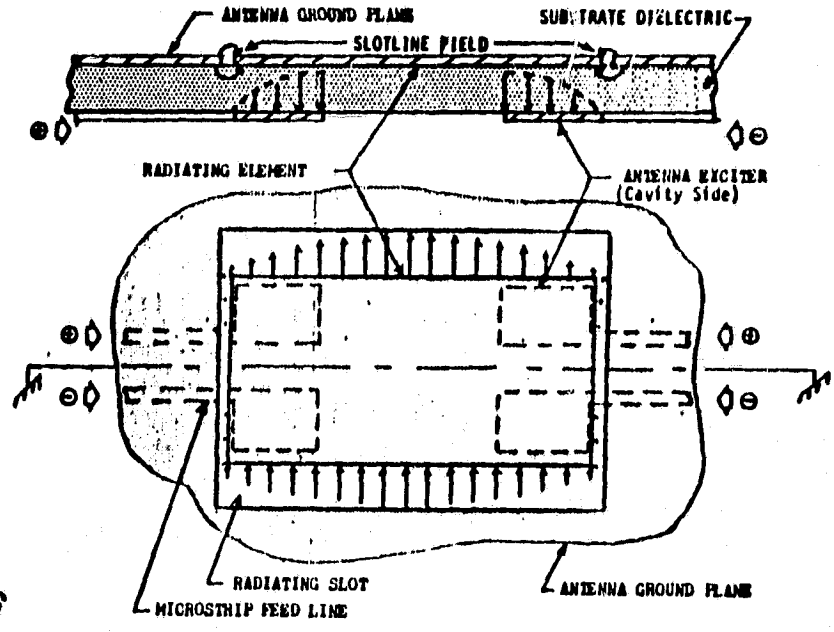

(b) "E" FIELD PROFILE

FIGURE 1.2 POWER COMBINING MICROSTRIP SLOTLINE ANTENNA

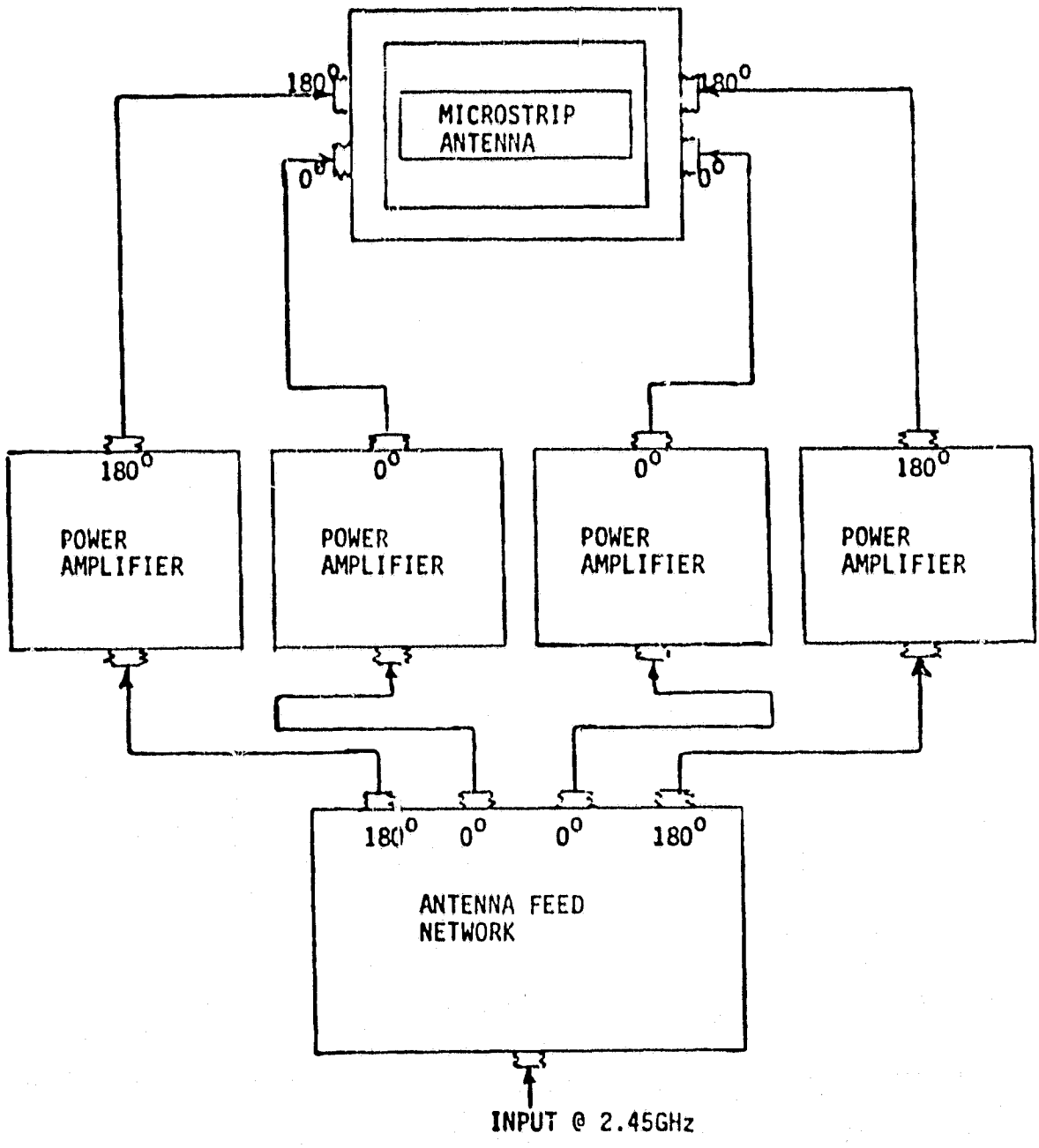

FIGURE 1.3 POWER COMBINING ANTENNA, FEED NETWORK AND POWER AMPLIFIER BLOCK DIAGRAM

2.0 POWER AMPLIFIERS

2.1 GENERAL DISCUSSION

Four gain-matched and phase-matched power amplifiers are required to evaluate their simultaneous performance with the power-combining antenna. Since there is no isolation between amplifiers when attached to the antenna it was decided that the amplifiers should be capable of surviving an infinite VSWR under all phase conditions. This can be achieved at lowest cost by permitting the amplifiers to operate Class "A". This mode of operation is acceptable at this stage of the solid-state module development since antenna efficiency with and without amplifiers is the only question of concern. The amplifier efficiency contribution is not a consideration in this study. Thus, four relatively low cost bipolar silicon transistor amplifiers each capable of an output power of at least 1/8 watt (+ 21 dBm) and each capable of operating in a fail-safe manner into any load VSWR were deemed sufficient and adequate for this study.

Since the objectives of the study was to evaluate the power combining efficiency of the antenna, it was desired that the amplifier gain and phase match be nearly perfect. In this way all test results would represent the antenna system itself under nearly ideal drive conditions. Thus, it was desired that the gain be matched to less than $\pm$ 0.1 dB and the insertion phase be matched to within $\pm$ 1°.

2.2 SPECIFICATIONS

The four matched amplifiers were supplied to the program by Trontech, Inc., Eatontown, N. J., to the specification shown in Figure 2.1. The thought was that the relatively loose gain-match and phase-match specification of $\pm$ .5 dB and $\pm$ 5°, respectively, could be further tightened upon receipt of the amplifiers by the requirement to supply a $\pm$ 10° phase control mechanism and by adjusting the supply voltage to control the gain. It turned out that the task was slightly larger than originally contemplated by Trontech, Inc. and four amplifiers were

finally delivered which met most of the requirements. With some rework on one of the amplifiers and retuning of all of them, Boeing, with substantially more equipment available than was available to Trontech, Inc., achieved the required matched amplifier performance needed b y the program.

2.3 AMPLIFIER REWORK AND FINAL PERFORMANCE

As noted above, the power amplifiers required retuning to achieve an acceptable insertion gain and insertion phase error window. In addition, a defective tuning capacitor in amplifier number 3 had to be changed. The net result is that they are all tuned to a gain of approximately 8.2 dB with a mean output power of 132 nw (+ 21.2 dBm). The gain match is to within $\pm$ 0.1 dB. The relative insertion phase for each of the units is within a phase error window of $\pm$ 1°. In addition, the input and output return loss is significantly better than specified, 11 dB on the input and 20 dB on the output.

The details of the amplifier rework and the resulting performance will now be described. The Trontech amplifiers can be approximately represented by the schematic diagram shown in Figure 2.2. When viewed with the cover removed, the components of Figure 2.2 are to be noted; however, some of the capacitors may in fact behave electrically more like variable inductances, due to the lead lengths involved. Nontheless, there are four variables (capacitors) with which to normalize two insertion parameters (phase and gain) while simultaneously optimizing the input and output return loss for a total of four amplifier parameters. It is not surprising that all four variables were needed.

The variable capacitor C2 in serial number 3 proved to be defective and a substitution capacitor was used which also required a change in C3. The shunt tuning combination of C2 and C3 performs the same tuning function as that of C1. C1, however, has a resistor in series (R1) which contributes loss needed to trim the gain of the amplifier. By obtaining additional input shunt capacity from C1, more of the input signal is absorbed in R1. Conversely, if the combination of C2 and C3 is used to obtain additional input shunt capacity (with a concurrent reduction in C1), less power is dissipated in R1 ard the amplifier input drive is increased.

After the rework it was noted that the gain should be set at no higher than 8.2 dB in order to allow sufficient tuning range to adjust them for equal phase and gain while maintaining a reasonably good input and output return loss. The output return loss is most critical for the antenna power combining test and therefore was targeted to be greater than 20 dB. This was achieved on all four amplifiers. Table 2.1 contains a tabular listing of input and output return loss measured under large signal conditions. Note that the input return loss is greater than 10 dB for each amplifier. The return loss now exceeds the original specification by a wide margin. To move the amplifiers further away from saturation effects, a higher collector voltage was selected, + 14 V instead of + 13 V . A comparison of the amplifier specifications with the results achieved are listed in Table 2.2.

A rather elaborate test setup was placed together to simultaneously measure the amplifiers gain, relative insertion phase, input return loss and output return loss under large signal conditions. A block diagram of the setup is shown in Figure 2.3. Figure 2.4 contains a photograph of the entire amplifier test setup.

To measure the ouptut return loss under large signal conditions a second cw signal generator was employed to inject a small signal into the amplifiers output slightly displaced from the signal at 2.45 GHz. The magnitude of the reflection of this signal was then monitored using a spectrum analyzer. The input return loss was measured by simply sampling the amplifier reflected 2.45 GHz input signal and displaying it on a second spectrum analyzer.

Figure 2.5 contains a plot of the gain and relative insertion phase of each of the amplifiers versus frequency. It will be noted that each of the amplifiers exhibit a gain peak at a frequency slightly higher than the design frequency of 2.45 GHz just as they did prior to the rework and tuning. One amplifier, serial number 3, behaves better because the gain for it is relatively flat (low gain versus frequency sensitivity) at 2.45 GHz. Serial number 3

is the amplifier which required the capacitor replacement and the extra attention it received enabled us to optimize the gain response better. All of the amplifiers could have been modified to move the peak gain to 2.45 GHz but would have required additional time. As a point of interest it was noted that the output tuning capacitor, C5, for all of the amplifiers except serial number 3 does not have sufficient tuning range to optimize the gain response. It was always at one extreme.

In Figure 2.5 the relative insertion phase of serial number 3 follows a different slope from that of the other amplifiers. This, of course, is due to the rework which makes this amplifier slightly different from the other three. No effort was made to match the amplifiers individual phase and gain response versus frequency since we only intend to operate at one frequency, 2.45 GHz. A gain and insertion phase versus frequency plot, however, is useful to illustrate the sensitivity of the amplifiers to small frequency changes.

A second set of amplifier performance plots are shown in Figure 2.6 where the input drive signal is changed $\pm$ 3 dB. The top plot contains the amplifier insertion phase, the lower plot contains the amplifier gain. Although difficult to see in the plot, the number 3 amplifier maintains a more constant phase and gain versus drive power than the other three amplifiers. This is to be expected since it is the only one whose gain response was peaked at 2.45 GHz. Detuning that occurs due to changing drive levels moves the response of an amplifier more when the amplifier is tuned on the edge of a response curve than when tuned for a flat response. The amplifier most sensitive to drive level is serial number 1. Referring back to Figure 2.5 it will be noted that the gain and relative phase response versus frequency was steepest for serial number 1. Therefore, the increased sensitivity of amplifier number 1 could have been predicted from its frequency response.

From Figure 2.6 it is seen that the phase and gain match between amplifiers is degraded if the input drive power is increased (as the amplifiers are driven further toward saturation). However, reduction in drive, even a

3 dB reduction is not significantly detrimental to phase and gain match. When operating the amplifiers with the power combining antenna it will be important to try to operate as near the + 13 dBm drive level as practical.

From Figure 2.6 it will be noted that the four amplifiers have been gain matched to within a .1 dB window (approximately) and phase matched to within a 1° window (approximately). In Figure 2.5 it appears that the window at 2.45 GHz may be slightly wider. Experience with repeatability within the measurement system suggests that subsequent reruns of the tests will yield slight variations which should be contained within a window double the value shown in Figures 2.5 and 2.6. Thus, as noted in Table 2.2, it is claimed that the amplifier gain match is $\pm$ .1 dB and that the relative insertion phase error is $\pm$ 1°. This $\pm$ .1 dB and $\pm$ 1° error represents the error window one gets when the measurement is repeated using the same equipment and includes errors which are traceable to one's ability to tune each amplifier to zero error. In addition for the absolute power gain for the amplifier, one must add the error imparted to the measurement by the equipment used in the measurement. This additional uncertainty is estimated to be on the order of $\pm$ 0.3 dB.

TRON-TECH

TRONTECH, INC., P.O. BOX 29, DEAL, N.J. 07723
542 INDUSTRIAL WAY WEST, EATONTOWN, N.J. 07724
TELEPHONE: (201) 229-4348 TELEX: 132-445

QUOTATION

TO: Mr. George Fitzsimmons
21206 Poplar Way
Lynnwood, Wash. 98036

DATE: 5-16-79
QUOTATION NO.: 87955
YOUR REFERENCE: Telecon. 5-16-79
QUOTATION FIRM FOR 90 DAYS

Dear Mr. Fitzsimmons:

We are pleased to offer the following quotation to your requirements.

SPECIFICATIONS

MODEL NO.	L245GB
FREQUENCY (GHz)	2.45
GAIN (dB)	6 min.
FLATNESS (dB)	±.5
NOISE FIGURE (dB)	10 typ.
VSWR IN VSWR OUT	2.5:1 max. 1.5:1 max.
PWR. OUT @ 1 dB GAIN COMPRESSION (dBm)	+21 min., +25 typ.
CASE/CONNECTORS	"C"/SMA
SUPPLY REQUIREMENTS	+20V± 0.2V, approx. 90 mA
GAIN MATCH (4 units)	±.5 dB max.
PHASE MATCH (4 units)	± 5° max.

Amplifiers to be supplied with mechanism to adjust phase by approx. ±10°. Amplifiers must withstand infinite VSWR at any phase on output. Data indicating measured values of above parameters to be supplied with amplifiers.

PRICING 1-9 sets of 4 amplifiers: $2,000.00 per set

Thank you for your interest in Trontech products.

Sincerely yours,
TRONTECH, INC.

FIGURE 2.1 COPY OF AMPLIFIER ORDER SPECIFICATION

FIGURE 2.2 TRONTECH AMPLIFIER SCHEMATIC DIAGRAM (2.45GHz)

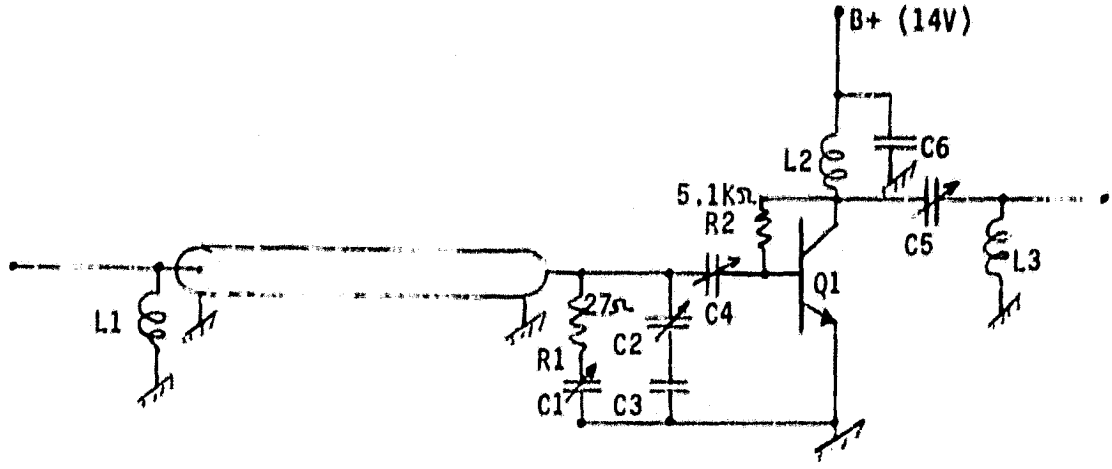

Q1 = Fujitsu 9215 rated @ 1 watt @ 2.3GHz

TABLE 2.1 TRONTECH AMPLIFIER PERFORMANCE AFTER REWORK & TUNING

SERIAL #	CURRENT (ma)	GAIN	PHASE (RELATIVE)	RETURN LOSS	
				INPUT	OUTPUT
1	161	8.2dB	0^o	14dB	20dB
2	172	8.2dB	0^o	12dB	22dB
3	178	8.2dB	0^o	11dB	23dB
4	157	8.2dB	0^o	12dB	20dB

P_{in} = +13dBm (20 mw), B+ = +14V f = 2,450 MHz

TABLE 2.2 AMPLIFIER SPECIFICATIONS & LARGE SIGNAL MEASURED VALUES

PARAMETER	SPECIFICATION	MEASURED
FREQUENCY:	2.45GHz	2.45GHz
POWER OUTPUT:	+21dBm (125mw)	+21.2dBm (132mw)
GAIN:	6dB	8.2dB
GAIN MATCH:	$\pm$.5dB	$\pm$.1dB
PHASE MATCH:	$\pm 5^{o}$	$\pm 1^{o}$
VSWR (RETURN LOSS):		
INPUT:	2.5:1 (7.4dB)	1.8:1 (11dB)
OUTPUT:	1.5:1 (14dB)	1.2:1 (20dB)

Note: The measured values were obtained after retuning the amplifiers under large signal conditions (one amplifier required some repair/rework).

FIGURE 2.3 HIGH POWER INSERTION GAIN & PHASE AND RETURN LOSS TEST CONFIGURATION BLOCK DIAGRAM.

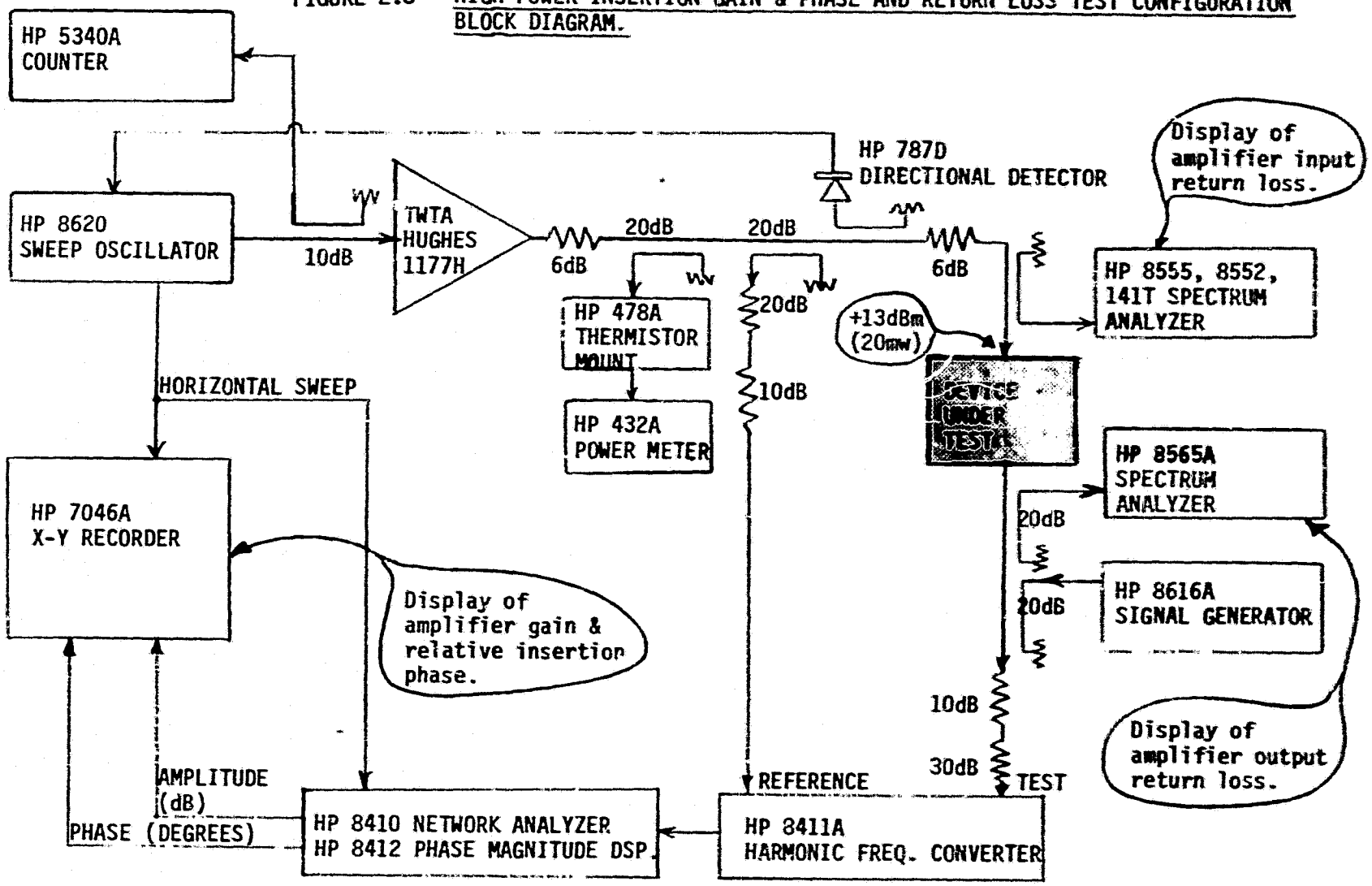

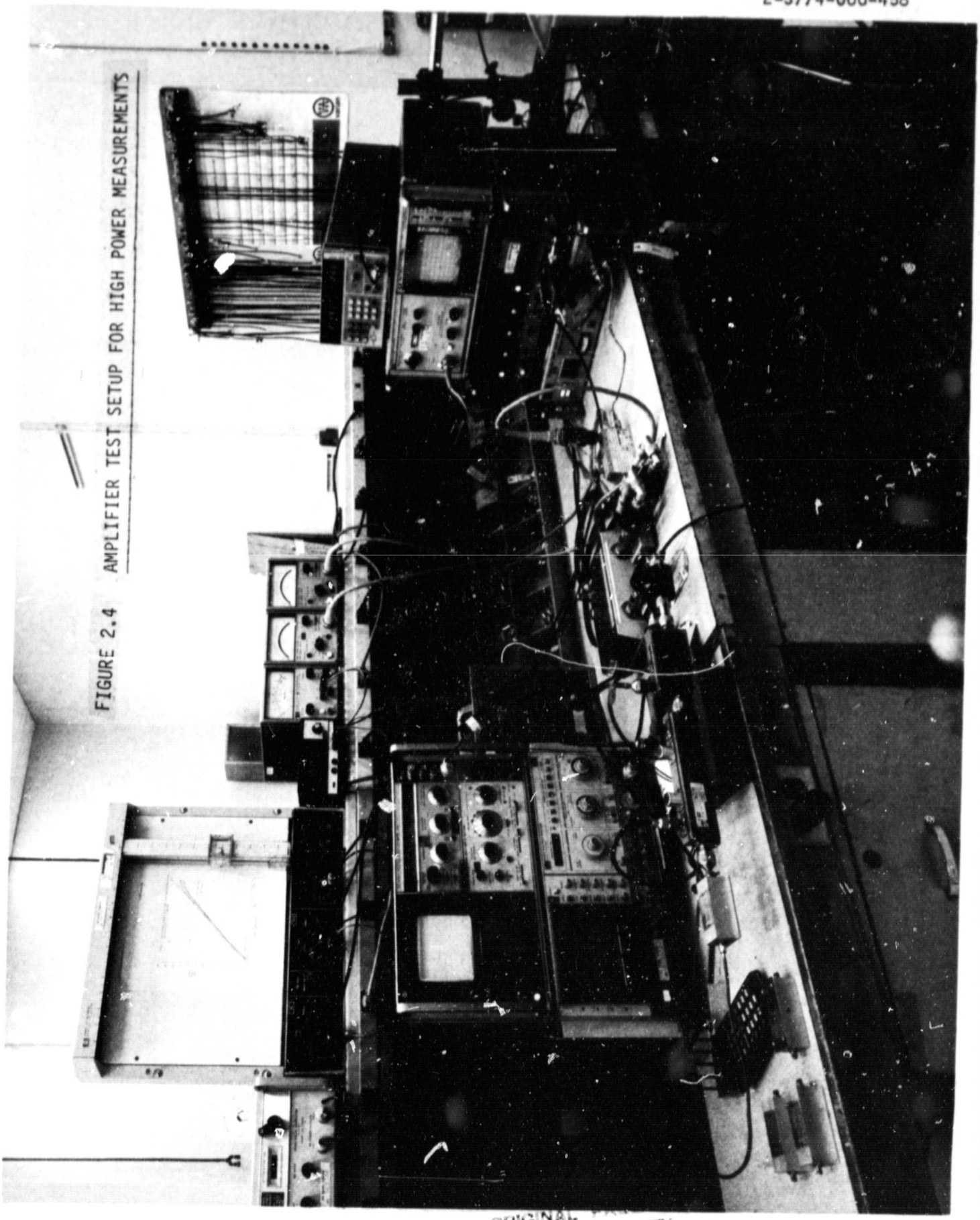

FIGURE 2.4 AMPLIFIER TEST SETUP FOR HIGH POWER MEASUREMENTS

FIGURE 2.5 AMPLIFIER GAIN & INSERTION PHASE VERSUS FREQUENCY (+13 dBm drive power, 20mw)

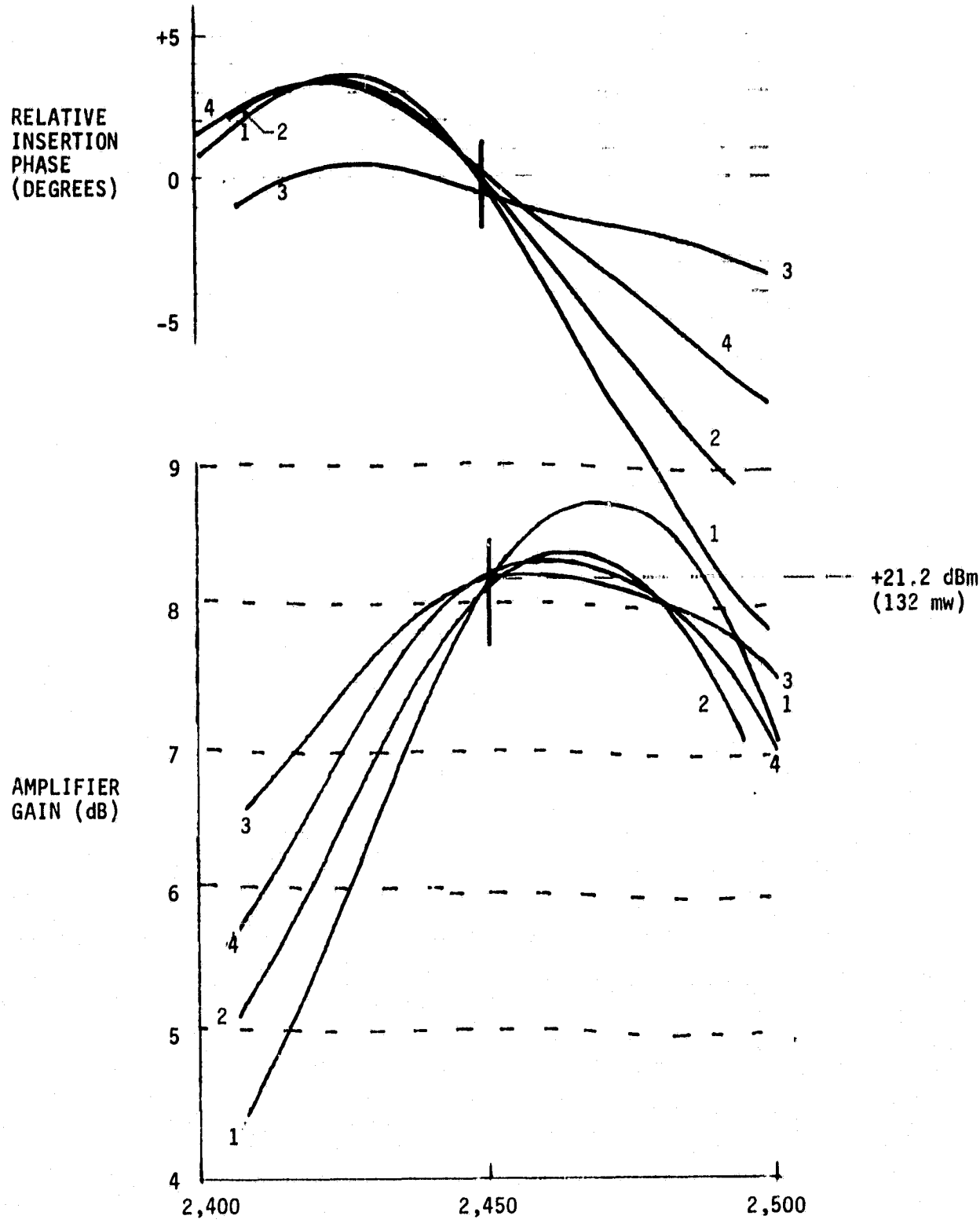

FIGURE 2.6 AMPLIFIER GAIN & INSERTION PHASE VERSUS DRIVE POWER

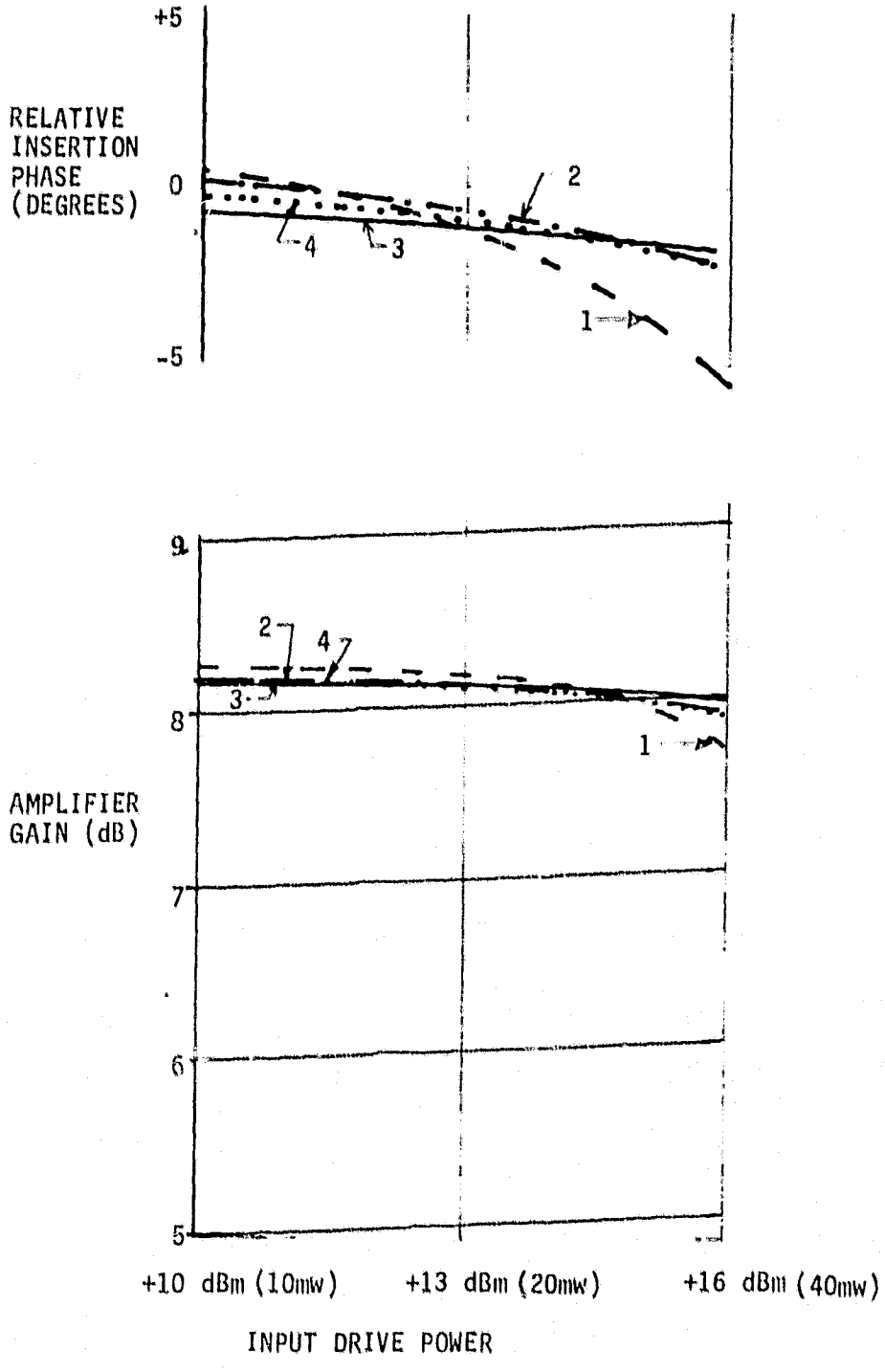

3.0 ANTENNA FEED NETWORK

To evaluate the four-way power-combining antenna a feed network is needed to supply four correctly phased 2.45 GHz signals that are all equal in amplitude. Two signals are needed that are in-phase while the remaining two signals are 180° out-of-phase at the design frequency. The required network was realized in stripline by cascading two 0°-180° rat-race hybrids at the output of a 2-way in-phase power divider. The three networks were then integrated into a single stripline circuit.

3.1 0° - 180° HYBRID

The 0° - 180° hybrid was realized using a 1-1/2 wavelength ring hybrid design. A reproduction of the printed copper metalization pattern is shown in Figure 3.1. For outputs of 0° and 180° a signal is introduced at the lower right hand side and the two outputs are taken at the top right and left hand sides. The top center port receives no power and is isolated. This latter port is generally terminated using a 50 ohm load. Such a termination will also insure that the two output ports of the hybrid are electrically isolated from each other (this assumes the input port is driven by a 50 ohm (matched) generator).

Figures 3.1 through 3.4 contain plots of the measured performance of the 0° - 180° hybrid. The arrows on the metallization pattern of Figure 3.1 correspond to the signal flow paths for the four measurements made to characterize the hybrids performance. The measurements were made using the HP 8542B automatic network analyzer.

In summary, the hybrid performs exactly as required at 2.45 GHz. The amplitude insertion loss balance between outputs is "perfect" (see Figure 3.1) with a total insertion loss of 0.12 dB, including connectors.

The isolation between output arms is greater than 30 dB (see Figure 3.2) and the return loss for all ports is also greater than 30 dB (see Figure 3.3). The relative insertion phase is exactly 180° as required at the center frequency of 2.45 GHz (see Figure 3.4). (The tabular data which is not attached revealed a measured relative insertion phase of 179.7°.)

3.2 2-WAY POWER DIVIDER

The two-way in-phase power divider was realized using a coupled line stripline design. A reproduction of the copper metalization pattern is shown in Figure 3.5. The input line (on the right) is split into two lines which remain coupled over a 1/4 wavelength distance at which point they part into two output 50 ohm lines. Just before the two lines separate a 100 ohm chip resistor is placed between the lines to function as a fourth port which is required to achieve isolation between the two output ports.

Figures 3.5 through 3.9 contains plots of the measured performance of the two-way power divider. As with the previous hybrid, the arrows on the metalization pattern of Figure 3.5 correspond to the signal flow paths for the three measurements made to characterize the hybrids performance.

In summary, the hybrid performs exactly as required at 2.45 GHz for the intended application. The insertion loss balance between outputs is "perfect" (see Figure 3.5) with a total insertion loss of 0.09 dB including connectors. The isolation between output arms (measure 3) is greater than 30 dB and the worst case return loss on all ports is 27 dB. The insertion phases measured are equal with less than 1/2 degree of error (see Figure 3.9).

3.3 INTEGRATED FEED NETWORK

The two hybrid networks described previously were integrated into a single printed circuit pattern to yield four output ports with equal power, two in-phase and two 180° out-of-phase. A reproduction of the printed copper metalization pattern is shown in Figure 3.10. It will be noted that two 0° - 180° hybrids have been attached to the output arms of a two-way power divider. The input port is Port 0. The output at Ports 1 and 4 are in-phase with each other and are both 180° out-of-phase with the outputs at Ports 2 and 3.

Figures 3.10 through 3.13 contain plots of the measured performance of the first (Serial No. 001) integrated feed network fabricated. Three units were made. Only one set of measured results are shown, however, it is typical of the other units assembled (a tabular summary of all three is given later). Two networks were made to permit work on more than one antenna at a time and the third network was made to provide a back-up unit.

Figure 3.10 graphically illustrates the inertion loss of the feed network over a 500 MHz bandwidth. At the design frequency, the insertion loss for all ports was nearly equal. The measured window of loss variation is .06 dB. The average insertion loss measured was 6.175 dB; 6.021 dB of this is attributable to the 1/4 power split leaving the total for circuit losses at 0.154 dB.

Figure 3.11 illustrates the relative insertion phase of all four output ports. It should be noted that at 2.45 GHz that two of the four ports should be 180° out-of-phase with the other two. Therefore, to compare, 180° has been added to the insertion phase for measurements 0-2 and 0-3 prior to plotting in Figure 3.11. The total phase error window measured is 1.5°. This result has been achieved without any trimming of the final

circuit. The small variations that remain can easily be taken out when cutting the hookup cables which will attach the feed network to the antenna.

The different slope of phase versus frequency for two of the ports is due to the difference in effective electrical insertion path length. From the diagram in Figure 3.10 it is seen that the path length to Ports 1 and 4 are equal. The path lengths to Ports 2 and 3 are also equal, but to a different (shorter) effective length. To flatten the phase versus frequency plot for Ports 1 and 4, the data for Figure 3.11 was taken relative to a reference length of 20.30 cm of air dielectric transmission line.

The return loss at all ports of the feed network when all other ports are terminated in 50 ohms is shown in Figure 3.12. The worst case return loss at 2.45 GHz was measured at 27.7 dB which corresponds to a VSWR of 1.09.

The final measurement of concern is the degree of isolation between output ports. Figure 3.13 contains a plot of isolation between Ports 1 and 2 and between Ports 1 and 3. At 2.45 GHz the worst case isolation is approximately 27 dB. This high isolation, coupled with the above mentioned high return loss, will insure that each of the solid state amplifiers are being fed from an independent (isolated) well-matched source.

A summary of the performance of the three integrated feed networks at 2.45 GHz is as follows:

TABLE 3.1: INTEGRATED FEED NETWORK PERFORMANCE SUMMARY AT 2.45 GHz

Serial No.	Phase Balance	Loss Balance	Insertion Loss	Isolation and Return Loss
001	± .73°	± .03 dB	.154 dB	>25 dB
002	± .39°	± .03 dB	.189 dB	>25 dB
003	± .81°	± .015 dB	.172 dB	>25 dB

The measured phase to all ports of each network deviates from a mean value by less than one degree, which is very acceptable. One degree was the goal. The measured loss was less than 0.2 dB for each of the units over and above the 6.02 dB that results from the four way power division. This value will be used again when the antenna efficiency is calculated. A more important parameter is loss balance which is so small that it is hardly measurable, a mere ± .03 dB worst case. Thus, the power delivered to all ports is within 0.7% of the mean value.

The isolation between the feed network output ports is greater than 25 dB for all units. This minimizes the ineraction between amplifiers in the final configuration by preventing reflected power from the input of each amplifier from reaching the input of one or more of the other amplifiers. Thus, the amplifiers are operated as if they were each driven from an isolated source. This is a particularly good operating procedure where one is primarily interested in how well the power combining antenna performs and in how well the solid state amplifiers interact with each other within the antenna circuitry.

The final figure of merit for the antenna feed network is the degree of impedance match realized at each port. As noted above, the return loss for all ports is greater than 25 dB. This means a VSWR of less than 1.12. It should be pointed out, however, that in actual operation a low output VSWR and good isolation is only available if the input power to the feed network is derived from a well matched source.

A photograph of one of the integrated antenna feed networks is shown in Figure 3.14. To simplify its use a copy of the circuit metallization pattern was printed as a label on the surface of one of the aluminum cover plates. Figure 3.15 contains a photograph of the automatic network analyzer used to measure the stripline circuits.

FIGURE 3.1

THE BOEING CO. GWF AUGUST 2, 1979

SPS SOLID STATE MODULE DEVELOPMENT

0-180 DEGREE HYBRID, CIRCUIT # SPS-5168

ENGINEERING MODEL

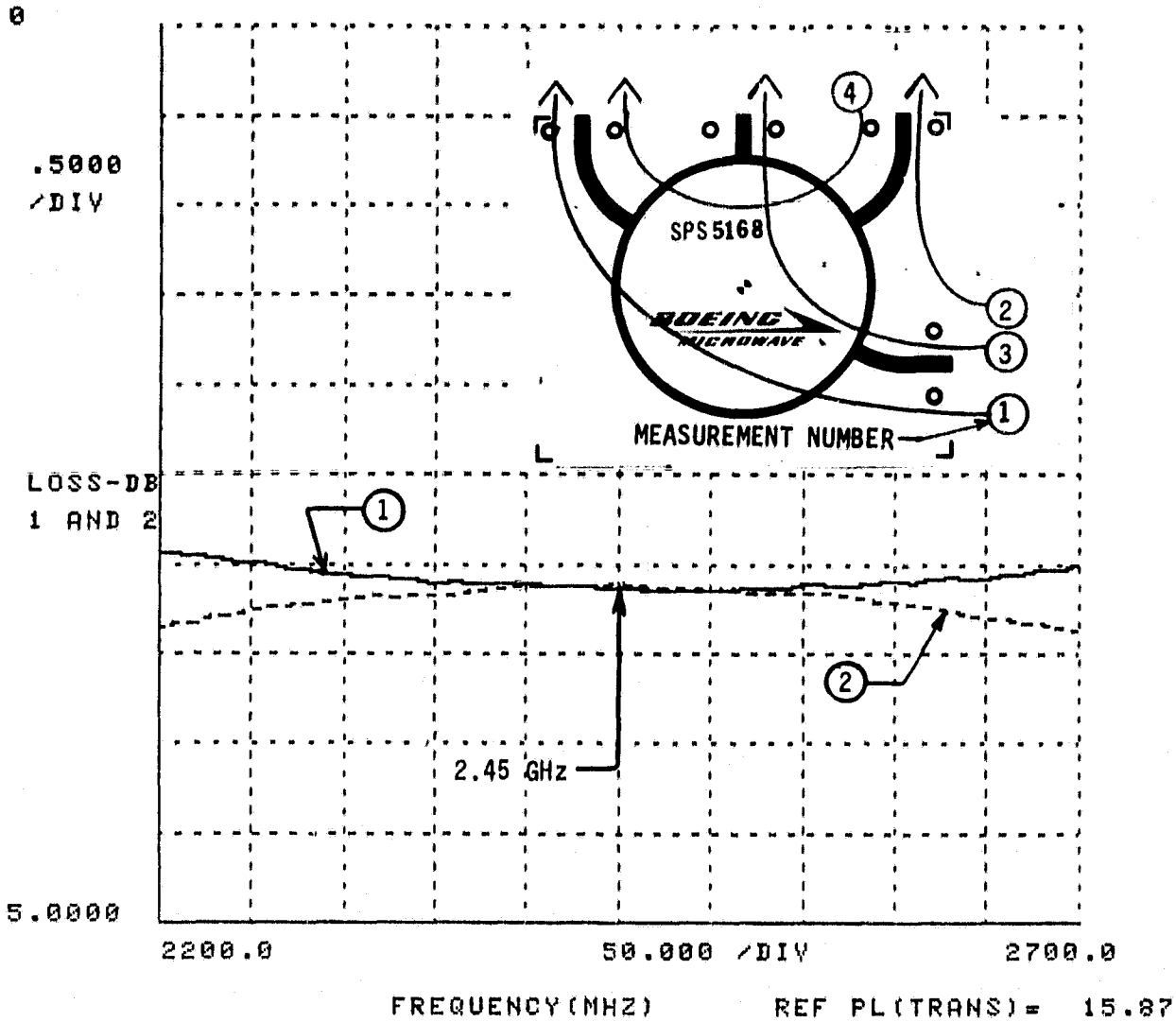

FIGURE 3.2

THE BOEING CO. GWF AUGUST 2, 1979

SPS SOLID STATE MODULE DEVELOPMENT
0-180 DEGREE HYBRID, CIRCUIT # SPS-5168
ENGINEERING MODEL

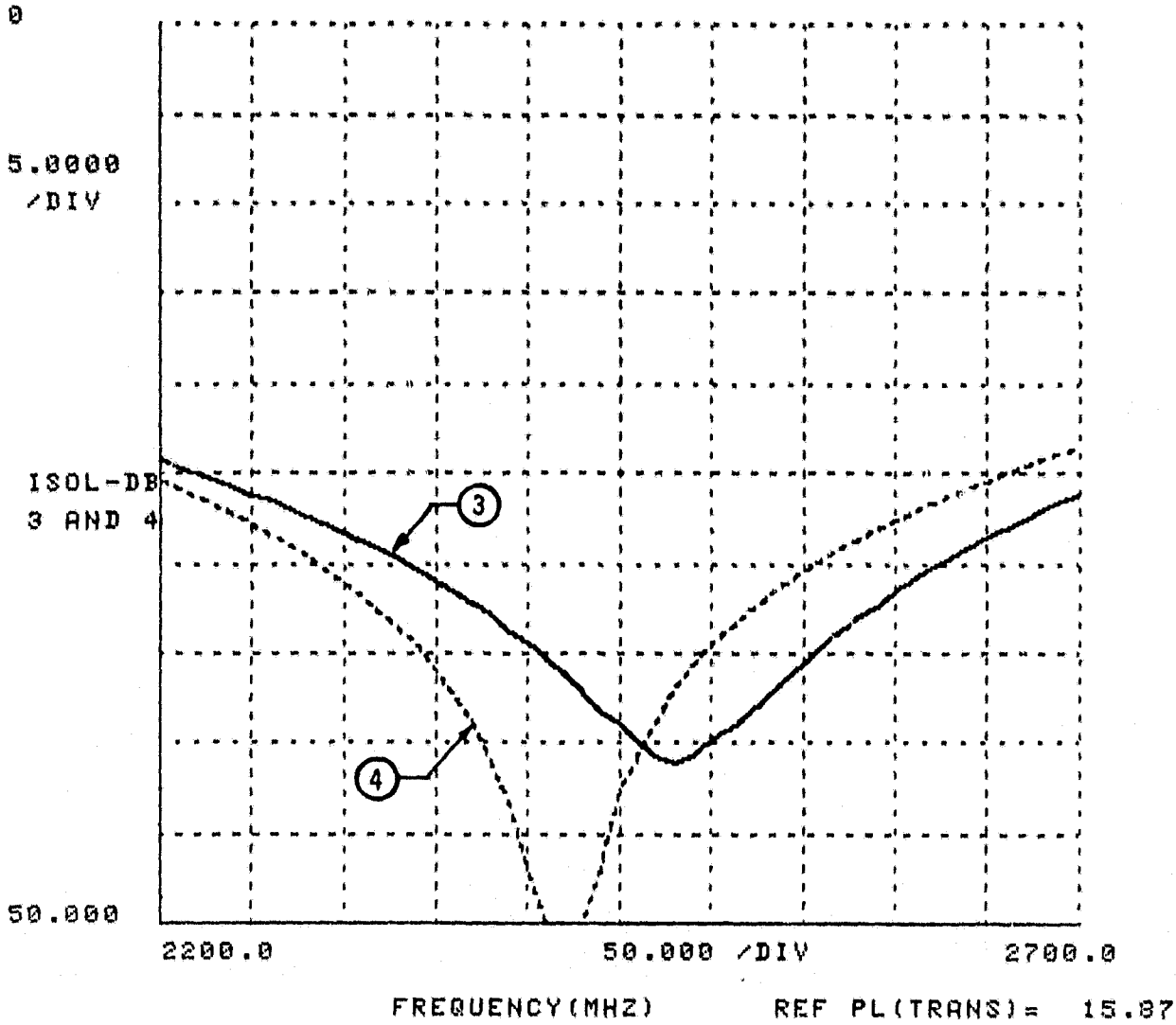

FIGURE 3.3

THE BOEING CO. CWF AUGUST 2, 1979

SPS SOLID STATE MODULE DEVELOPMENT

0-180 DEGREE HYBRID, CIRCUIT # SPS-5168

ENGINEERING MODEL

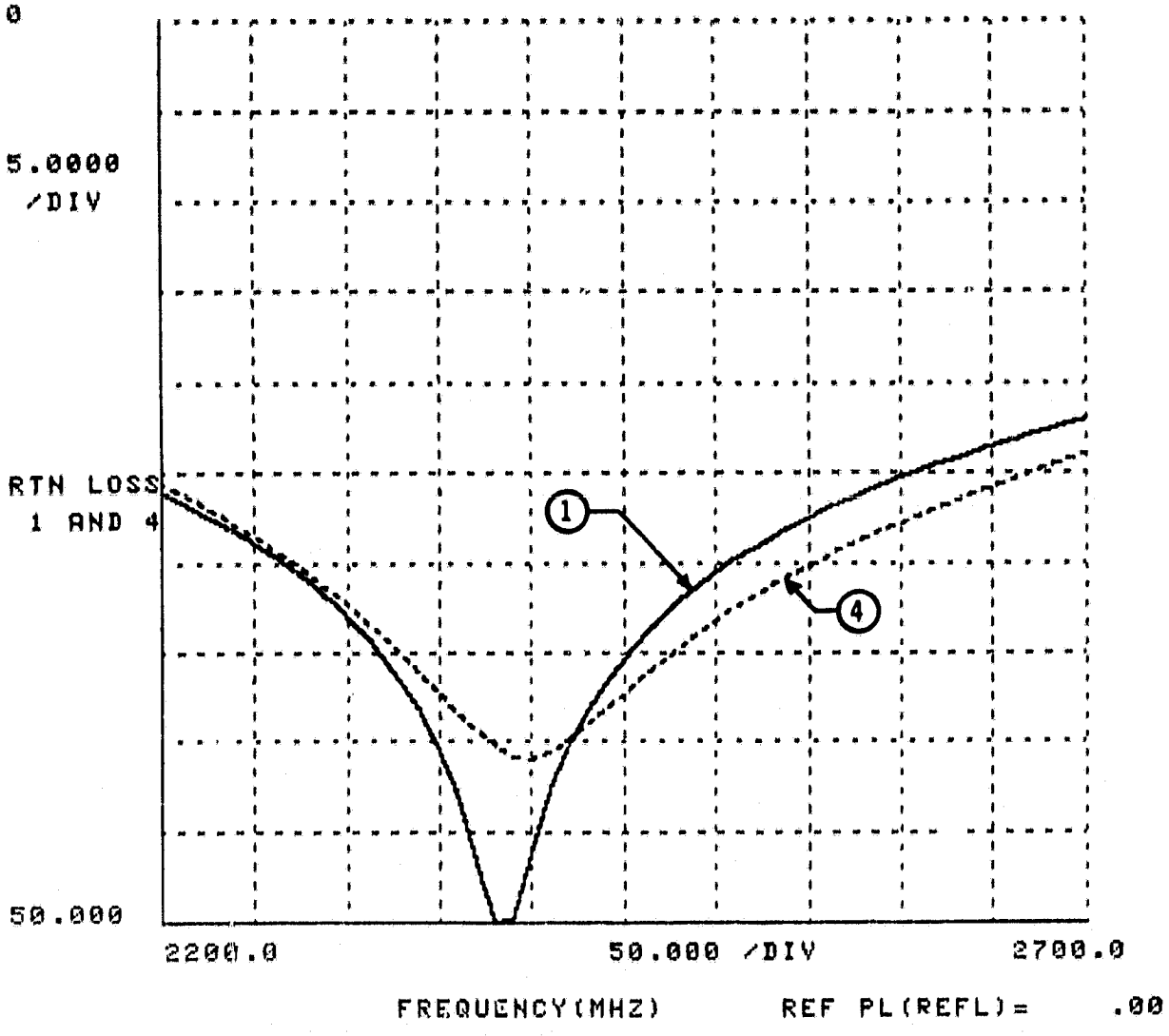

FIGURE 3.4

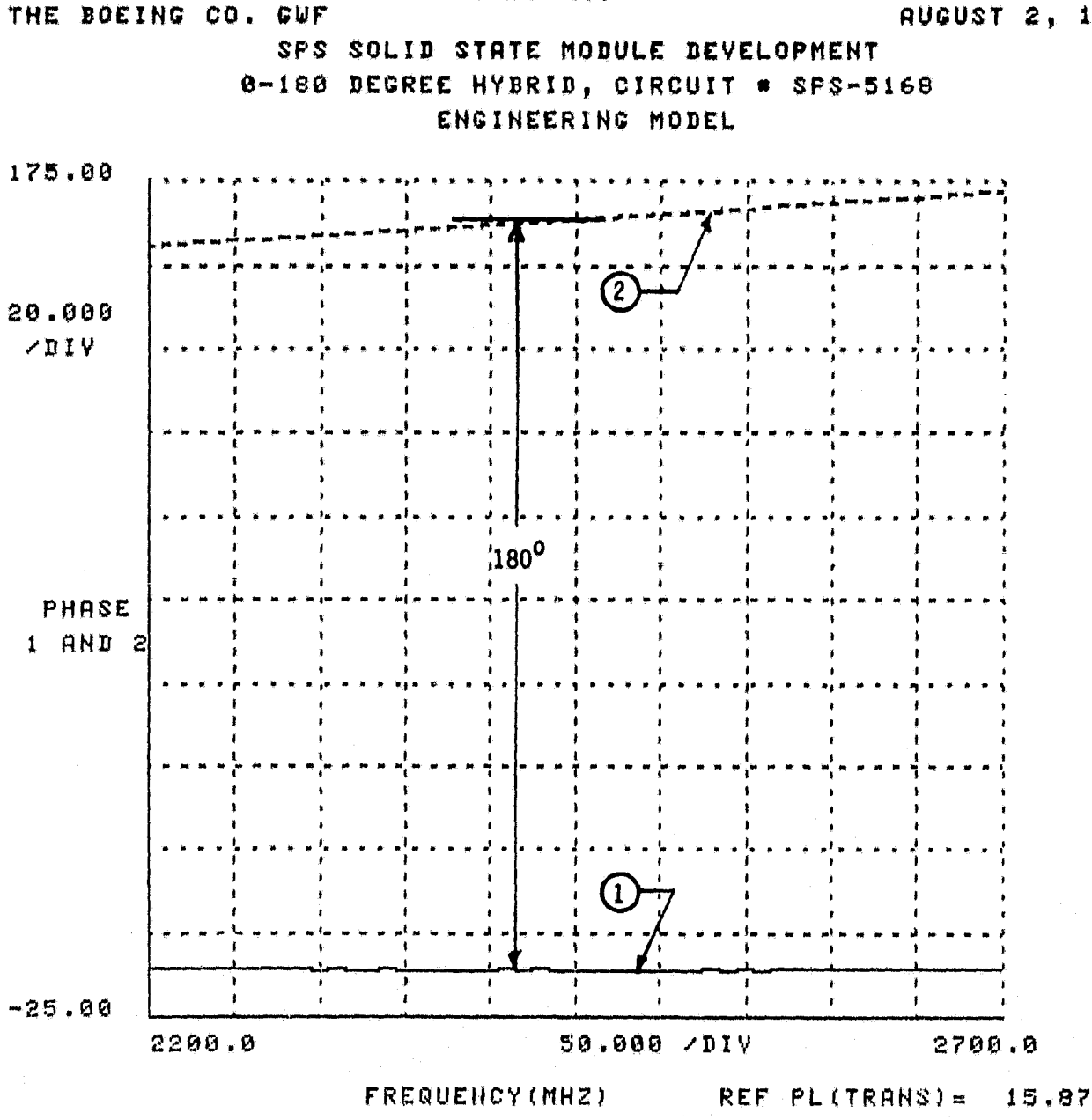
THE BOEING CO. GWF
AUGUST 2, 1979
SPS SOLID STATE MODULE DEVELOPMENT
0-180 DEGREE HYBRID, CIRCUIT # SPS-5168
ENGINEERING MODEL
175.00
20.000
/DIV
PHASE
1 AND 2
180°
-25.00
2200.0
50.000 /DIV
2700.0
FREQUENCY(MHZ)
REF PL(TRANS)= 15.87
1
2

FIGURE 3.5

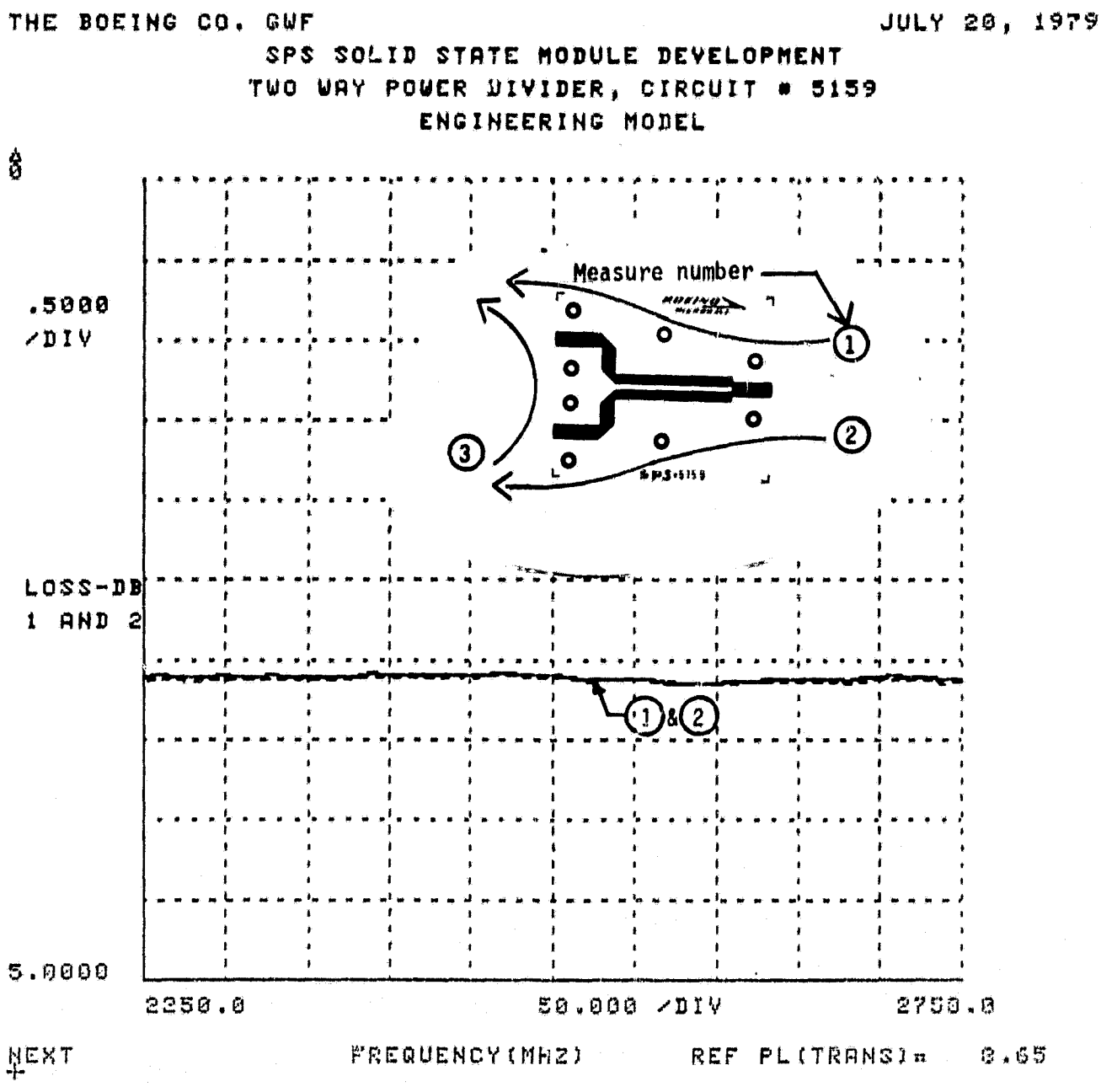
THE BOEING CO. GWF
JULY 20, 1979
SPS SOLID STATE MODULE DEVELOPMENT
TWO WAY POWER DIVIDER, CIRCUIT # 5159
ENGINEERING MODEL
0
.5000
/DIV
LOSS-DB
1 AND 2
5.0000
Measure number
1
2
3
1&2
2250.0
50.000 /DIV
2750.0
NEXT
FREQUENCY(MHZ)
REF PL(TRANS)= 0.65

FIGURE 3.6

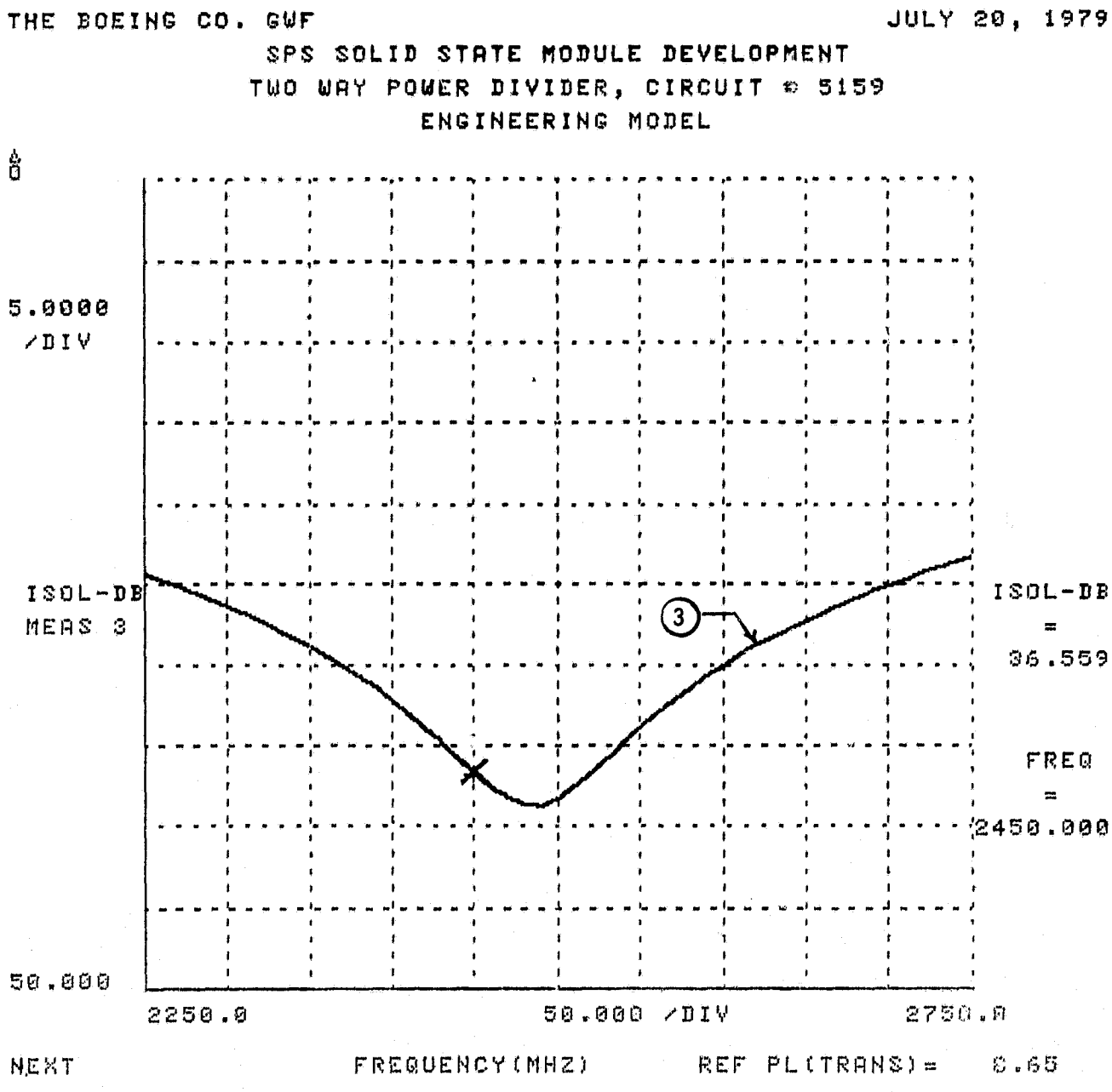
THE BOEING CO. GWF
JULY 20, 1979
SPS SOLID STATE MODULE DEVELOPMENT
TWO WAY POWER DIVIDER, CIRCUIT # 5159
ENGINEERING MODEL
dB
5.0000
/DIV
ISOL-DB
MEAS 3
50.000
3
ISOL-DB
=
36.559
FREQ
=
2450.000
2250.0
50.000 /DIV
2750.0
NEXT
FREQUENCY(MHZ)
REF PL(TRANS)= 0.65

FIGURE 3.7

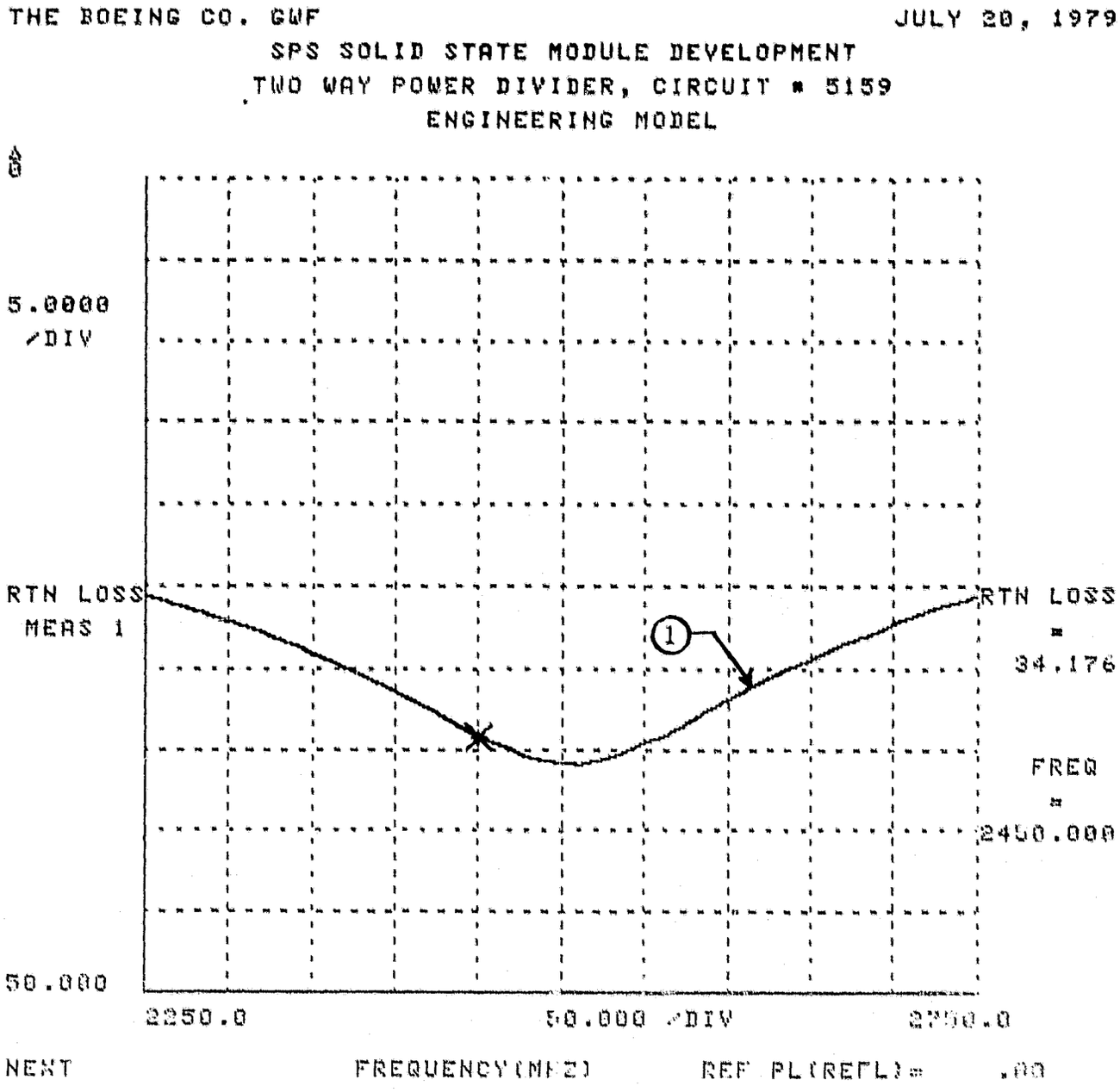
THE BOEING CO. GWF
JULY 20, 1979
SPS SOLID STATE MODULE DEVELOPMENT
TWO WAY POWER DIVIDER, CIRCUIT # 5159
ENGINEERING MODEL
5.0000
/DIV
RTN LOSS
MEAS 1
50.000
RTN LOSS
=
34.176
FREQ
=
2450.000
2250.0
50.000 /DIV
2750.0
NEXT
FREQUENCY(MHZ)
REF PL(REFL)=
.00

FIGURE 3.8

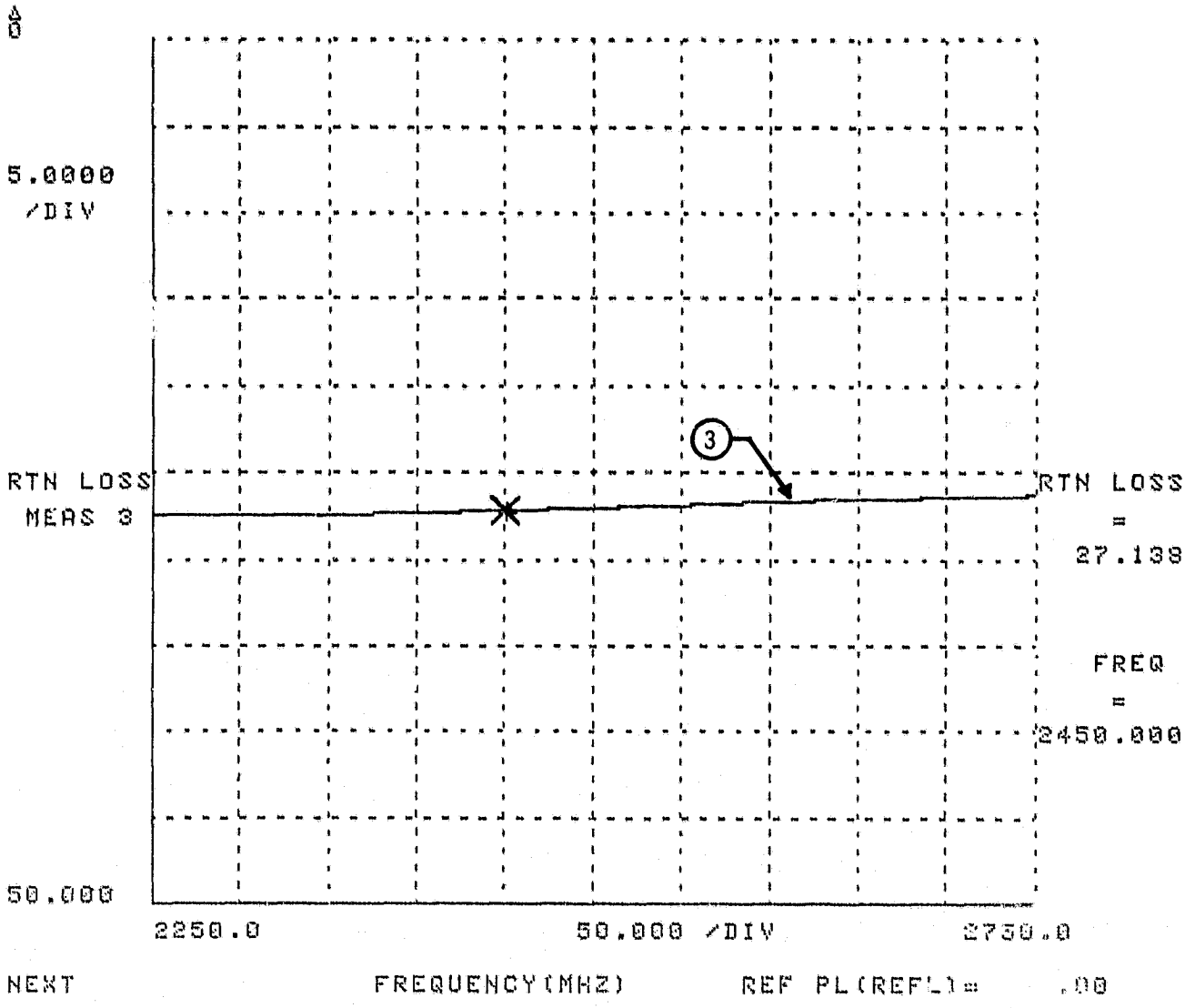
THE BOEING CO. GWF
JULY 20, 1979
SPS SOLID STATE MODULE DEVELOPMENT
TWO WAY POWER DIVIDER, CIRCUIT # 5159
ENGINEERING MODEL
dB
5.0000
/DIV
RTN LOSS
MEAS 3
3
RTN LOSS
=
27.138
FREQ
=
2450.000
50.000
2250.0
50.000 /DIV
2750.0
NEXT
FREQUENCY(MHZ)
REF PL(REF'L)= .00

FIGURE 3.9

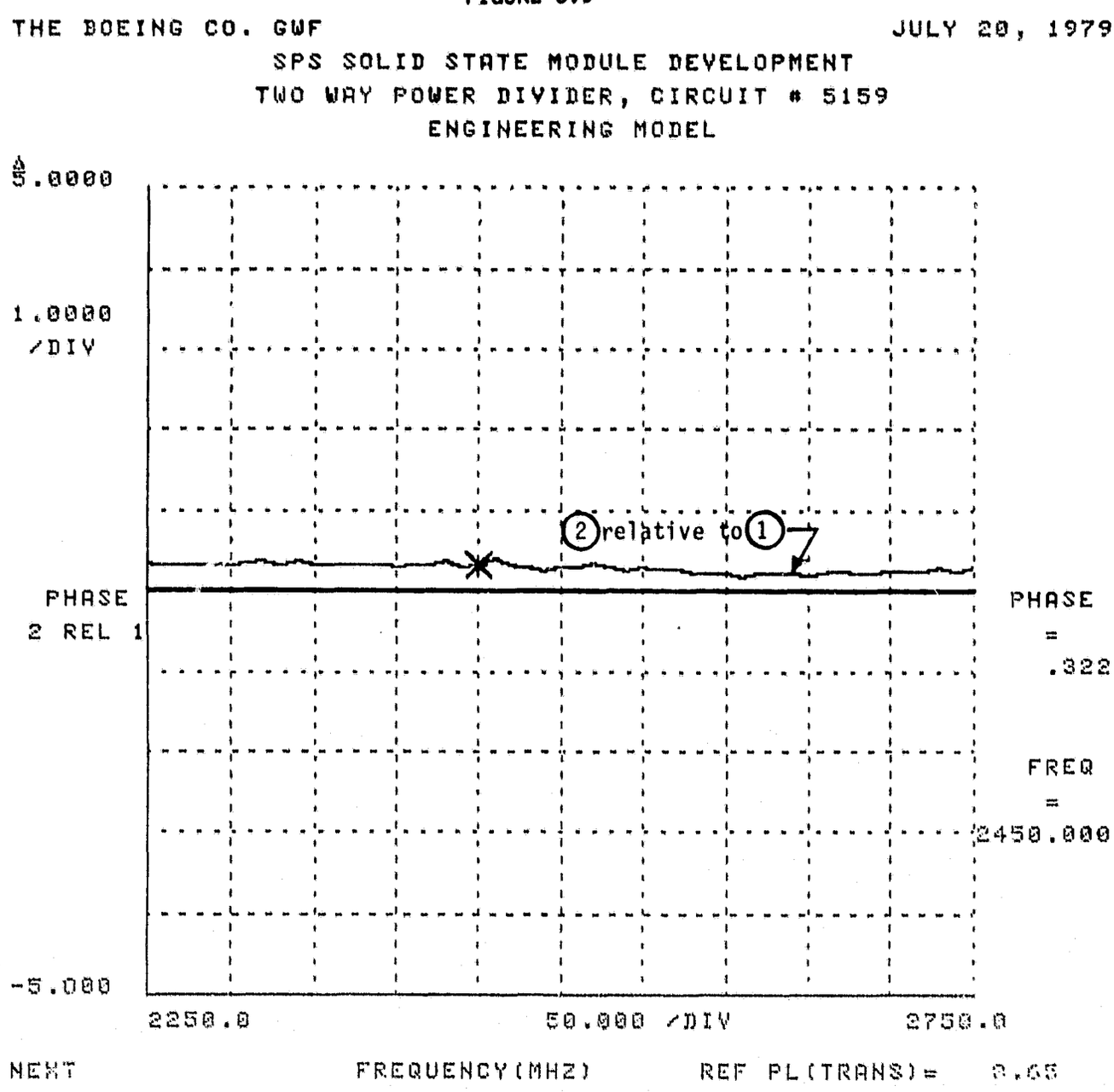
THE BOEING CO. GWF
JULY 20, 1979
SPS SOLID STATE MODULE DEVELOPMENT
TWO WAY POWER DIVIDER, CIRCUIT # 5159
ENGINEERING MODEL
5.0000
1.0000
/DIV
2 relative to 1
PHASE
2 REL 1
PHASE
=
.322
FREQ
=
2450.000
-5.000
2250.0
50.000 /DIV
2750.0
NEXT
FREQUENCY(MHZ)
REF PL(TRANS)= 0.00

FIGURE 3.10

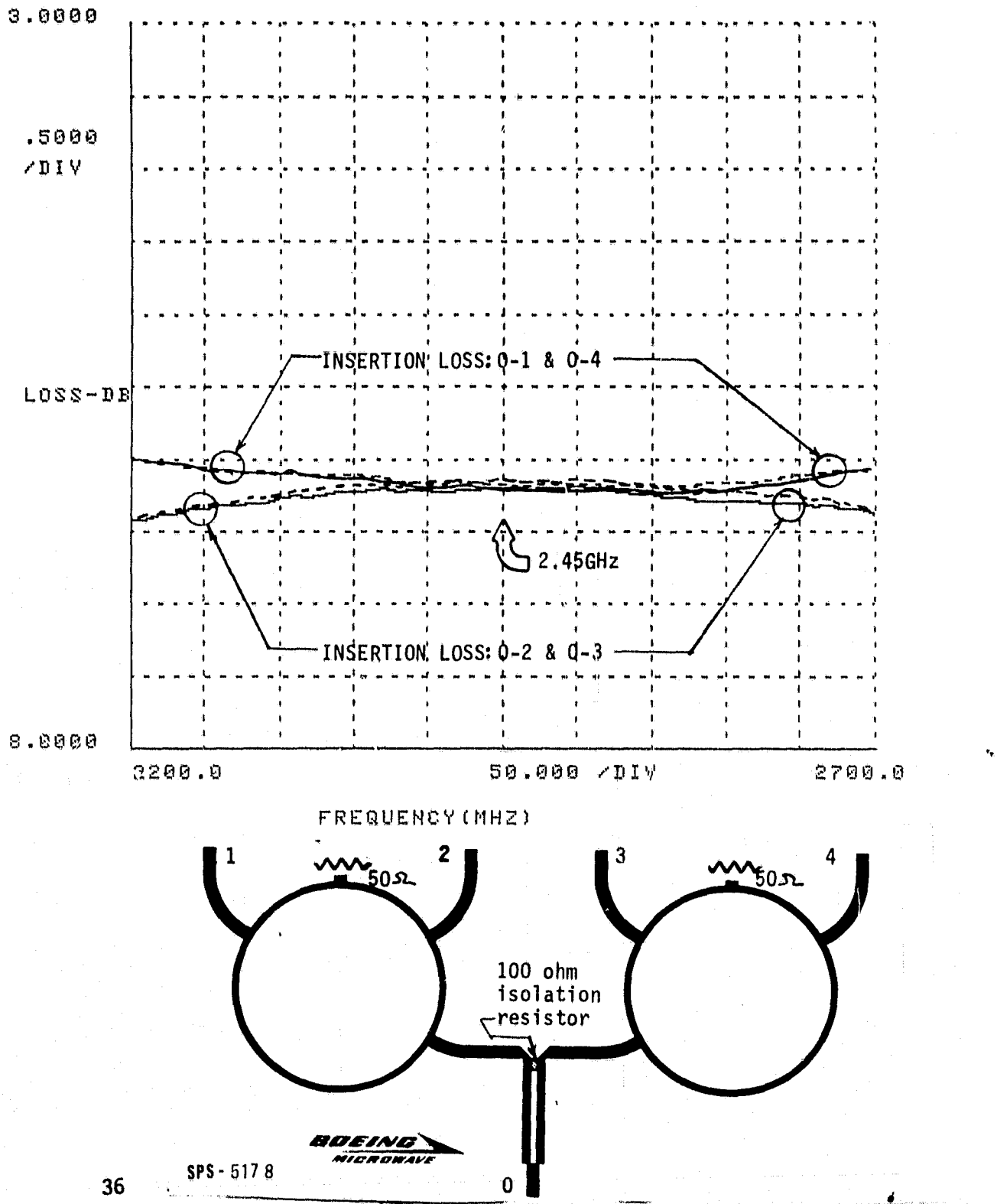
THE BOEING CO. GWF
SEPTEMBER 10, 1979
SPS SOLID-STATE ANTENNA MODULE FEED NETWORK 2.45 GHZ
SPS-5178, SER. *01
3.0000
.5000 /DIV
LOSS-DB
8.0000
INSERTION LOSS: 0-1 & 0-4
2.45GHz
INSERTION LOSS: 0-2 & 0-3
3200.0
50.000 /DIV
2700.0
FREQUENCY(MHZ)
1
2
3
4
50Ω
50Ω
100 ohm isolation resistor
0
BOEING MICROWAVE
SPS-5178

FIGURE 3.11

THE BOEING CO. GWF SEPTEMBER 10, 1979
SPS SOLID-STATE ANTENNA MODULE FEED
NETWORK 2.45 GHZ
SPS-5178, SER. #01

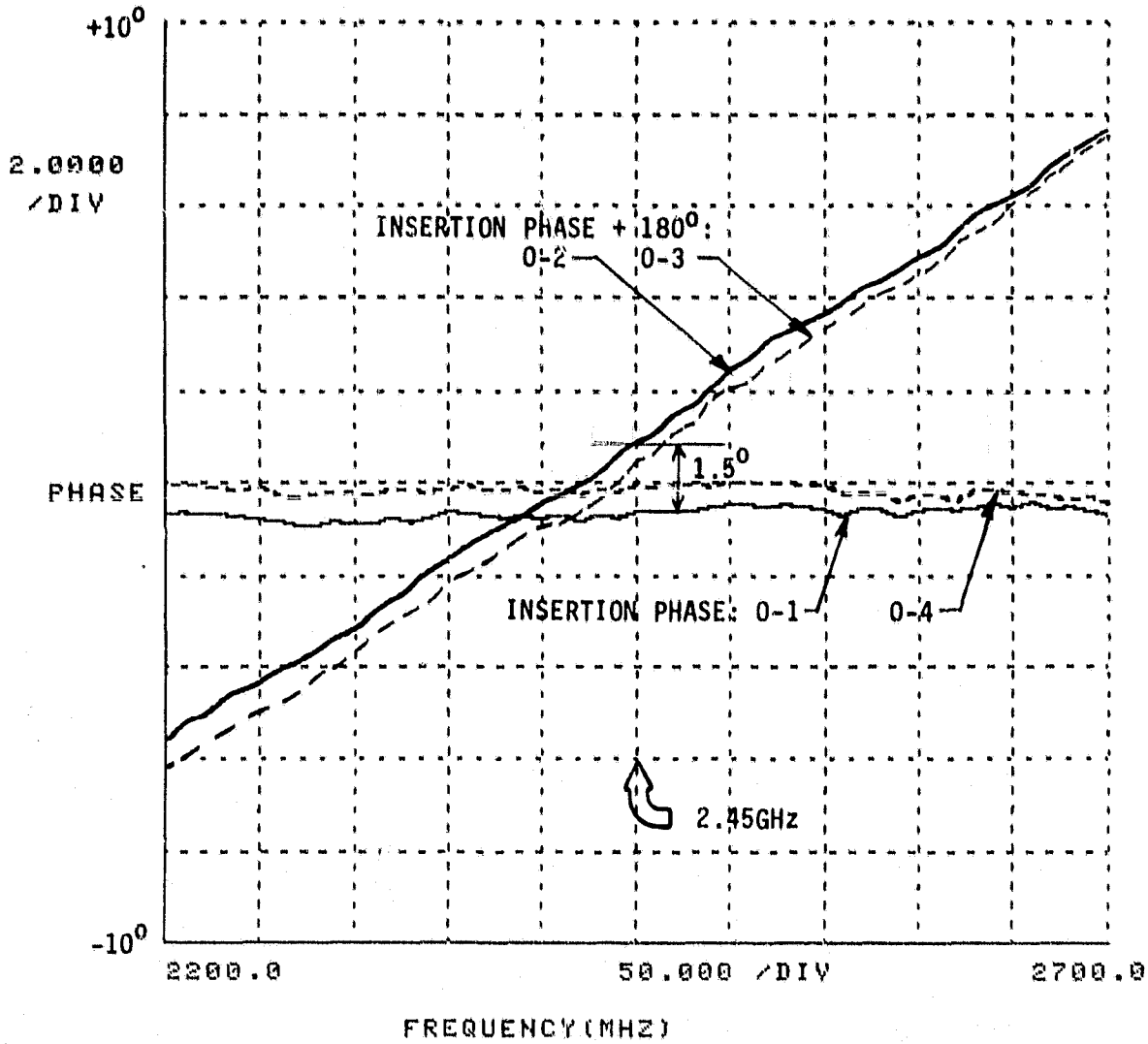

FIGURE 3.12

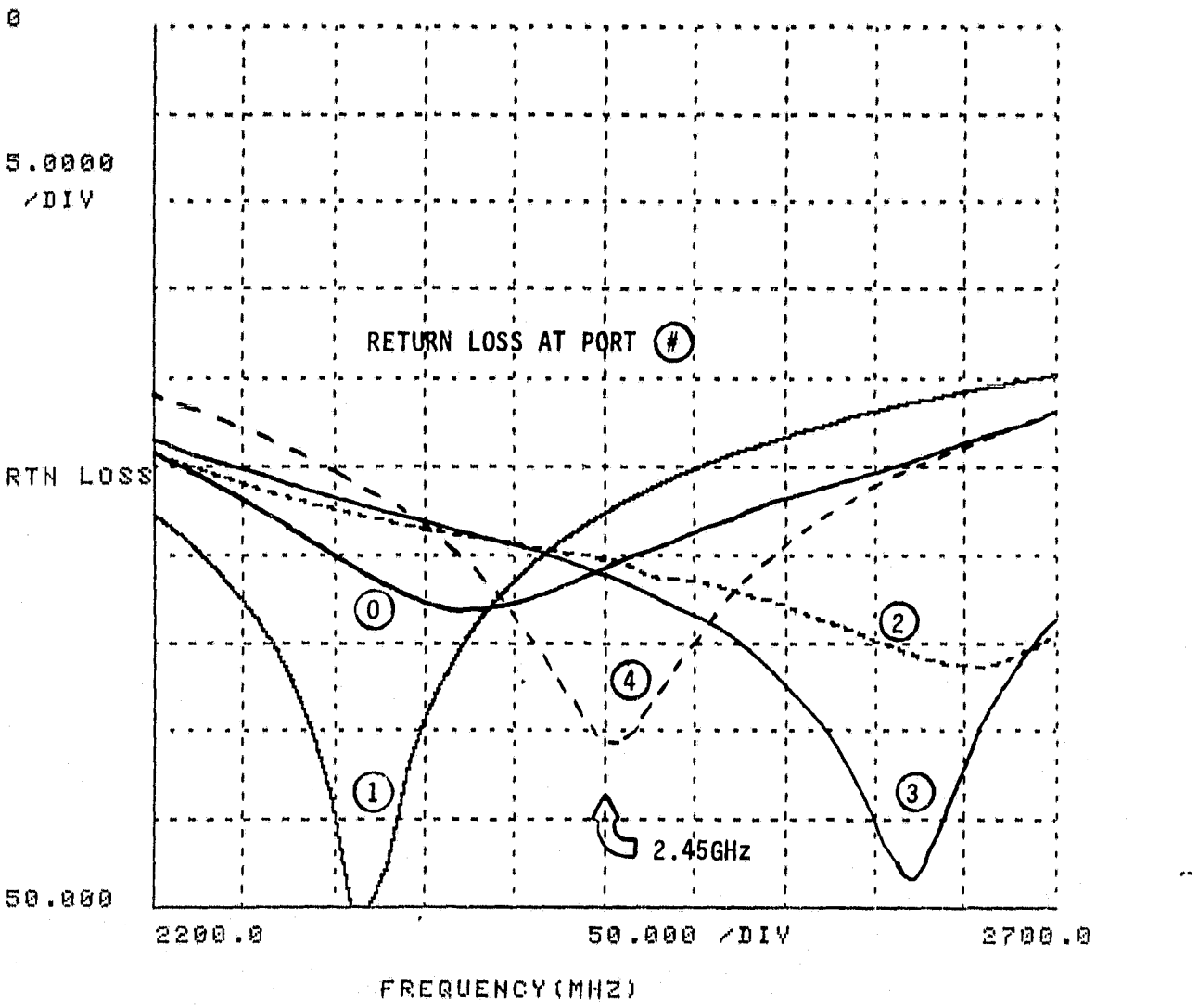
THE BOEING CO. GWF
SEPTEMBER 10, 1979
SPS SOLID-STATE ANTENNA MODULE FEED NETWORK
2.45 GHZ
SPS-5178, SER. #01
0
5.0000 /DIV
RETURN LOSS AT PORT #
RTN LOSS
0
1
2
3
4
2.45GHz
50.000
2200.0
50.000 /DIV
2700.0
FREQUENCY(MHZ)

FIGURE 3.13

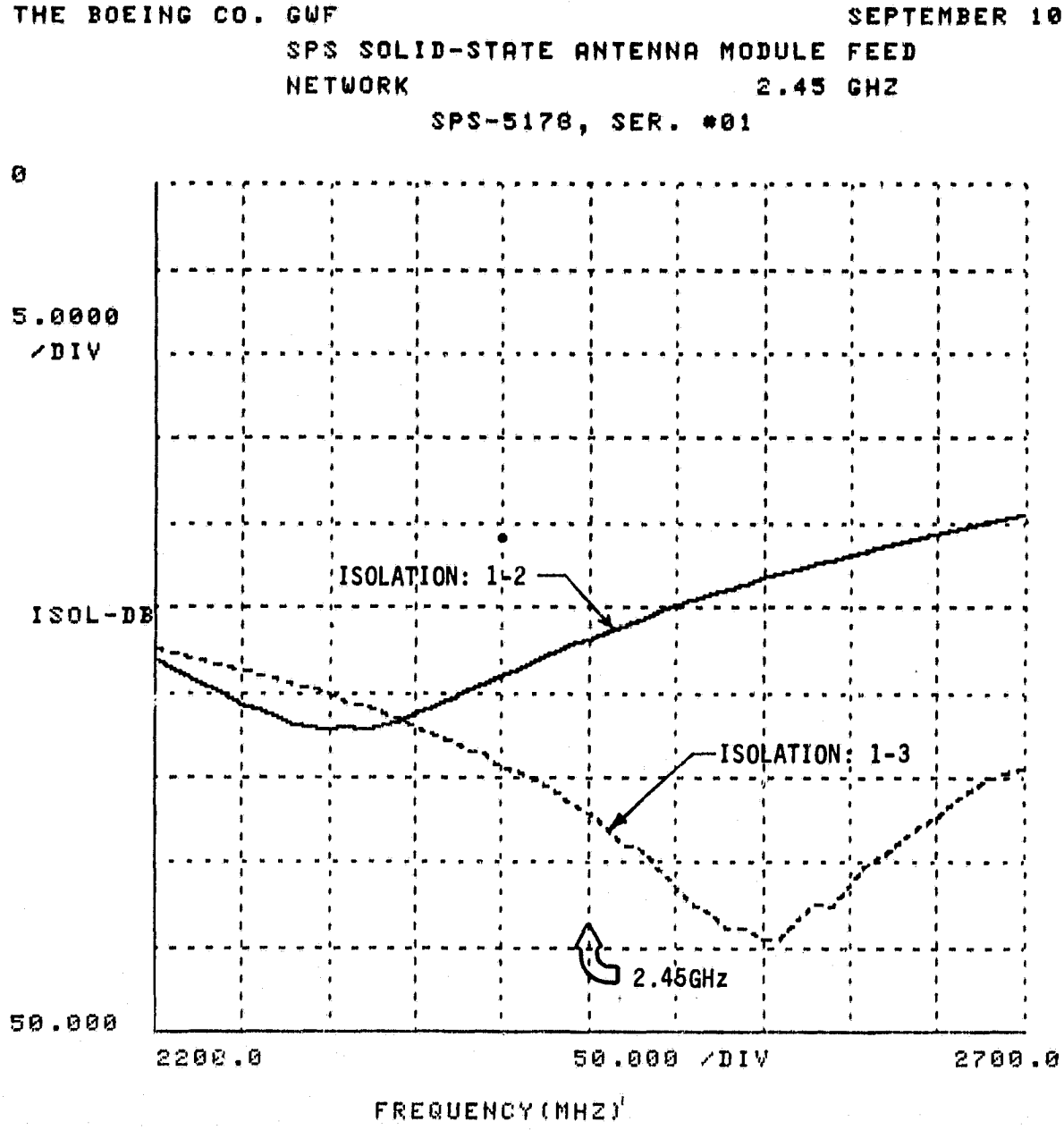
THE BOEING CO. GWF
SEPTEMBER 10, 1979
SPS SOLID-STATE ANTENNA MODULE FEED NETWORK
2.45 GHZ
SPS-5170, SER. #01
0
5.0000 /DIV
ISOL-DB
50.000
ISOLATION: 1-2
ISOLATION: 1-3
2.45GHz
2200.0
50.000 /DIV
2700.0
FREQUENCY(MHZ)

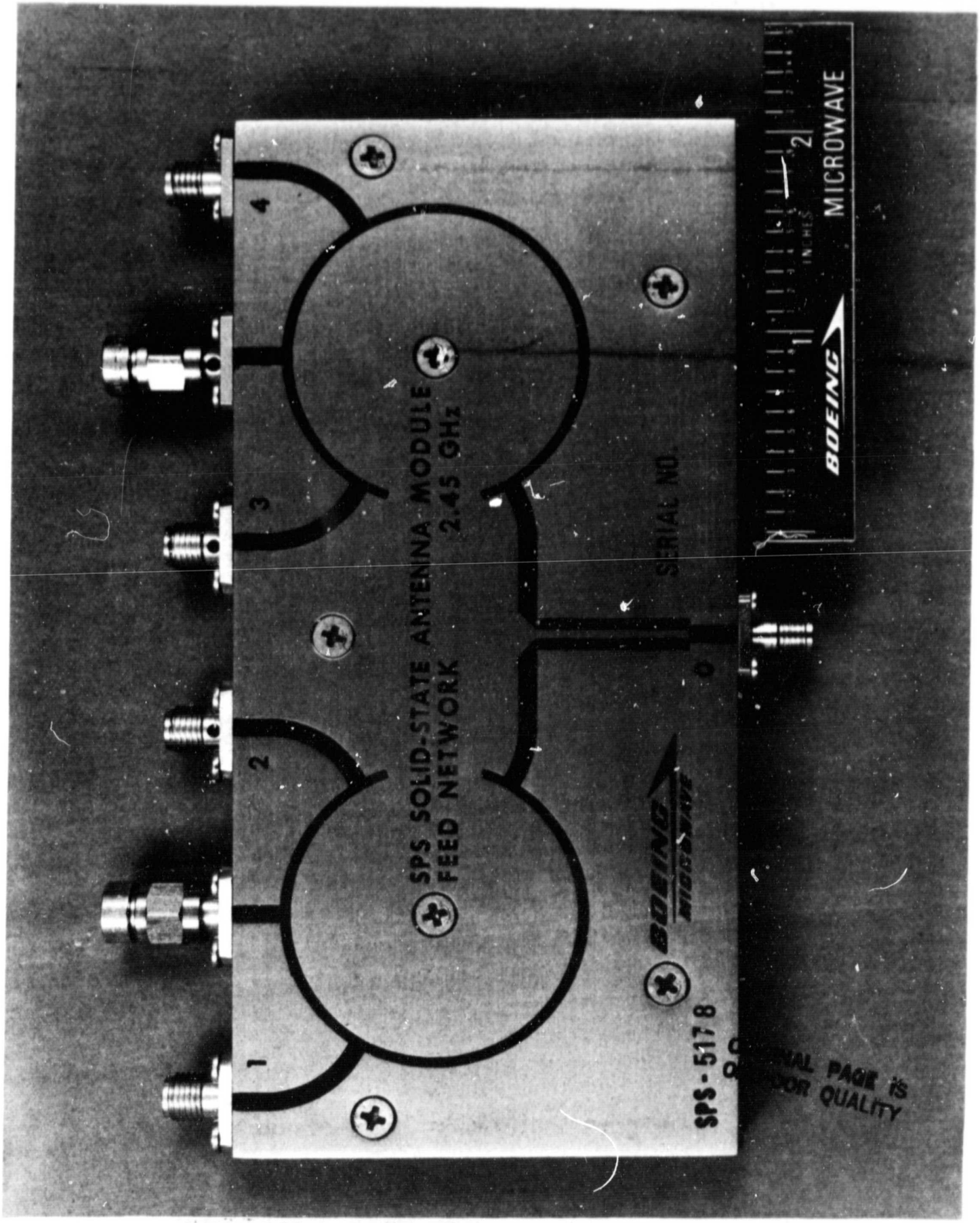

FIGURE 3.14 PHOTOGRAPH OF THE ANTENNA FEED NETWORK (STRIPLINE)

FIGURE 3.15 AUTOMATIC NETWORK ANALYZER

4.0 POWER COMBINING ANTENNA

4.1 BACKGROUND

The antenna developed and evaluated under the program looks very much like the antenna proposed (see Figure 1.2). The major differences between this antenna and the four-feed power-combining antenna previously developed by Boeing (IR&D) is in the mechanism of coupling to the antenna and further additional attention was given to reduce leakage of cross-polarized radiation. The four coupling mechanisms are more optimally located to achieve a smaller reactance (detuning) slope versus frequency which yields a broader bandwidth antenna. To reduce the cross-polarized radiation, surface slotlines orthogonal to the principal radiating slot were kept very narrow in an attempt to confine most of the field within the dielectric substrate.

The basic antenna is essentially a twin slot radiator in which the two slots are directly coupled in that they share a common cavity. The advantage of coupling the two slots is to leave open the option that a single phase error correction integrated circuit (see Figure 1.1) may be used to control the radiated phase of four power amplifiers by sampling the common phase within the cavity.

With the exception of cabling mechanisms the antenna consists of only two parts. A dielectric substrate which is metalized on both sides with an appropriate circuit pattern and a rectangular metal cavity. The two are then electrically attached using solder or conducting epoxy. The subsections that follow describe the antenna design in detail.

4.2 SUBSTRATE MATERIAL

A low loss dielectric material with a relative dielectric constant of approximately 10 was desired for the antenna substrate which must also suffice as the substrate for the input microstrip feed lines. A material

with a higher dielectric constant would unnecessarily increase the input feed line copper loss due to smaller line widths unless the dielectric was made thick which would result in more mass than necessary per radiating element. A lower dielectric constant material would probably be workable if an acceptable material were available (with a high thermal conductivity). Ceramic (Al_2O_3) seems desirable for this application since it is relatively low cost in large quantities and has better thermal conducting properties than most other lower dielectric constant materials which have similar costs. SPS requires a microwave quality material that is available in large quantities, preferably a good thermal conductor with good thermal stability at low cost. Thus, for this program ceramic substrates of Al_2O_3 were judged the first choice.

A competitive material manufactured by 3M, Co. called Epsilam-10 exhibits a dielectric constant of approximately 10 and is available in 9" x 9" double copper clad sheets. The mechanical and thermal properties are not competitive for SPS applications; however, for this program it was judged adequate to demonstrate the solid-state power combining antenna features required. In addition, it was readily available in standard sheet sizes much larger than the usually available 2" x 2" size for microwave quality ceramic substrates.

With Epsilam-10 work could begin sooner without special order delays for microwave quality ceramics of sufficient size. Further, the ceramic approach involved additional metalization processing which would contribute to the program cost. The relatively thick one-ounce copper layer (.0014") available on the Epsilam-10 was judged excellent with regard to copper losses when compared to ceramic where thinner metalization layers (.0003") are generally used. The advertised loss tangent for Epsilam-10 is .002 (.001 on data sheets used at program start). This is much higher than the .0001 of ceramic but was considered acceptable since a loss tangent of .002 would probably not contribute as much loss as would be expected for the copper loss alone for the same 50 ohm line. Thus dielectric loss in Epsilam-10 although higher than for ceramic still should not dominate the loss mechanisms expected.

The above rationale describes the justification of why Epsilam-10 was selected for the dielectric substrate. Looking back over the results of the seven month effort, however, it appears that perhaps the wrong choice was made. A great deal of difficulty was experienced when soldering the cavity to the substrate or when soldering the finished antenna to the larger ground plane due to cracks forming in the dielectric. The cracks were caused by the material's inability to tolerate the thermal gradients imposed by the heat of soldering. These cracks altered the effective dielectric constant and caused detuning and various unbalanced conditions within the antenna. The problem was finally solved by substituting silver bearing conductive epoxy (COMREX #584).

Another problem experienced is that the dielectric constant of Epsilam-10 is not consistent between sheets. Detuning occurred whenever a design was repeated using material from a different 9" x 9" copper clad dielectric sheet. A significant E field exists within the radiating slots that is parallel to the dielectric surface which means that the dielectric constant in all directions must be repeatable to avoid detuning effects. Epsilam-10 is also known to be anisotropic with a higher (different) dielectric constant for fields parallel to the surface of the sheet than for fields perpendicular to the surface. Thus, for results to be repeatable the surface parallel dielectric constant must also be controlled.

A final problem associated with the material is a significantly higher loss than anticipated. Since the copper is quite heavy (0.0014"), approximately 27 skin depths thick (the skin depth is 52.5 microinches for copper at 2.45 GHz) the added loss observed is believed to be associated primarily with dielectric loss. Subsequent to the work it has been learned that the substrate material will absorb water which can significantly increase losses. The substrates were always baked after etching to dry them out; however, precautions were not observed to control future exposure to moisture which could have produced uncontrolled variations in circuit losses.

Several test strips of 50 ohm line were fabricated for evaluation to determine the Epsilam-10 dielectric constant and loss properties. In summary, it was found that the relative dielectric constant is a little larger than advertised by 3-M Co. If one assumes the effective value of the relative dielectric constant is slightly greater than 12 (instead of the 10.2 claimed by 3M), the impedance values versus line width obtained may be justified. A 50 ohm line in this material was found to be slightly narrower than 0.020" which can only be reconciled with theory by placing the relative dielectric constant near 12. (The discrepancy was not due to substrate thickness variation.)

Two 50 ohm test strips that had lengths of 1 inch and 2 inch were measured using the automatic network analyzer with the result that the insertion loss of the line was determined to be 0.126 dB/in (.218 dB/wavelength). This is 35% greater than what has been Boeing's experience for microstrip lines on ceramic (Al_2O_3) where the loss is 0.093 dB/inch using gold metalization instead of copper. (The conductivity of gold is approximately 70% of that for copper.) With the thicker metalization on Epsilam-10 combined with the superiority of copper as a conductor it was expected (hoped) that the line insertion loss would be at least as low as for ceramic.

Subsequent to the work it has been learned that the inner copper surface roughness for Epsilam-10 is on the order of 4 skin depths thick at 2.45 GHz. This is at least 20 times the surface roughness value quoted for standard microwave quality ceramic substrates where a surface roughness of 8 to 10 microinches rms is typical. This copper surface roughness would increase the expected copper loss and the hoped-for gain to make up for the higher dielectric loss tangent for Epsilam-10 may have never existed.

The potential for experiencing added Epsilam-10 dielectric losses as a result of water absorption further clouds the issue of what caused the losses observed to be so high. A best estimate is that the principal contributor is dielectric loss and the failure to adequately control the exposure of the substrate to moisture. Dielectric loss, however, if

increased above the level specified by the manufacturer becomes of concern since dielectric loss may dominate in the slot lines used for the antenna.

4.3 COUPLING NETWORK

To transfer power from the antenna feed network to the radiating slots two transformations are required. The first transformation is between coaxial cable and microstrip transmission line. The second is a transformation between microstrip line and slotline.

A number of commercial adaptors are available to transform from coaxial cable to microstrip. For this program a realiable connector was desired since identical properties for each connector in sets of four are required. We particularly wanted to avoid stress being applied on the soldered center conductor that could cause the solder to yield to an open circuit. The final soldered center pins would be hidden from view and a poor connection could be very difficult to diagnose in an antenna system that is integrated with a four-feed phasing network.

The microstrip connector (adaptor) which was used is made by Solitron Microwave, Number 2975-6300. This connector holds the center pin stationary by a glass metal seal. The center pin is sleeved on each end to two sliding center pin extensions which are permitted to move as stresses dictate.

This connector has been characterized on other Boeing programs up through 4.3 GHz as a reliable component. The glass-to-metal seal does contribute more loss than some other competitive approaches which do not offer the physical integrity. The manufacturer specifies the connector insertion loss at less than or equal to .08 dB/connector at 2.45 GHz. When two sample pairs were measured on each end of a microstrip transmission line the loss was estimated at .052 dB per connector. This value will be used later to estimate the antenna coupling losses.

The coupling between microstrip line and slotline will now be considered. As can be seen by examining the sketches in Figures 1.1 and 1.2 the energy is first coupled into a relatively narrow slotline which immediately opens up to the wider slotline needed to match to the high impedance of free space. Thus, the slotlines needed have been broken in two. One narrow line for coupling from microstrip and another wider slotline for coupling to free space.

By using a narrow slotline for coupling in, the coupling bandwidth will be wider, wide enough to present only negligible impact on the overall antenna bandwidth. In addition, the reduced radiation from this narrower slot permits one to fold it and take advantage of other feed geometrics which might be desired.

The coupling approach used was to extend the microstrip line across the slot and simulate a short to the other side of the slot by further extending the microstrip line 1/4 wavelength beyond the slotline edge. The open circuited 1/4 wavelength stub reflects an effective rf short at the edge of the slotline. The rf voltage that propagates on the microstrip line is thus impressed across the narrow slotline. Once the signal is transferred to the slotline, it is free to travel in both directions. To insure one-way propagation a short is placed across the slotline at a position 1/4 wavelength away from the microstrip-to-slotline transition. S. B. Cohn discusses this type transformation in "Slotline on a Dielectric Substrate", IEEE-MTT-17, October 1969.

Slotlines are generally employed with dielectric materials that are thicker than those used here and the diectric constant selected is usually higher. However, at some risk of over-extension of theory, the work of Mariani, et al., has been extrapolated to help design the narrow coupling slot. The graph shown in Figure 4.1 gives the impedance and wavelength expected as a function of the slotline width.

It is known for couplers such as required here that the physical geometry transforms the slotline impedance down to a lower value. Thus, a 70 ohm slot line will appear matched to a 50 ohm microstrip line when transformed according to the geometry described above. This is fortunate since tolerances will be unmanageable if as per Figure 4.1 the slot was required to be 1.5 mils for 50 ohms. Instead, a 70 ohm slotline requires a more relaxed slot width of approximately 6 mils and for that width the wavelength within the slotline is approximately 2.5 inches.

To examine the validity of the impedance and wavelength values a test substrate consisting of a long shorted slotline coupled to a microstrip line was tested. The slot width was measured to be near 7 mils and the line was well matched when a 80 ohm chip resistor was placed across the line. The wavelength measured was 2.46 inches neglecting end effects. Thus, from Figure 4.1, the wavelength data suggests that the line width was 5 mils while the impedance data suggests the line width was 10 mils. Thus, while the theory projected by Figure 4.1 didn't match the measured results perfectly, there was reasonable confirmation. Certainly enough to permit one to use the theory to obtain near optimum results.

A second experiment was undertaken to attempt to quantify the losses that one might expect from a slotline using the proposed coupling techniques. In this experiment two microstrip line-to-slotline couplers were placed a fixed slotline distance apart to measure the total insertion loss of the slotline, microstrip lines and transitions. Two such lines were fabricated, one with one-inch separation and one with two-inch separation. Figure 4.2 contains a photograph of both test fixtures. The objective of this experiment was to obtain a measure of the slotline insertion loss.

Figure 4.3 contains a plot of the insertion loss versus frequency for both test fixtures. It will be noted that even though the two lines are of different lengths, the insertion loss for both is nearly identical. The return loss for both fixtures is shown in Figure 4.4.

One explanation for this might be that the slot line loss is very small (not significant) and that all of the loss is associated with the two microstrip connectors, the two microstrip lines and the radiation losses primarily of the slot line.

It is reasonable to expect that the slot line copper losses might be quite small since the fields are not well confined by the substrate which is relatively thin and for which the dielectric constant is relatively low. Thus, the slot line currents spread out over a wide area of copper surface with the net result being low copper loss. Also, by the same argument one might expect relatively low dielectric losses for the slot line since the fields are only loosely confined to the diectric substrate. It should be pointed out, however, that this same lack of confinement can lead to radiation losses.

The microstrip line loss using 0.126 dB/inch has been calculated to be 0.155 dB for both input and output lines (includes the contribution of the open circuited 1/4 wavelength microstrip stub). The Tech-Wave coax-to-microstrip adaptors used have a loss of .035 dB/pair. The total loss thus accounted for is 0.19 dB leaving a balance of approximately 0.26 dB (5.8% of the power) believed to be lost in the slotline transmission process. Due to the above arguments it is thought that much of this loss may be due to radiation.

If, indeed, the 0.26 dB of loss is due to radiation from the slot line there is still the question of how significant it is with the actual four feed antenna where the total length of the narrow coupling slot is only 0.30". If the coupling slot radiates it will be orthogonal to the desired radiation and all such losses would be wasted. If it proves to be significant, the coupling slot could be aligned with the radiating slot where all such losses would contribute to the desired radiated signal. Or, the narrow slot could be overcoated with a dielectric to more fully confine the energy and reduce radiation.

During antenna range testing orthogonal radiation was measured as part of evaluating the antennas efficiency. The result is that the cross-polarization component was measured as 1% of the total radiated signal. This result confirms that at least part of the .26dB is due to radiation.

The open circuit 1/4 wavelength microstrip coupling stub, shown in Figures 1. and 1.2, is a square metalization block which was used in some early microstrip line-to-slotline coupling experiments but had to be discarded. The 1/4 wavelength block is slightly broader band than a simple extension of the 50 ohm microstrip line for 1/4 wavelength and was, therefore, initially proposed. However, tests revealed a difficulty in achieving repeatable results. Figure 4.5 illustrates the original discarded method and the revised method. The difficult was thought to be associated with the accuracy of registration of the microstrip open circuited 1/4 wavelength stub (block) with respect to the .006" wide slotline on the opposite side of the dielectric card. It was speculated that the square microstrip block might overlap a portion of the .006" wide coupling slotline changing its characteristics and therefore detuning the coupling network. To eliminate this possibility, the microstrip portion of the coupling network was changed by simply extending the 50 ohm line beyond the slotline by 1/4 wavelength. For this configuration a slight error in registration does not change the characteristics of the shorted 1/4 wavelength slotline stub.

4.4 ANTENNA DESIGN

The required antenna consists of a pair of 1/2 wavelength radiating slots fed on both ends and backed by a metalic cavity. The cavity serves two purposes, it restricts radiation to only one direction and, secondly, it couples the two slots together for coherent radiation in a common phase.

Figure 4.6 contains a plan view of three slotline radiator configurations together with the metalization pattern of the input microstrip line.

This illustrates a progression of designs that were fabricated before arriving at the final four-feed antenna. In general, the wider one makes the slot radiator, the broader the radiator bandwidth. The length of the radiating slot, of course, determines the frequency. Finally, the length of the narrow 1/4 wavelength shorted slotline stub achieves the required match with the 50 ohm input transmission line. All of these controlling parameters interact with each other to some degree, however, the preceeding general statements are accurate at least in a gross sense.

The energy propagating within the slot antenna radiates in both directions. The energy radiating within the cavity propagates through the cavity in the $TE_{1,0}$ mode (similar to) toward the opposite slot antenna. Similarly, the other slot antenna couples an equal magnitude signal into the cavity with the opposite polarity. These two waves interact to cancel (yielding a net zero E field) at the center of the cavity creating a standing wave pattern similar to that shown pictorially in Figure 4.7. The width of the cavity must be larger than 1/2 wavelength (above waveguide cutoff) in order to insure that the two radiating slots are tightly coupled. A small cavity dimension was selected to approximate the length of the radiating slot. The dimension used is 2.5 inches, whereas 1/2 wavelength at 2.45 GHz is 2.41 inches. The cavity was made 2.5 inches square with a depth of 0.3 inches. Additional depth would increase the cavity unloaded Q (increased volume-to-surface ratio) which would reduce the cavity losses slightly, but not appreciably compared to the remaining circuit losses associated with the antenna substrate.

If one were to shrink the distances between the radiating slots (to increase the packing density) the bandwidth will decrease. The reason for this is that the cavity loads the radiating slot with an inductive reactance which gets smaller as the slots are placed closer together. The antenna reactance slope versus frequency increases under these conditions which reduces the bandwidth.

Considerably more analysis and developmental testing is needed to optimize such an antenna for the SPS application especially considering the large number of variables available. The antenna arrived at, is however, a first level low budget cut at a compromise design suitable for range evaluation.

Figure 4.8 contains a photograph of the final antenna prior to attachment to the ground plane for antenna range tests. The article at the right in the photograph is a printed copy (on paper) of the antenna metalization pattern. Note that the bottom and top metalizations are connected together on all edges by using silver conducting epoxy (COMREX #584). This epoxy was also used to attach the microstrip transition adaptor blocks and the antenna cavity to the substrate as well as attaching the finished antenna to the 18-inch square ground plane employed.

Figure 4.9 contains a photograph of the microstrip antenna epoxied into the center of the ground plane. The ground plane consists of an 18-inch square sheet of copper clad epoxy-fiberglass cloth circuit board. The holes located at each connector were needed to permit room for the right angle coaxial elbows. Conducting adhesive copper foil tape was used to cover these holes prior to antenna range testing.

Figure 4.10 contains a photograph of the rear view of the antenna when the power amplifiers were in place. Note at the bottom of the photograph there are four straight coaxial cables. These sections of cable are used to replace the amplifiers when the antenna is evaluated without the amplifiers. The lengths of these cables have been adjusted to make each electrically identical to within a 1° window ($\pm$ 1/2°). At 2.45 GHz one degree of electrical length in the .141" diameter semi-rigid cable is 9.4 mils.

The feed network (Ser. #002) together with the four output cables (the four that connect between the feed network and the amplifiers or the straight sections of cable) was measured to be equal phase within a 1° window ($\pm$ 1/2°). With the straight sections of cables installed

including the elbow adaptors which mate with the antenna, the insertion phase error window was again measured to be 1° (± 1/2°). This latter result was achieved by specifying the location where the straight section was installed and then color coding them so they could be easily reinstalled.

Thus, for purposes of antenna evaluation, the antenna is being fed by a feed network that exhibits nearly perfect balance. The phase is measured to be within a 1° window and the amplitude similarly is within a 0.02 dB window. When the amplifiers are installed the error increases to an estimated window of 3° in phase and 0.2 dB in amplitude.

The estimated losses anticipated for the input signal after it is delivered by the feed network to the antenna is as follows:

1/2" microstrip line + 1/4 wavelength opencircuited stub loss:	.058 dB
Solitron 2975 -6300 coax to microstrip adaptor loss:	.052 dB
Total Loss Estimate:	.11 dB

An insertion loss of 0.11 dB corresponds to a loss of approximately 2.5%. In a final SPS version of the antenna, the Solitron connector would not be required which would delete half of the above loss. Further, as discussed earlier, at least part of the microstrip loss may be avoided by using ceramic substrates. Thus, only a portion of the above loss (less than half) should actually be held against the antenna being tested. Those losses that remain represent losses that would be found with any solid state appropriate antenna concept and are not characteristic specifically of the power-combining feature.

The input return loss of the four-way power-combining antenna imbedded within the 18 inch square ground plane prior to delivery to the antenna range for tests, is shown in Figure 4.11. The return loss at 2.45 GHz is greater than 30 dB and the bandwidth at the 15 dB down points is approximately 100 MHz (4%). The relatively large ground plane diameter of 18 inches was selected to yield a smooth antenna gain response. A large ground plane will minimize antenna gain undulations versus angle which are caused by ground plane edge radiation.

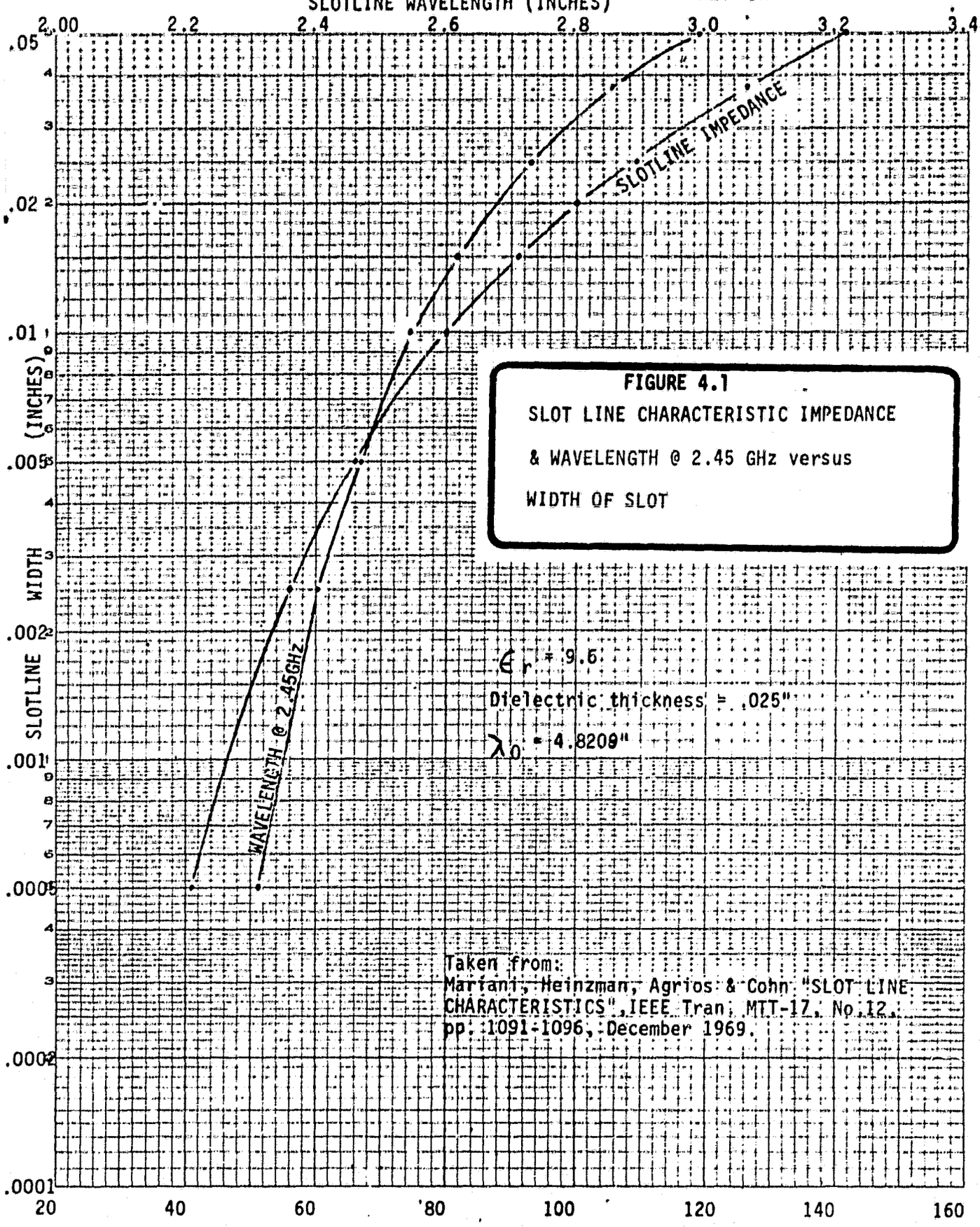

FIGURE 4.1

SLOT LINE CHARACTERISTIC IMPEDANCE & WAVELENGTH @ 2.45 GHz versus WIDTH OF SLOT

Taken from:
Mariani, Heinzman, Agrios & Cohn "SLOT LINE CHARACTERISTICS", IEEE Tran, MTT-17, No.12, pp. 1091-1096, December 1969.

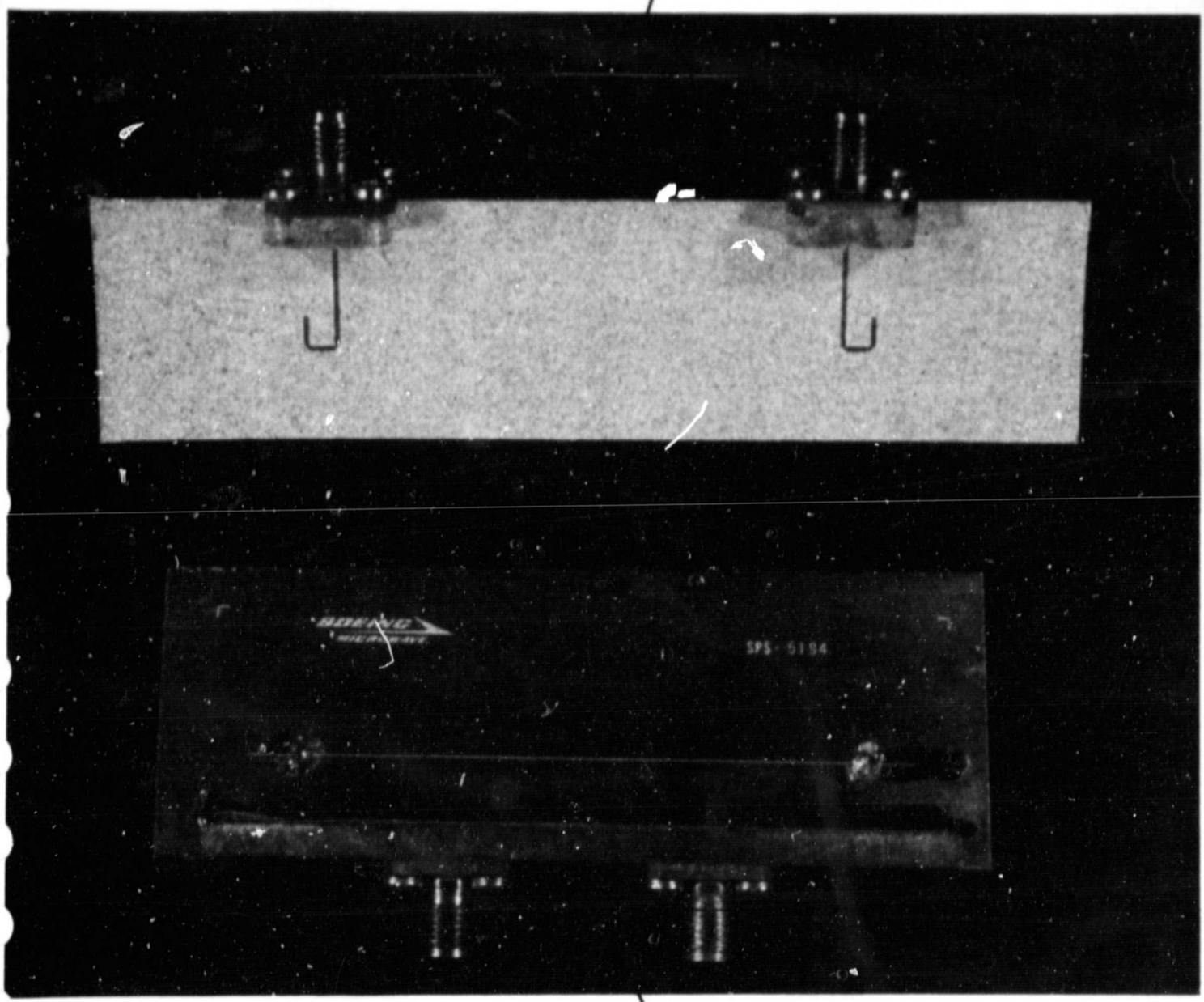

Spacing between microstrip to slotline couplers: No. 1: 1.0" No. 2: 2.0"

FIGURE 4.2 MICROSTRIP-SLOTLINE-MICROSTRIP LINE TEST FIXTURES

FIGURE 4.3

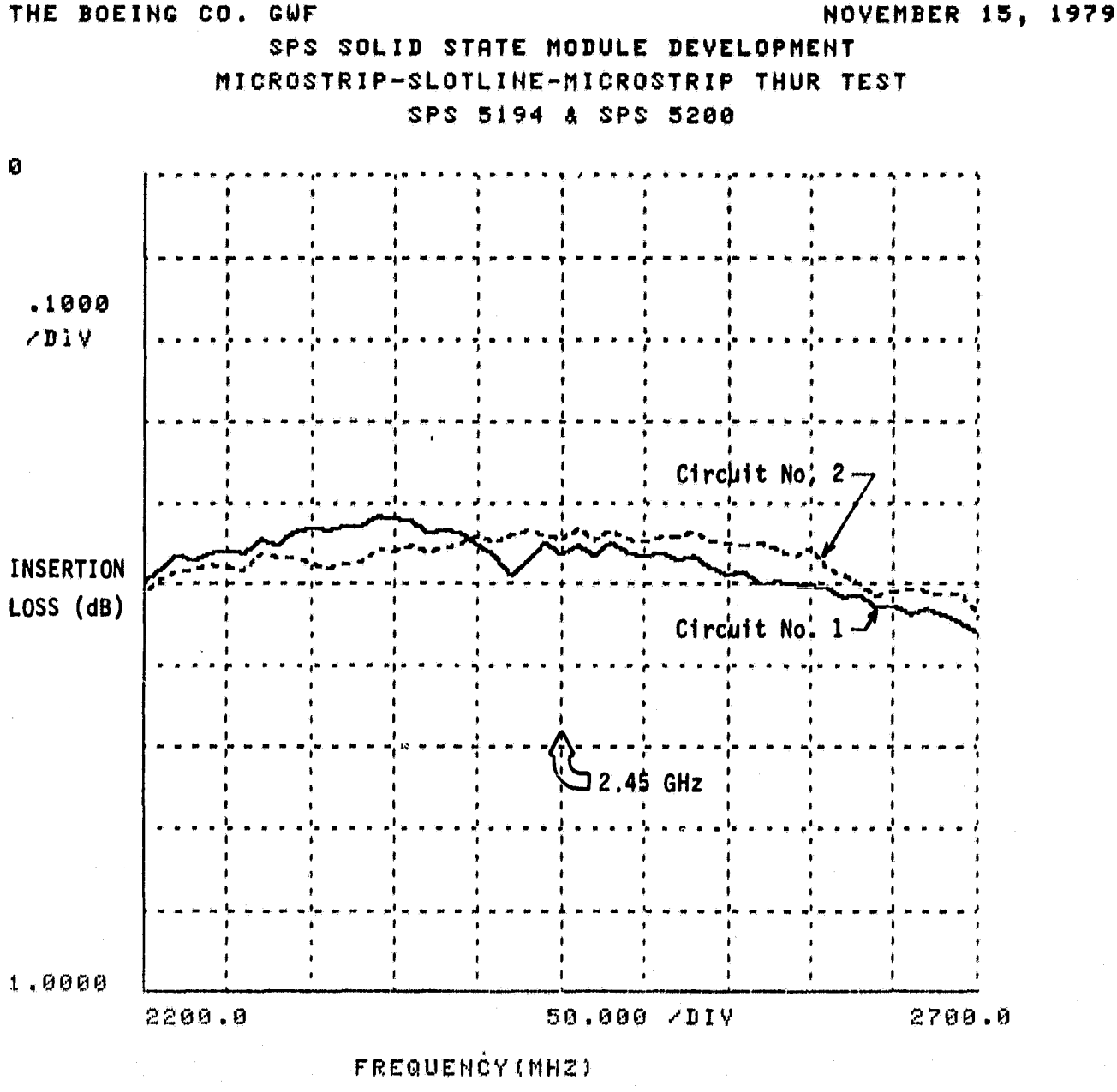
THE BOEING CO. GWF
NOVEMBER 15, 1979
SPS SOLID STATE MODULE DEVELOPMENT
MICROSTRIP-SLOTLINE-MICROSTRIP THUR TEST
SPS 5194 & SPS 5200
0
.1000
/DIV
INSERTION
LOSS (dB)
1.0000
Circuit No. 2
Circuit No. 1
2.45 GHz
2200.0
50.000 /DIV
2700.0
FREQUENCY(MHZ)

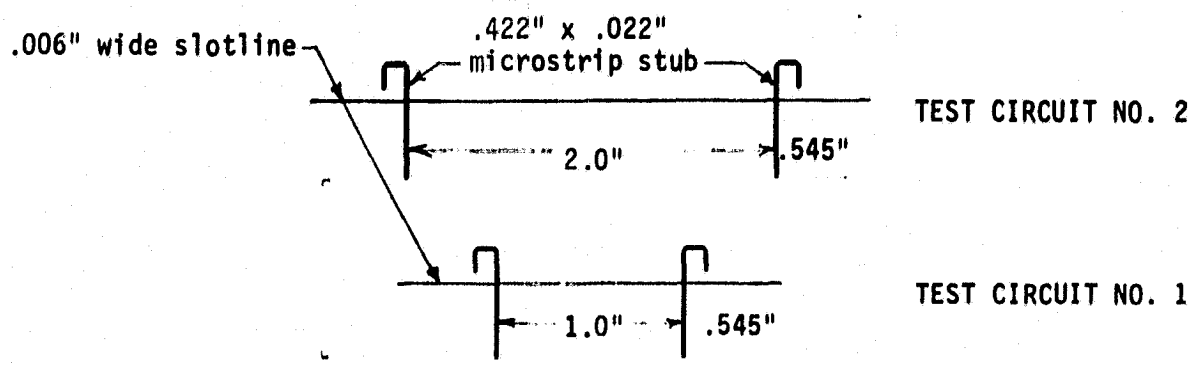
.006" wide slotline
.422" x .022"
microstrip stub
2.0"
.545"
TEST CIRCUIT NO. 2
1.0"
.545"
TEST CIRCUIT NO. 1

FIGURE 4.4

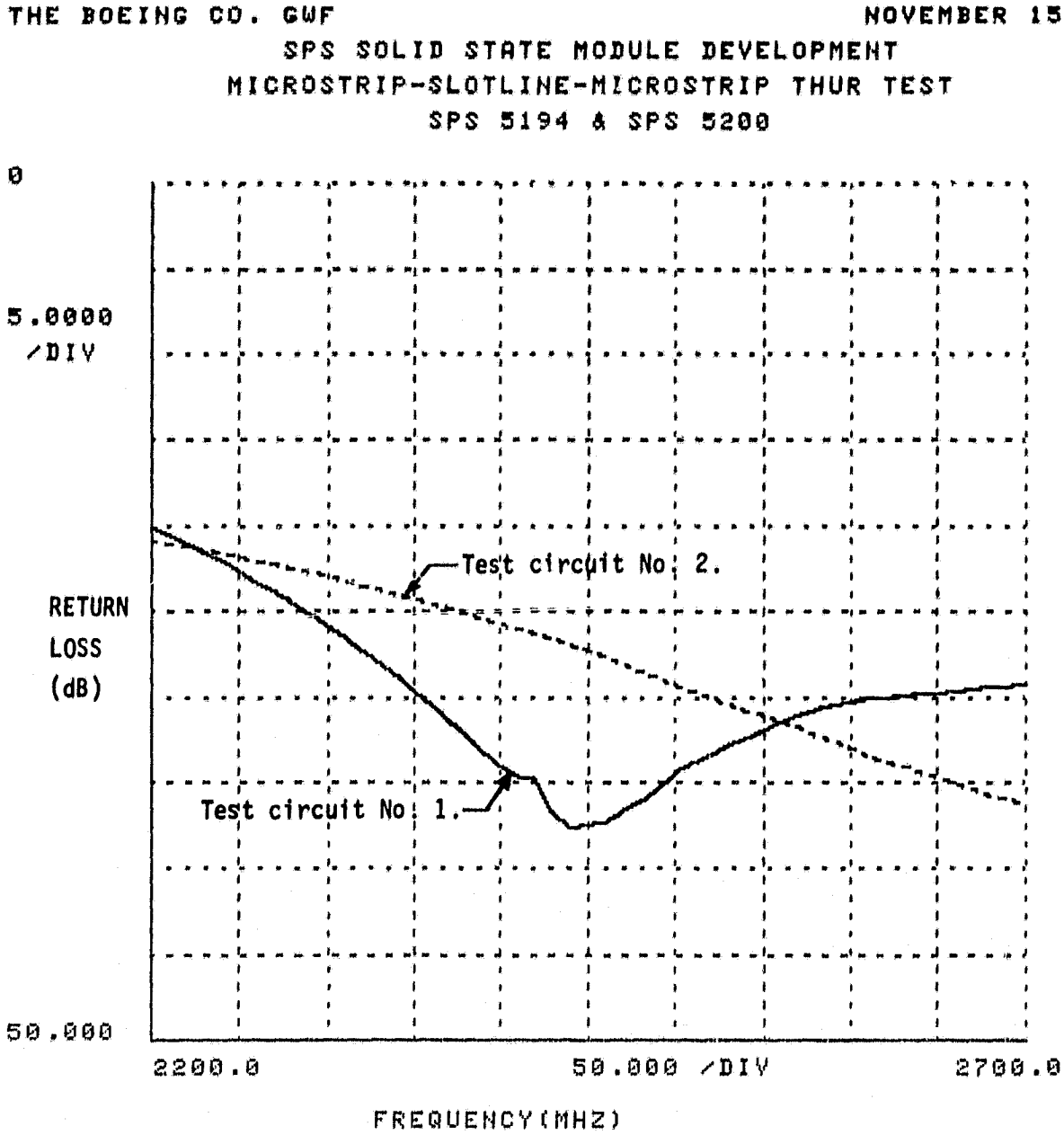
THE BOEING CO. GWF
NOVEMBER 15, 1979
SPS SOLID STATE MODULE DEVELOPMENT
MICROSTRIP-SLOTLINE-MICROSTRIP THUR TEST
SPS 5194 & SPS 5200
0
5.0000
/DIV
RETURN
LOSS
(dB)
50.000
Test circuit No. 2.
Test circuit No. 1.
2200.0
50.000 /DIV
2700.0
FREQUENCY(MHZ)

FIGURE 4.5

SLOTLINE ANTENNA COUPLING METALIZATION PATTERNS

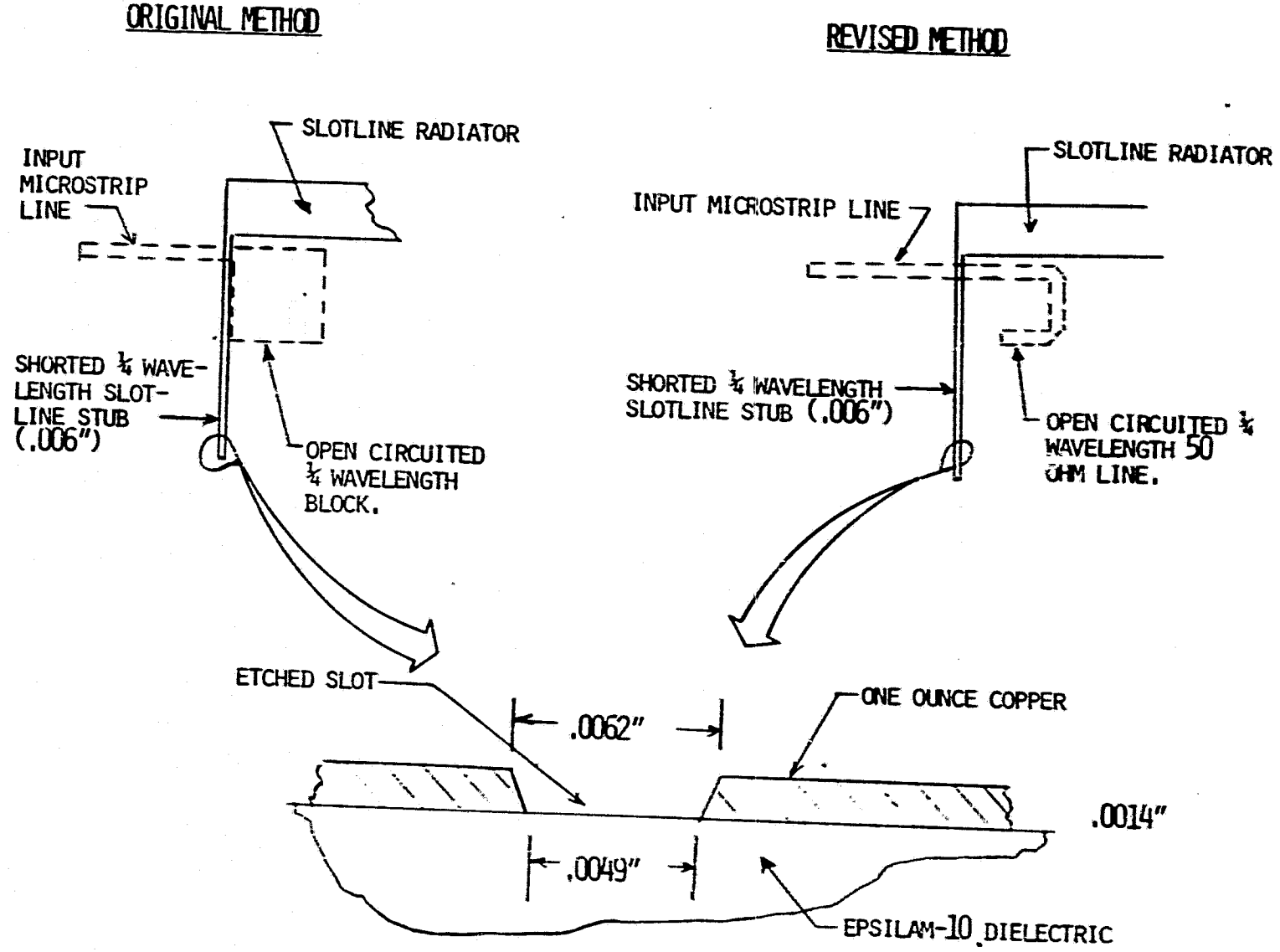

BOEING TECHNOLOGY MICROWAVE CIRCUITS

FIGURE 4.6

EVOLUTION OF A SLOTLINE ANTENNA

(METALIZATION PATTERN)

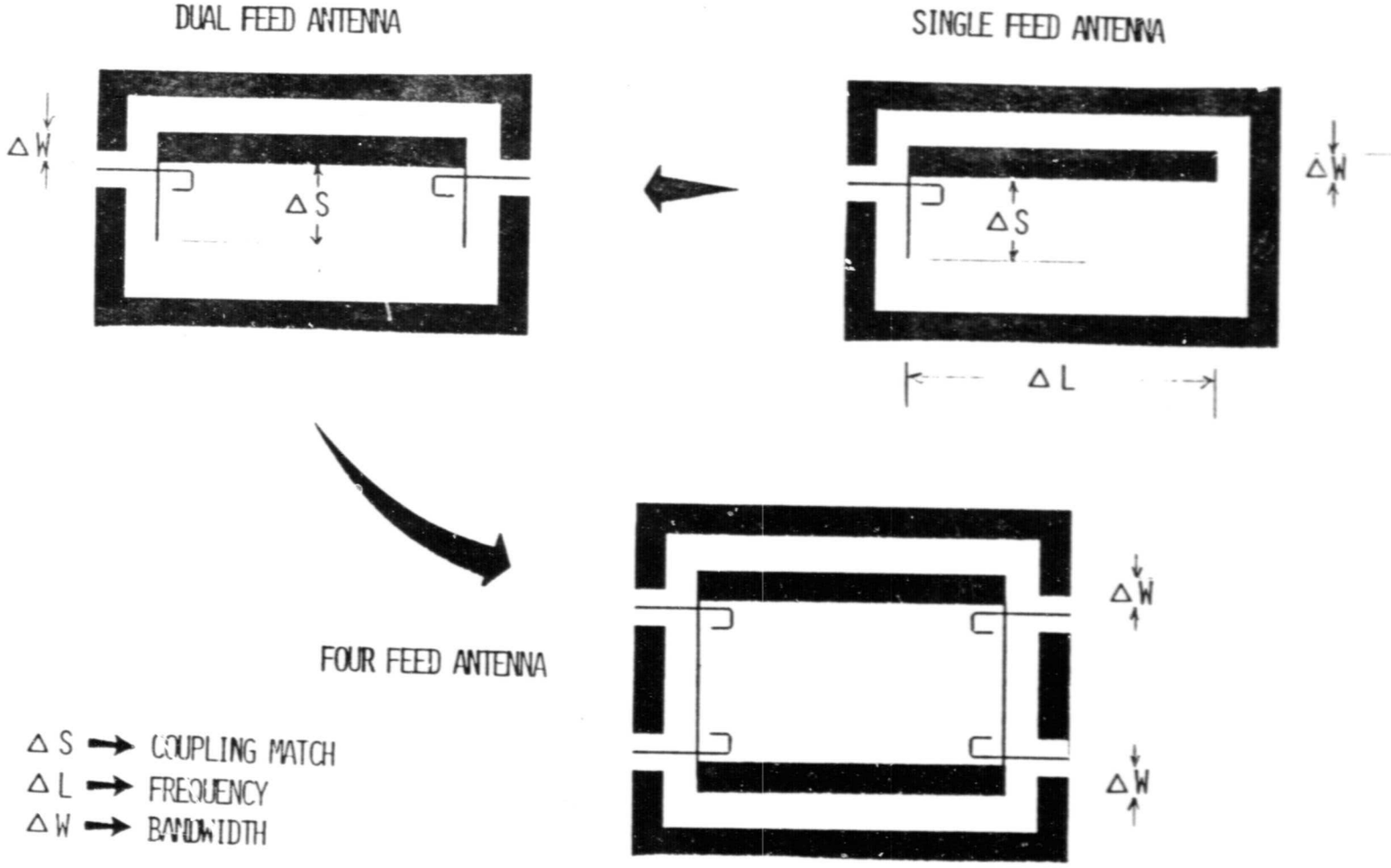

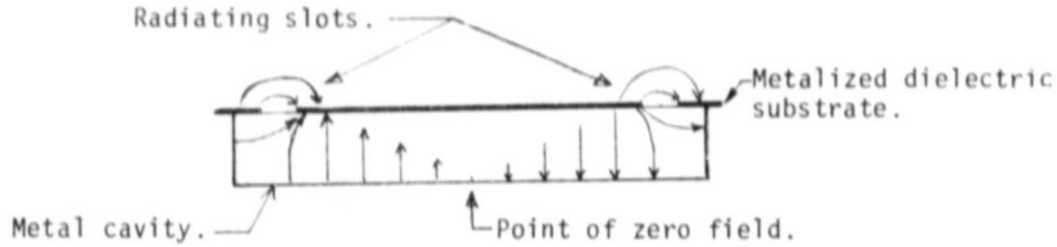

CAVITY "E" FIELD PROFILE

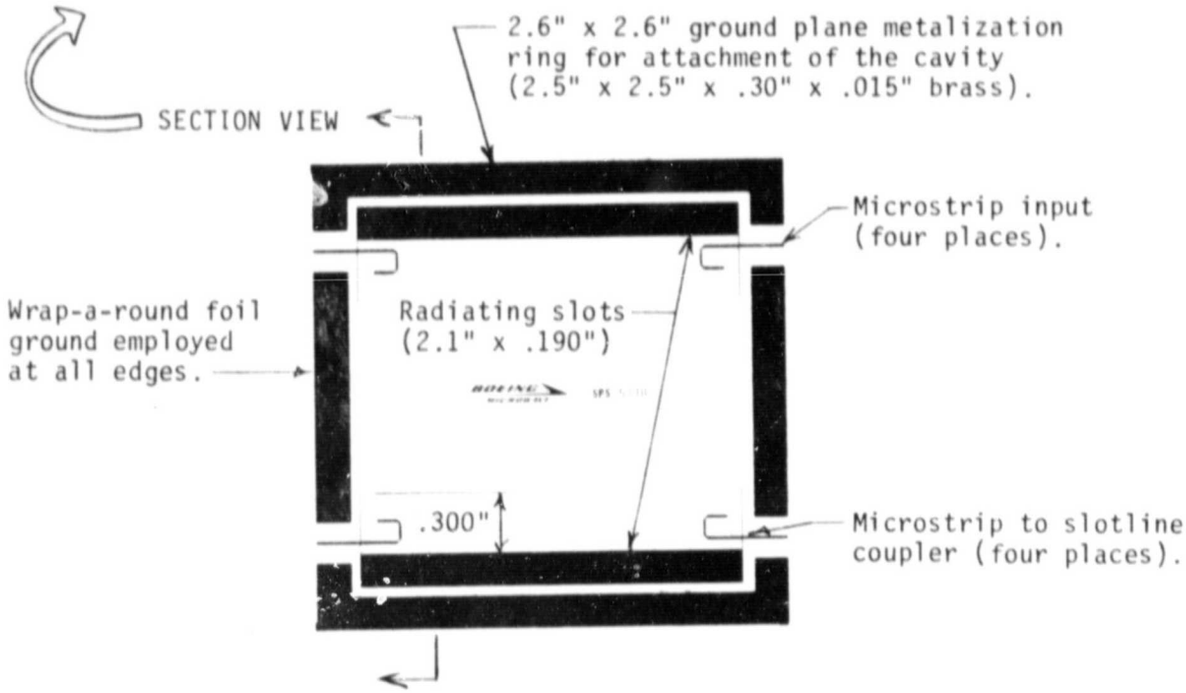

FIGURE 4.7 COPPER METALIZATION PATTERN FOR FOUR FEED MICROSTRIP ANTENNA
(Two patterns superimposed)

FIGURE 4.8 FOUR-WAY POWER COMBINING MICROSTRIP / SLOTLINE ANTENNA

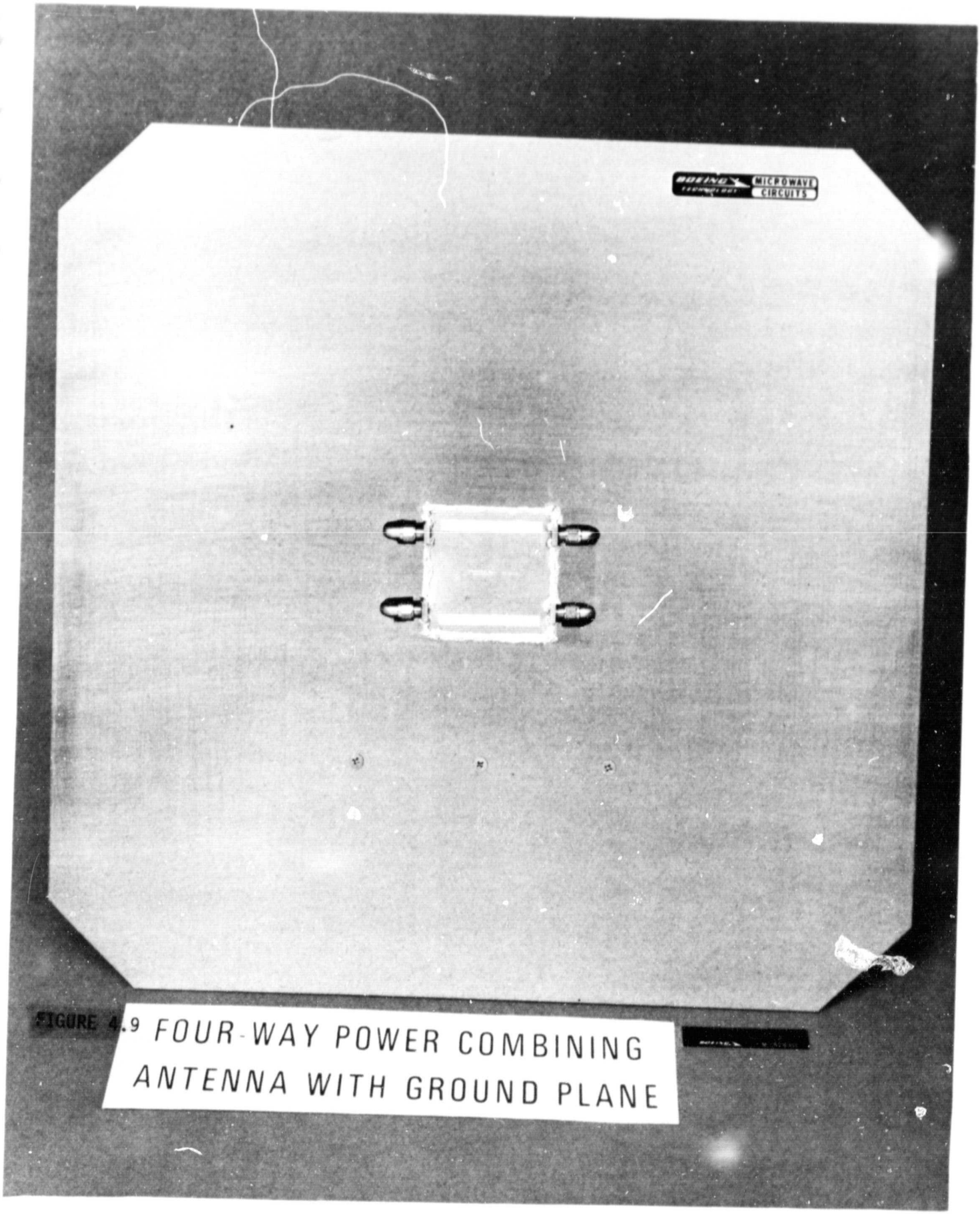

FIGURE 4.9 FOUR-WAY POWER COMBINING ANTENNA WITH GROUND PLANE

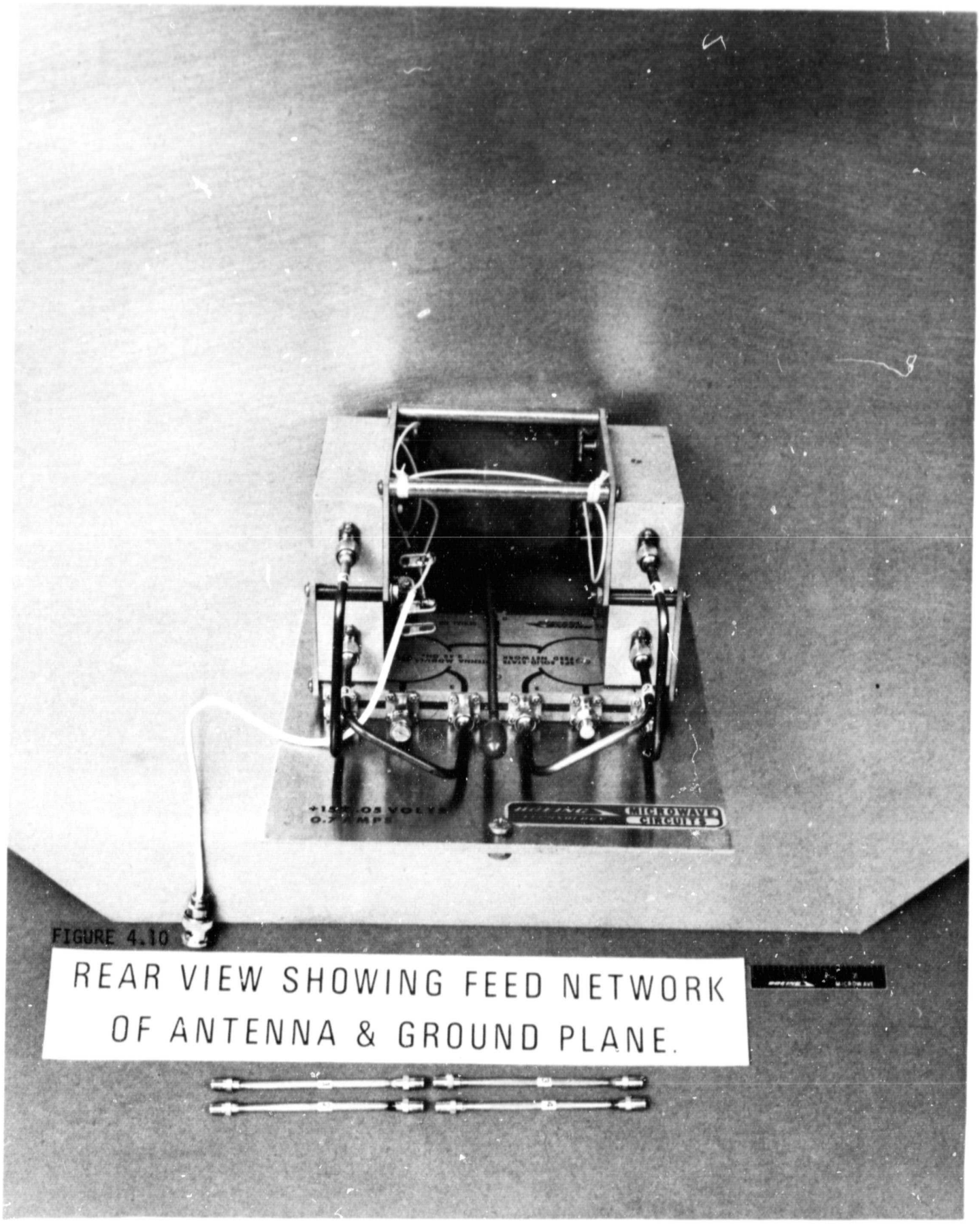

FIGURE 4.10

REAR VIEW SHOWING FEED NETWORK OF ANTENNA & GROUND PLANE.

FIGURE 4.11

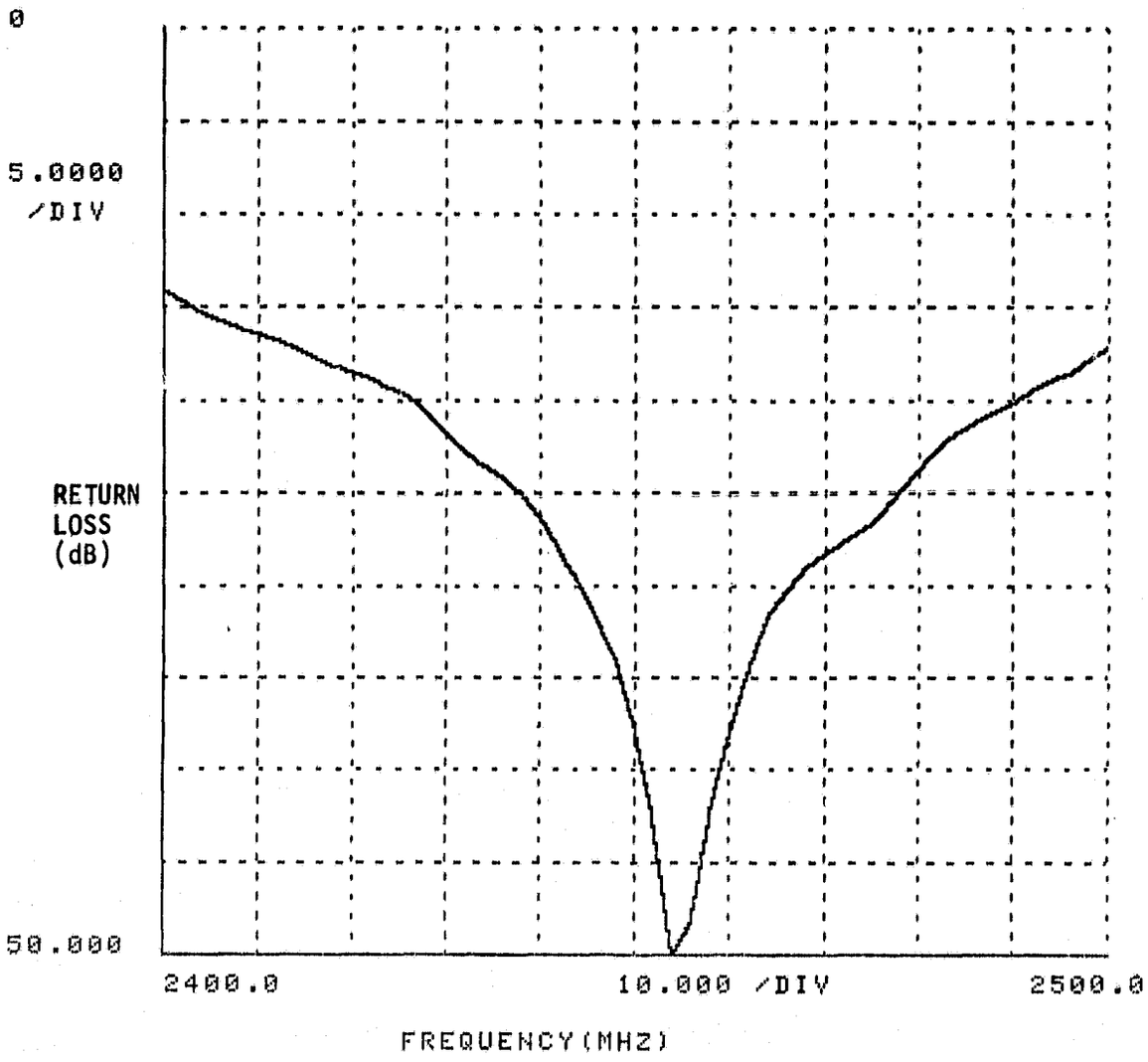
THE BOEING CO. GWF
FEBRUARY 1, 1980
SPS SOLID STATE MODULE DEVELOPMENT
FOUR FEED ANTENNA & FEED NETWORK # 002
WITH GROUND PLANE
0
5.0000
/DIV
RETURN
LOSS
(dB)
50.000
2400.0
10.000 /DIV
2500.0
FREQUENCY(MHZ)

5.0 ANTENNA RANGE EVALUATION

The primary purpose of the antenna range tests is to: (1) Determine the efficiency of the four-way power-combining microstrip antenna when fed by a nearly perfect feed system and (2) Evaluate the ability of the antenna to efficiently combine the energy from four solid state amplifiers putting out a total power of 1/2 watt. This has been accomplished and, in summary, it has been found that: (1) The basic antenna exhibits a measured efficiency of approximately 88.3% (.54 dB of loss) and (2) The antenna behaved nearly identical with the amplifiers installed as it did without the amplifiers. The cross-polarized component of radiation was measured to be approximately 1% (.05 dB of loss). The connector and microstrip line loss is believed to represent approximately 2.5% (.11 dB of loss). The balance of the measured loss, 8.2% (.37 dB loss), is attributable to antenna copper and dielectric losses (which are more difficult to quantity) and to measurement uncertainty (which is believed to be $\pm$ 10% ($\pm$ .46 dB)). In other words, the loss is accountable except for a value of 8.2% which is smaller than the measurement uncertainty of $\pm$ 10%.

5.1 ANTENNA RANGE PATTERNS

Figures 5.1 through 5.8 contain the antenna range patterns through the two principal planes of the antenna with and without amplifiers co-polarized and cross-polarized. The patterns were taken on an indoor antenna range that is associated with the Boeing Terminal Guidance Laboratory. It will be observed that the patterns are reasonably well behaved and that the maximum sidelobes are approximately 20 dB down.

The origin of the slow undulation with a periodicity of approximately 36° is not believed to be due to ground plane edge effect which one might first suspect. Edge effects from an 18" ground plane if of significance would have a periodicity of more like 7°. The 36° period appears to have been made by scattering from points separated by on the order of 3". The culprit in this case is believed to be the conducting epoxy used to attach the antenna to the ground plane (the antenna substrate is 2.6" x 2.6").

The conductivity of the epoxy is probably less than copper at 2.45 GHz and this ring of change in conductivity surrounding the antenna is believed to cause the observed undulations in the pattern in all planes.

The 36° undulations were not observed with the earliest antenna fabricated on the program. This earlier antenna, however, was put together with solder which tends to confirm the validity of the conducting epoxy's roll in the pattern undulations.

The last four patterns (Figures 5.5 through 5.8) are for the same antenna with the four amplifiers attached. The combined output and power under test was 1/2 watt. It will be observed that the antenna patterns are nearly identical to those taken without the amplifiers. Components 20 dB and more down appear to be carbon copies of those without the amplifiers. This is as would be expected if each radiating slot is being excited in phase and with equal amplitude signals. Thus, the pattern similarity suggests that each amplifier is connected and performing. However, one should keep in mind that since the two radiating slots are tightly coupled (via the antenna cavity) the patterns should be reasonably consistent, even if a partial amplifier failure is present.

Two cross-polarization patterns are shown for each of the two conditions with and without amplifiers in Figures 5.3 and 5-4 and 5.7 and 5.8. In all of these the peaks of the cross-polarization components are approximaterly 30 dB below the peak copolarized level.

5.2 ANTENNA GAIN

The power combining antenna gain was measured via the three antenna gain measurement method using the Developmental Center Antenna Range 3 and a value of 7.67 dB was obtained. A review of the records caused us to question the data and with a bit of good fortune we were able to re-measure

the antenna in conjunction with a Boeing Primary Standards Laboratory exercise involving standard gain horn calibrations. The measured gain came to 7.85 dB ± .20 dB. The other two antennas used in the test were two Scientific Atlanta Model SA12-1.7 standard gain horns of 15.58 dB. The specifics of the three antenna gain method together with an error analysis is given in the Appendix (Section 7).

For future work the mechanism of achieving an accurate antenna gain measurement will be eased somewhat due to the recent calibration of three standard gain horns by the Boeing Primary Standards Laboratory. To assist S.P.S. the frequency of 2.45 GHz was added as one of the specific frequencies certified.

The antenna system block diagram, shown in Figure 5.9, illustrates the lossy elements that are connected ahead of the antenna. The loss of these elements should not be held against the antenna under test since they would not be there immediately preceding the antenna at high power in the SPS application. Thus, the actual measured antenna gain was 7.38 and a correction of 0.47 dB was added to achieve the corrected value of 7.85 dB.

5.3 ANTENNA DIRECTIVITY

The antenna directivity D is defined as the ratio of the peak radiated power to the average isotropic radiated power (average power radiated over the unit sphere). To arrive at the average isotropic radiated power, one must measure and total up the radiated power over the spherical surface in both polarizations with the unknown antenna at its center and average that value by dividing by the number of measurements. Typically at Boeing a 2° x 2° cell is employed which requires 16,200 measurements. The error associated with the directivity measurement described below is ± .41 dB. A more detailed discussion on directivity and errors is contained in the Appendix (Section 7).

The directivity measured for the power-combining antenna is 8.39 dB. The cross-polarization component is measured and recorded separately from copolarization component after which they are added together to compute the isotropic radiated level. The contribution to the isotropic level made by the cross-polarization components was measured to be slightly under 1% (20 dB down).

A look at the cross-polarization E and H plane patterns, Figures 5.3 and 5.4, would suggest that the average level of cross-polarization is greater than 25 dB below the isotropic level. (Note that the isotropic level is approximately -10 dB on Figures 5.1 through 5.4. This value is found by subtracting the directivity from the peak copolarization value of -2-8.39 = 10.39 dB.) A cross-polarization level of 25 dB to 30 dB down would change the measured 1% downward to .3% to .1%, respectively.

Further study of the directivity raw data printout (the radiation distribution plot), however, reveals that the 1% level indeed is probably correct. If a cross-polarization pattern cut was taken at approximately $\pm$ 45° to either the E or H plane, the principal contributors to the cross-polarization would have shown up. In each of the four quadrants, at approximately $\pm$ 90° (in the plane of the radiator), values as high as -18.8 dB down from the copolarized peak were observed. These cross-polarization components appear at an azimuth angle of $\pm$ 90° and above or below horizon at $\pm$ 70° with the antenna positioned vertically polarized.

The source of these four lobes is not known, however, one would first suspect radiation from the four narrow coupling slotlines which are arranged orthogonal to the radiating slot. A consideration of the fields present within these slots reveals that they should contribute zero energy to an E or H plane cut. That, in fact, their principle contribution if available should appear approximately where the cross-polarization was found to peak.

Thus, if these components are to be reduced below the current 1% level, it is believed that the narrow feedline slots will have to receive additional attention. Obvious steps that could be considered are: (1) Overcoat the slots with a dielectric cover (an idea which may be necessary to eliminate shorts within the narrow slots due to contaminants), (2) Employ a dielectric substrate with a relative dielectric constant that is higher than the 10 employed here, or (3) Rearrange the narrow slots to lie in line with the principle radiating slots.

A shortcut (approximate) estimate of what the antenna directivity (loss free gain) should be would be to calculate the gain expected from two sinusoidally excited dipoles spaced a distance equal to the mean of the slot spacings. If this were done it would look like the following:

Dipole (Full)		2.14
Ground Plane		3.01
Array Factor		3.01
Mutual Coupling		-.36
Directivity	=	7.80 dB

Thus, we see that the directivity measured (8.39 dB) is 0.59 dB greater than that calculated via this simple means. It should be observed that the assumption of sinusoidal excitation is not quite correct for the twin slot antenna under consideration. The fields at the edge of the slot are not zero but are well developed which would produce a more uniform aperture distribution which would raise the measured directivity slightly. Also, the slots are wide while the assumption was for two narrow dipoles spaced a distance equal to the center-to-center spacing of the slots. Thus, the experimental antenna may have a slightly larger effective area which would bias the measured directivity upward. Thus, the measured directivity is relatively close to what might be expected. When the power-combining antenna

was driven by the four amplifiers at the 1/2 watt level the measured directivity was 8.46 dB compared to 8.39 dB measured without amplifiers. The slight increase of 0.07 dB is believed to be related to repeatability errors since a pattern improvement would be required to yield a higher directivity which isn't very likely. The narrow difference simply says that the amplifier combining process is being performed properly and that the measurement equipment repeats nicely.

5.4 ANTENNA EFFICIENCY

The efficiency of the Power Combining antenna is computed by forming the ratio of the measured gain (G) to the measured directivity (D), efficiency = G/D. Thus

$$\eta = \frac{G}{D} = G_{dB} - D_{dB}$$
$$= 7.85 - 8.39$$
$$= -0.54 \text{ dB}$$
$$= 88.3\%$$

and approximately 11.7% of the power is lost. The 3 sigma uncertainty of this result has been estimated to be $\pm$ .455 dB or $\pm$ 10%. Thus, the true value of efficiency ranges between 78% and 98%. 1% of the 11.7% loss can be accounted for in the cross-polarized radiation. The Solitron coax-to-microstrip connector loss and the substrate microstrip line loss is estimated to be 0.11 dB, which represents another 2.5% of the loss (most of this can be avoided if a ceramic substrate is employed). This leaves a balance of approximately 8.2% attributable to the antenna copper and dielectric loss and to measurement uncertainty. In dB terms, the 8.2% is a loss of 0.37 dB which might well be accounted for primarily as dielectric loss within each of the slots as dielectric loss. Also, some loss can probably be attributed to the conducting epoxy since the imprint of the epoxy loss appears to have impacted the antenna pattern.

5.5 AMPLIFIER COMBINING

A comparison test was performed on the indoor Terminal Guidance Laboratory Antenna Range to determine the antenna gain change when the power amplifiers were added. The expected gain increase is just the power gain of the amplifiers which were previously measured to be 8.2 ± .3 dB (each of the amplifiers were amplitude and phase matched to within ± 0.1 dB and ± 1°).

The range test yielded an antenna combining gain of 8.3 dB ± .15 dB which is 0.1 dB higher than recorded for the amplifiers alone. RSSing these two independent uncertainties yields ± .33 dB. The net result is that since the added gain is equal to what was expected to within ± .33 dB that no combining loss was observed. Also, under these idealized conditions the 1/2 watt of amplified rf power appears to have been perfectly combined (subject to an uncertainty of ± .33 dB) within the radiating element.

The insertion loss that the 1/2 watt signal incurs by combining within the antenna is identical to that incurred when the amplifiers were deleted. Another way of viewing the results is that the output of all four amplifiers were summed without the added loss of conventional circuit type power combiners. The total antenna loss is comparable to what one would incur with any selected solid-state antenna approach except the dual role of power-combining is also achieved.

The measurement uncertainty for the above described test could have been reduced by approximately 1/2 by observing more precautions when bench-testing the amplifiers. A shortage of time, however, precluded our re-running the test.

Figure 5.10 contains a block diagram of the amplifier combining range test setup and a plot of the recorded results versus frequency. The top line represents the reference insertion loss of the link. The bottom line is the link insertion loss when the amplifiers were installed along with a 9.8 dB $\pm$ .15 dB attenuator. It will be noted that the attenuator exceeded the gain of the amplifiers at 2.45 GHz by an amount equal to 1.5 dB. Thus, the measured gain is 9.8 - 1.5 or 8.3 dB. Note that the two lines come even closer together at higher frequencies (the gain increases) which is not surprising since the amplifiers gain peaked at a frequency above 2.45 GHz.

5.6 ANTENNA EFFICIENCY WITH AMPLIFIERS

To obtain a measure of the power combining antenna efficiency with the amplifiers installed an extended definition of directivity needs to be made. The measured antenna directivity with the amplifiers installed was 8.46 dB $\pm$ .41 dB which is nearly identical with that measured without the amplifiers. Let us now add to that number the amplifiers gain as measured on the test bench which was 8.2 dB $\pm$ .3 dB. This new number, 16.66 dB $\pm$ .51 dB is the peak gain expected for the antenna if it were loss-free and lost none of its power in cross-polarization. Thus, 16.66 dB is the new equivalent directivity (D_e) when the amplifiers are installed.

In the preceding section, when the amplifiers are added to the antenna, a gain component of 8.3 dB $\pm$ .15 dB is observed. We know from the three antenna test that the antenna gain without the amplifiers is 7.85 dB $\pm$ .20 dB. Therefore, the measured antenna gain with the amplifiers installed is 16.15 dB $\pm$ .25 dB.

The efficiency with the power amplifiers added this becomes:

$$\eta = \frac{G}{D_e} = G_{(dB)} - D_e \text{ (dB)}$$

$$= 16.15 - 16.66$$

$$= -.51 \text{ dB}$$

$$= 88.9\%$$

This is 0.6% larger than the efficiency measured without the amplifiers. The uncertainty associated with this efficiency, however, has been increased by the added uncertainty associated with establishing the amplifiers gain which was $\pm$ 0.30 dB and the uncertainty associated with measuring the added gain when the amplifiers were installed with the antenna of $\pm$ .15 dB. The uncertainty estimate obtained by RSS-ing in these two new added uncertainties brings the efficiency 3 sigma value to $\pm$ .566 dB or $\pm$ 12%. This is up from the previous 10% uncertainty obtained for the antenna without amplifiers. Thus, the efficiency of the antenna with amplifiers differs from the efficiency of the antenna without amplifiers by a number (0.6%) that is less than the increase in measurement uncertainty associated with the second measurement. The conclusion is that the efficiency of the antenna with the amplifiers is the same as that exhibited by the antenna without the amplifiers.

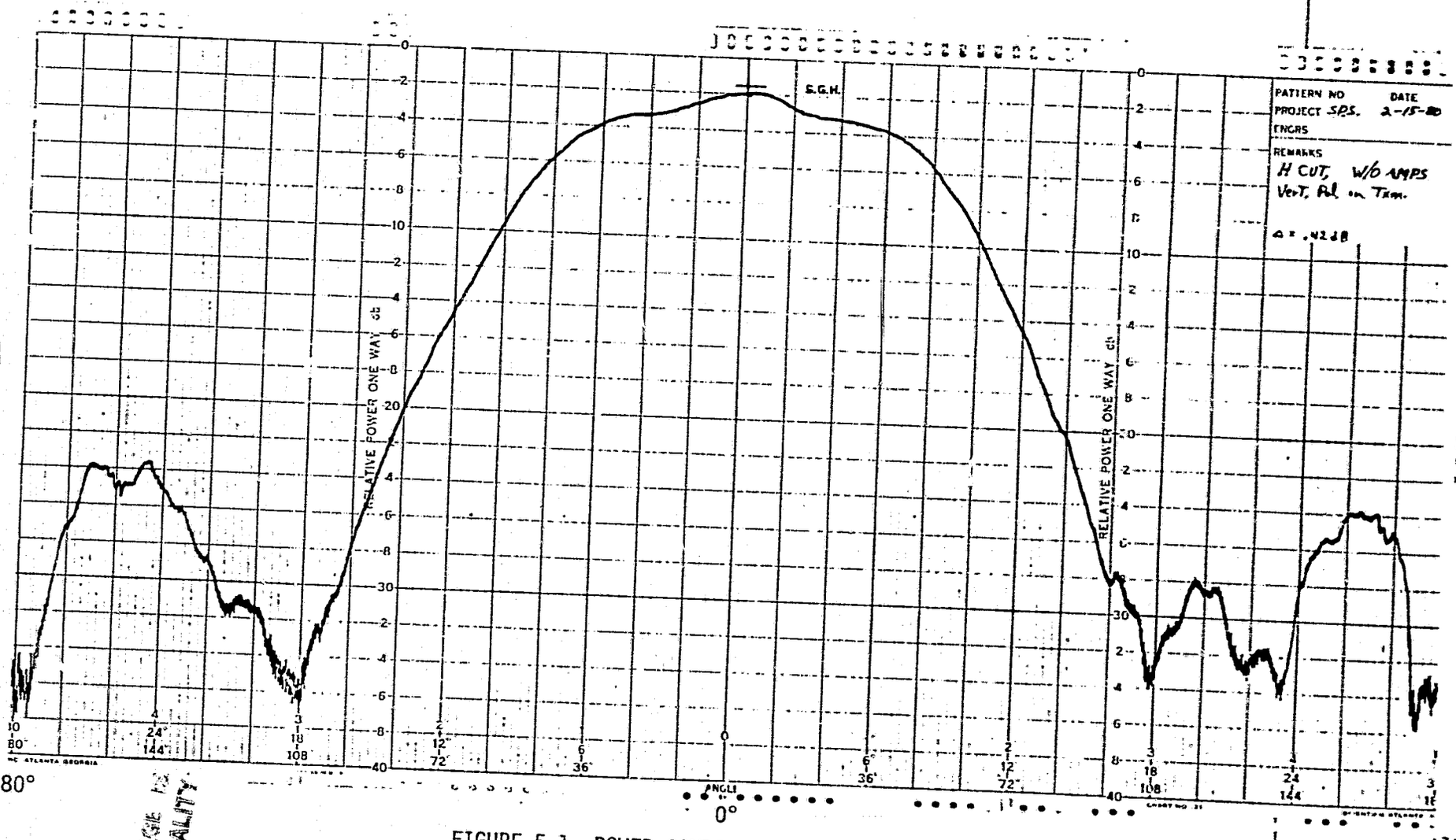

FIGURE 5.1 POWER COMBINING ANTENNA PATTERN
(H CUT COPOLARIZED)

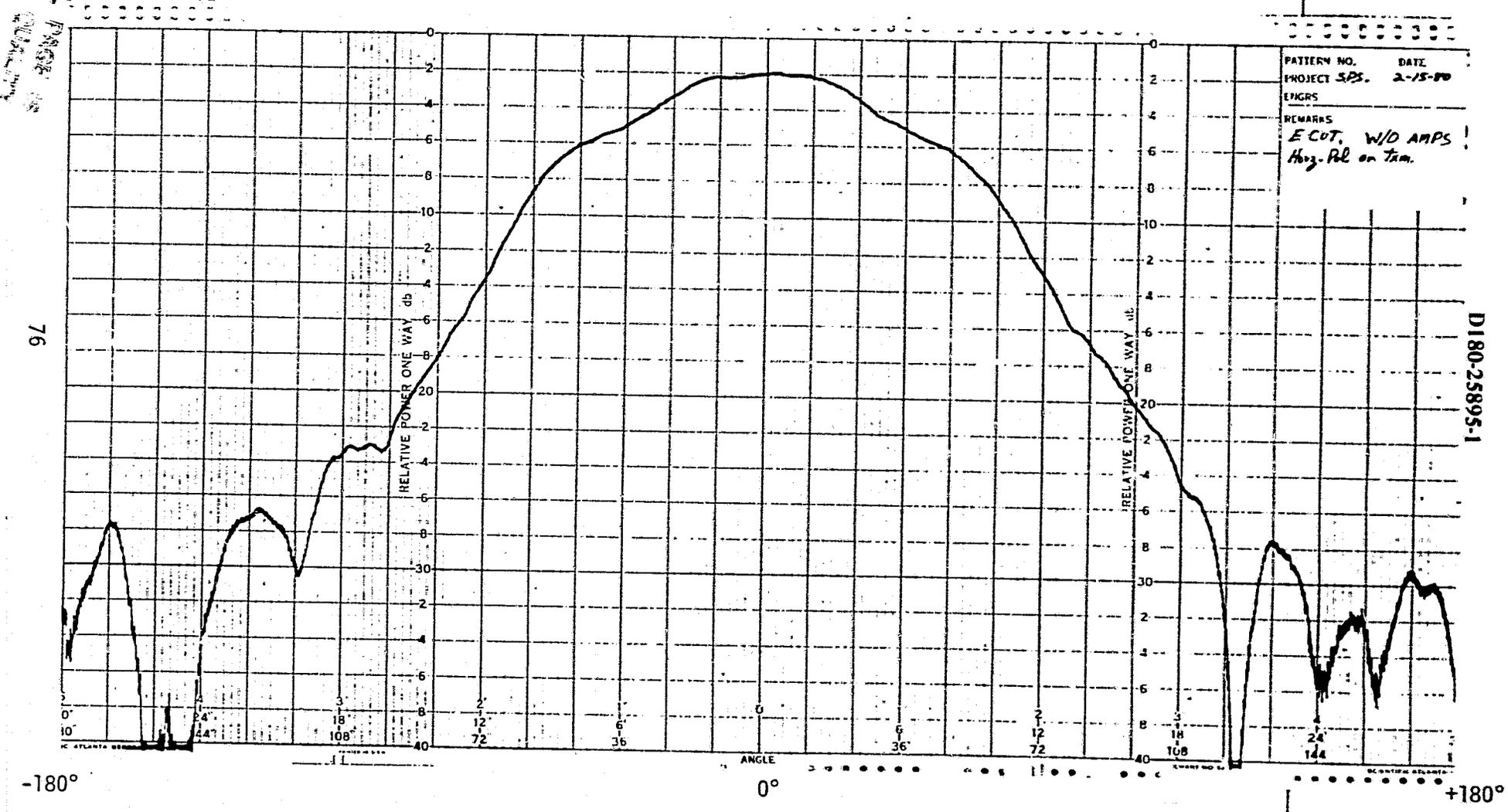

FIGURE 5.2 POWER-COMBINING ANTENNA
(E CUT COPOLARIZED)

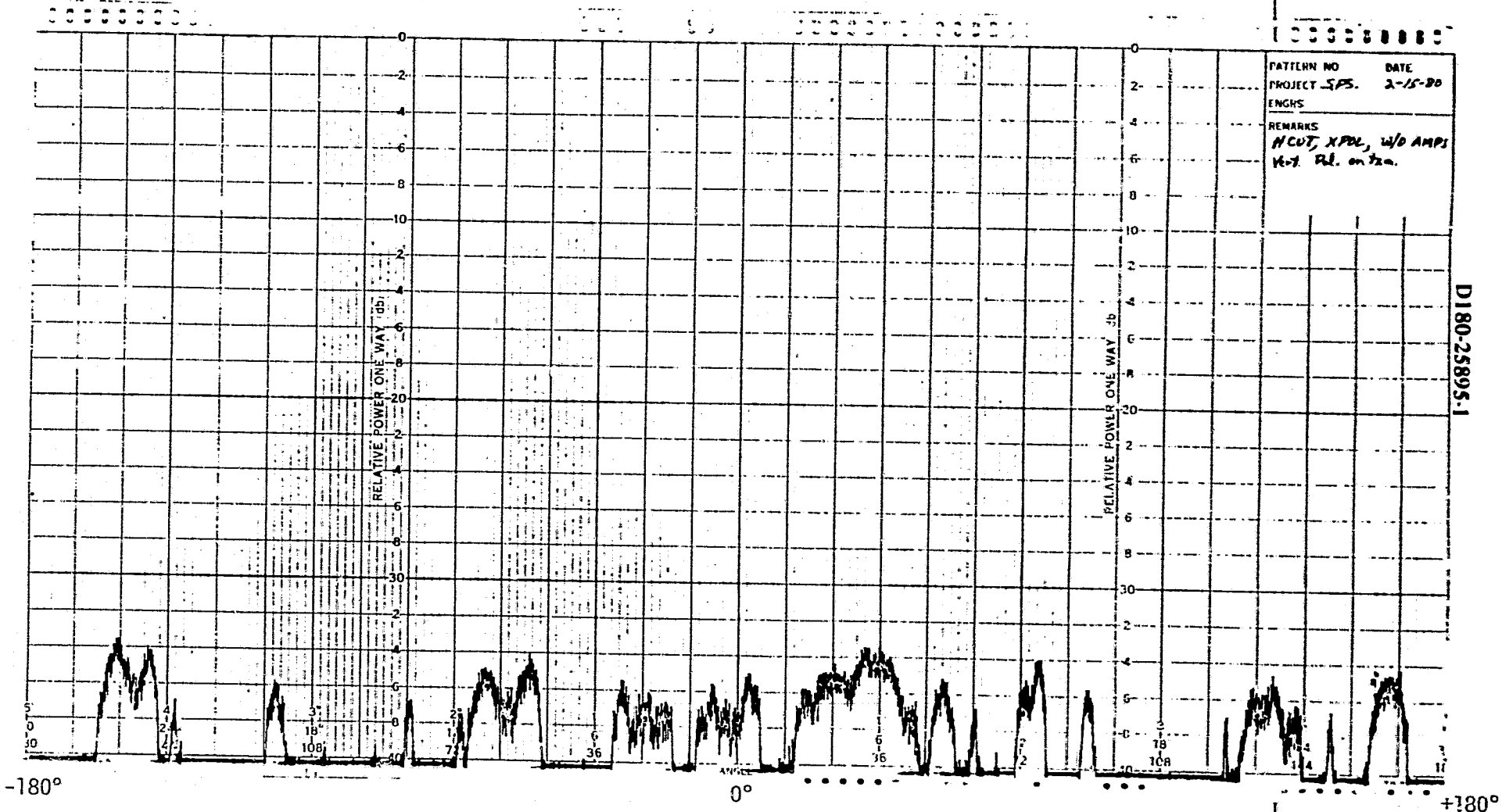

D180-25895-1

FIGURE 5.3 POWER-COMBINING ANTENNA
(H CUT, CROSS-POLARIZED)

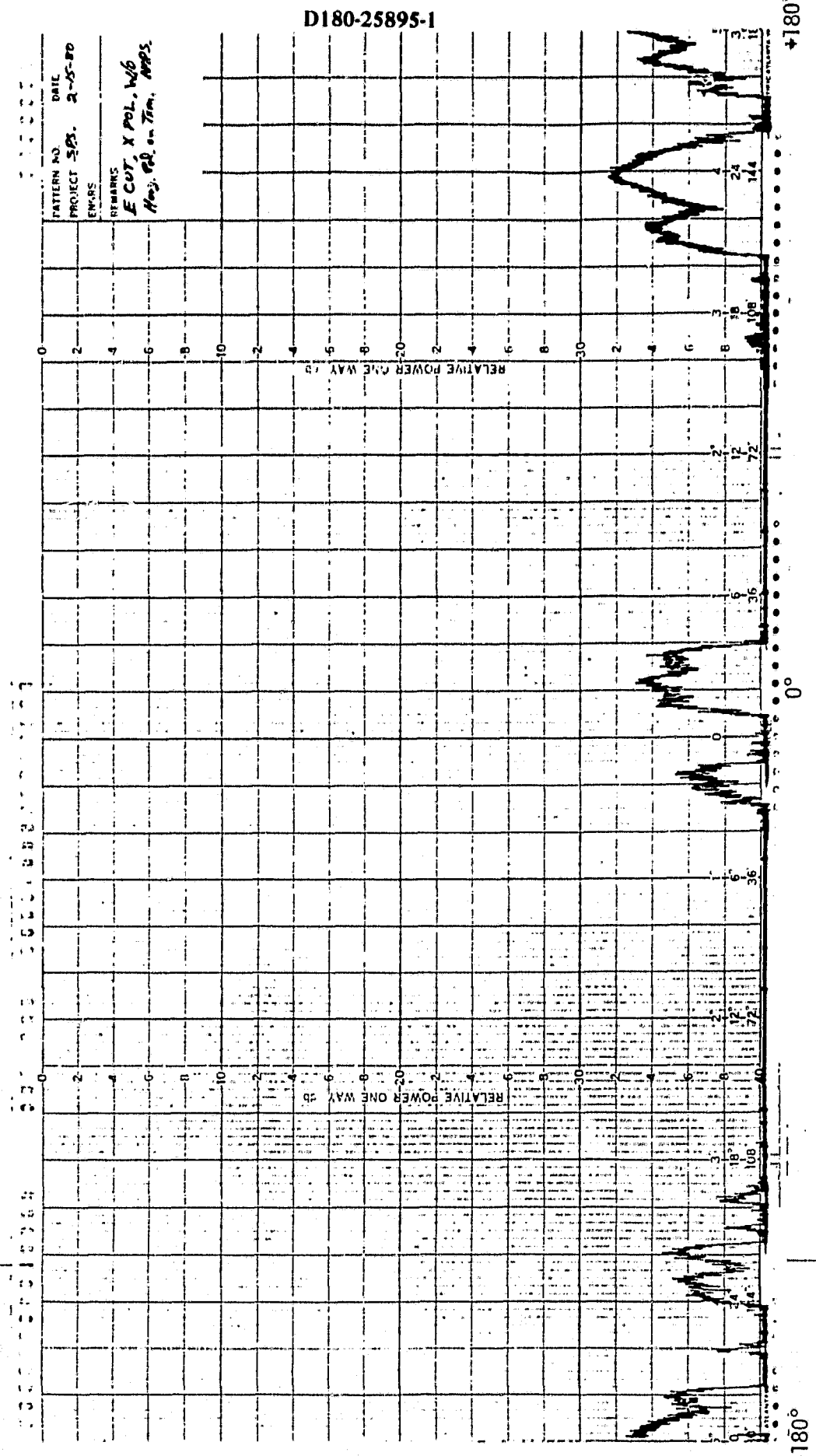

FIGURE 5.4 POWER-COMBINING ANTENNA PATTERN
(E CUT CROSS-POLARIZED)

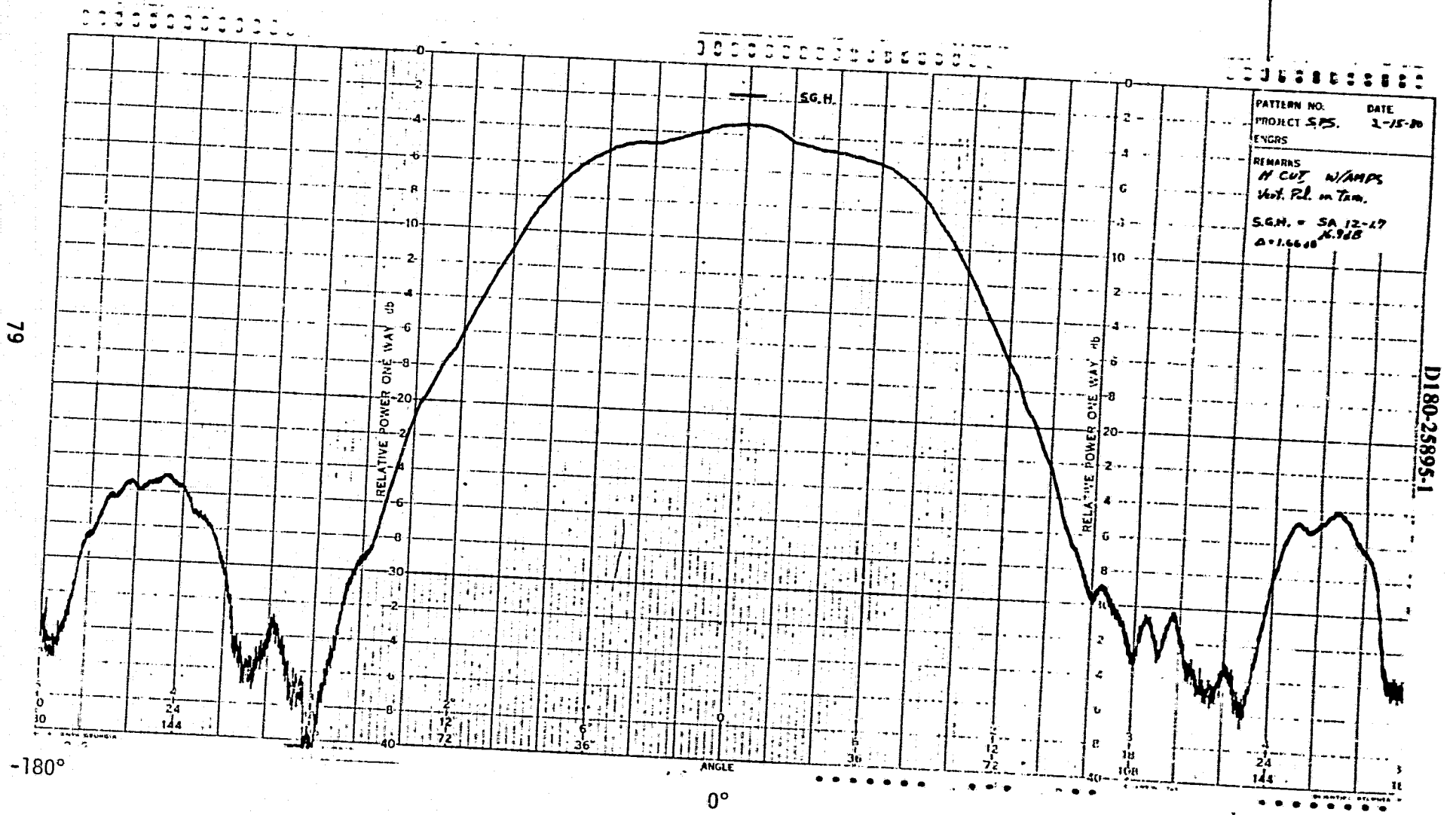

D180-25895-1

79

FIGURE 5.5 PATTERN OF POWER-COMBINING ANTENNA WITH AMPLIFIERS
(H CUT COPOLARIZED)

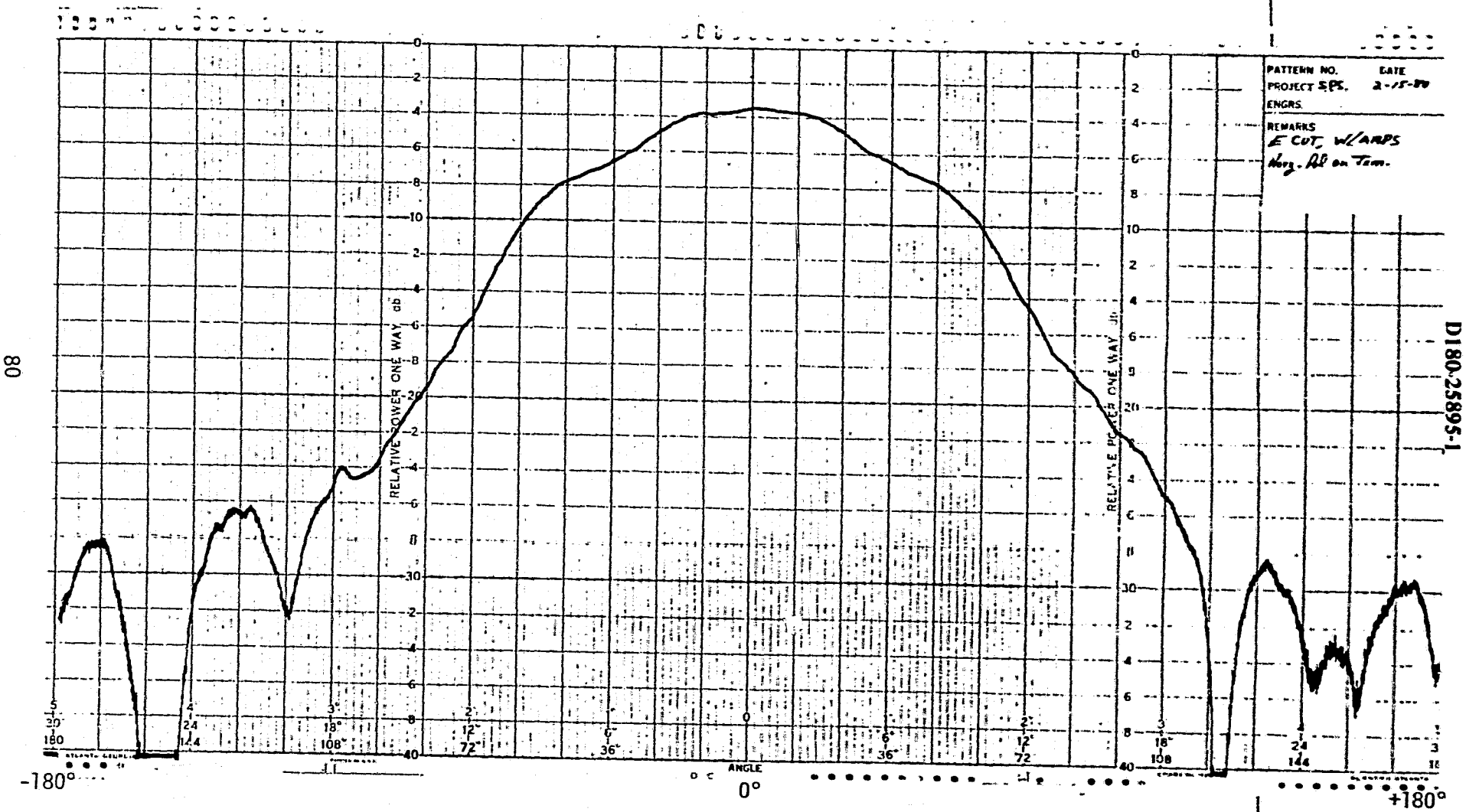

D180-25895-1

80

FIGURE 5.6 PATTERN OF POWER-COMBINING ANTENNA WITH AMPLIFIERS
(E CUT COPOLARIZED)

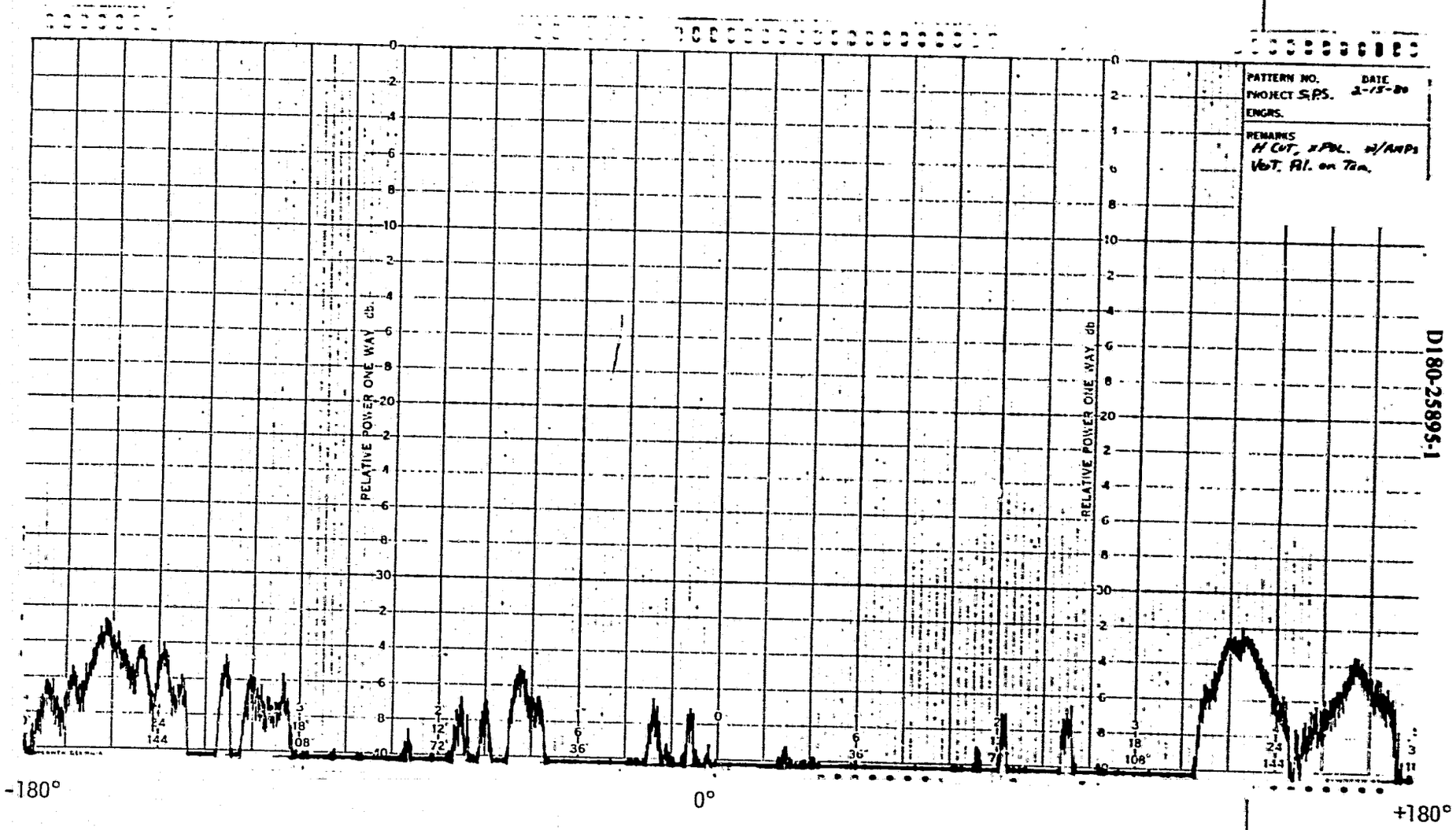

FIGURE 5.7 PATTERN OF POWER-COMBINING ANTENNA WITH AMPLIFIERS
(H CUT CROSS-POLARIZED)

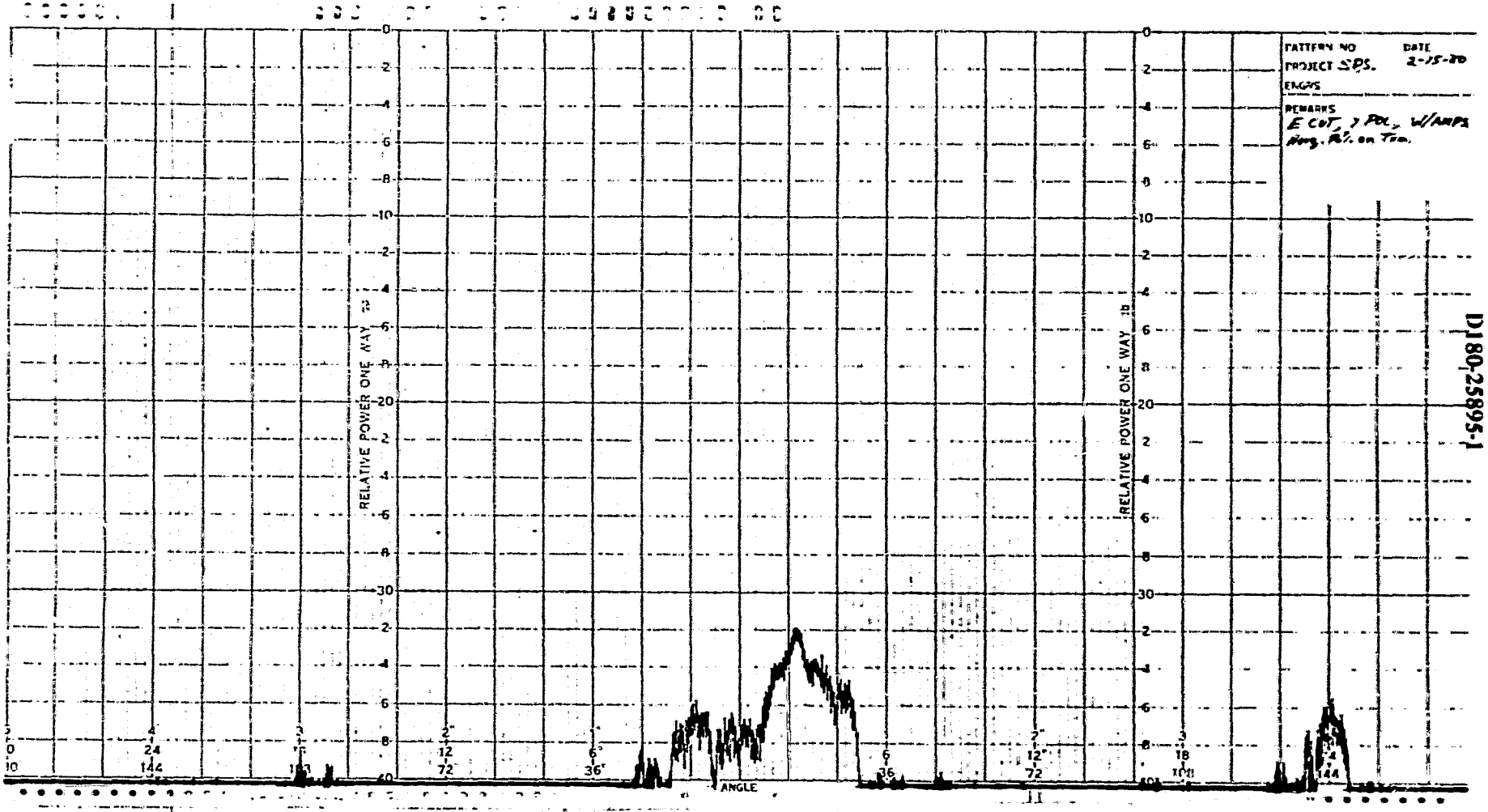

D180-25895-1

FIGURE 5.8 PATTERN OF POWER-COMBINING ANTENNA WITH AMPLIFIERS
(E CUT CROSS-POLARIZED)

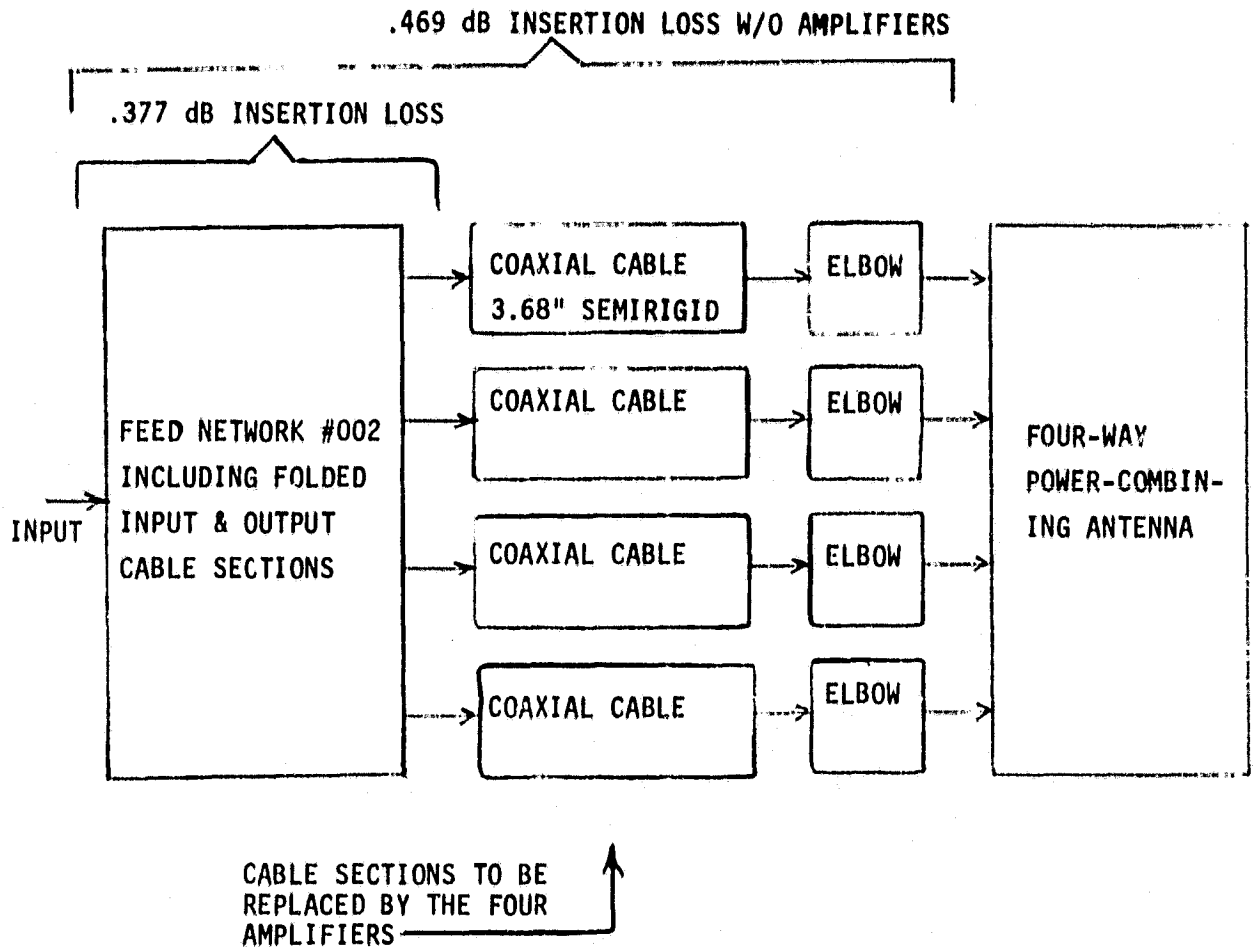

NOTE: 1. Amplifier gain = 8.2 dB @ +21.2 dBm (132mw) output each.

2. Total input drive required with four amplifiers = +19.4 dBm (87.2mw).

FIGURE 5.9 ANTENNA SYSTEM BLOCK DIAGRAM

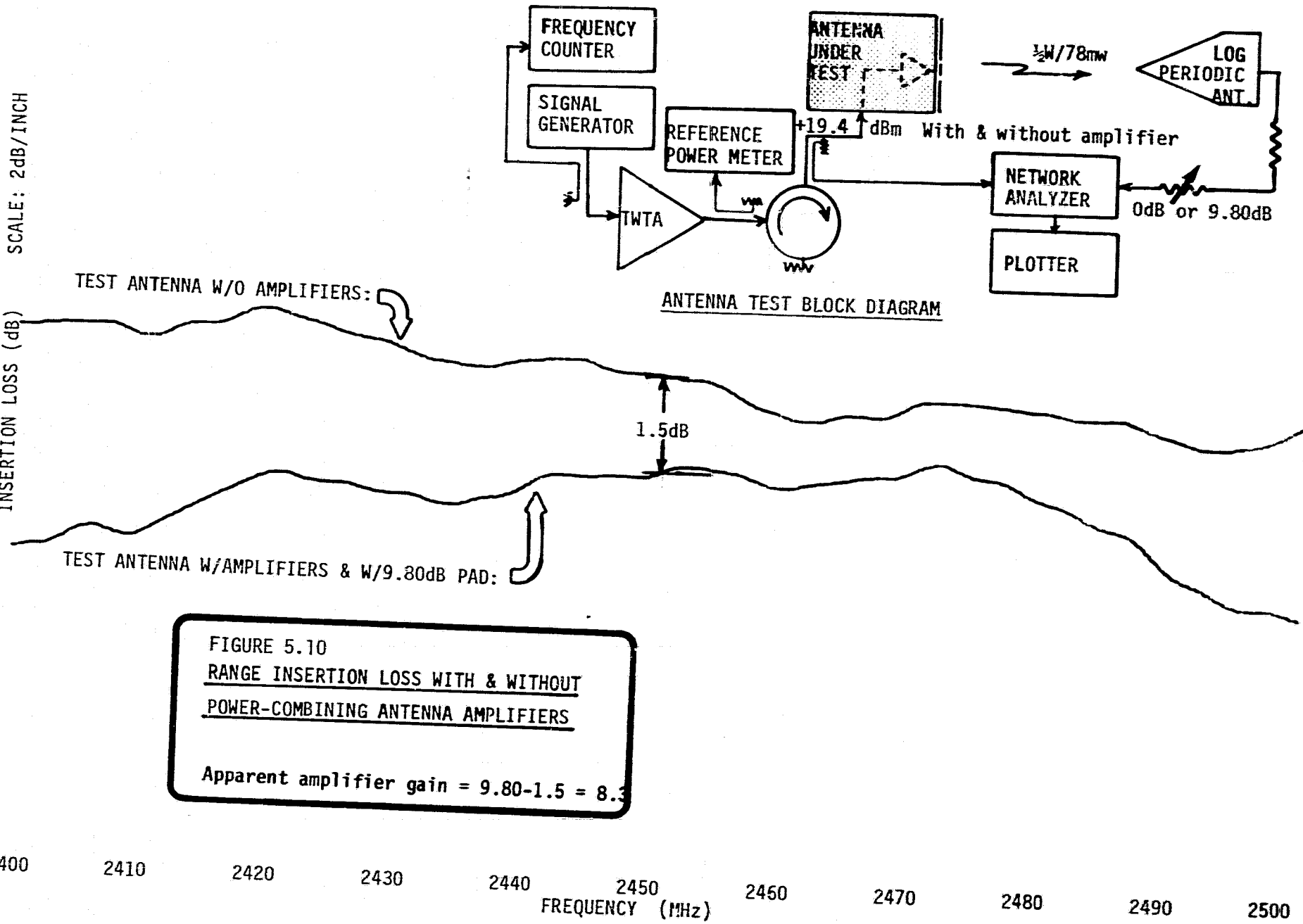

FIGURE 5.10
RANGE INSERTION LOSS WITH & WITHOUT POWER-COMBINING ANTENNA AMPLIFIERS

Apparent amplifier gain = 9.80-1.5 = 8.3

6.0 CONCLUSIONS AND RECOMMENDATIONS

A summary of the measured results for the four-way power combining antenna is as follows:

1. The antenna measured efficiency (G/D) is 88.3% $\pm$ 10%.
2. The radiated cross-polarized energy represents 1% of the antenna's loss.
3. 2.5% of the antenna loss results from microstrip loss. Much of this could be reduced by avoiding the relatively lossy dielectric Epsilam-10.
4. The remaining 8.2% (.37 dB) of loss is attributable to dielectric and copper loss and to measurement uncertainty. A substantial portion of this is believed to be associated with the Epsilam-10 dielectric loss and to a lesser degree the losses in conducting silver epoxy used to assemble the antenna. The losses associated with the power combining process are insignificant, as further confirmed by gain and pattern tests with the addition of four active amplifiers.
5. When the four amplifiers yielding a combined output power of 1/2 watt were added to the antenna the gain of the antenna (7.85 dB) increased by the gain of the added amplifiers within measurement uncertainty. Thus, the amplifier output power was summed perfectly in the antenna beam without any measurable added loss over that obtained without the amplifiers.
6. The solid-state antenna system demonstrated under the contract is substantially as originally proposed. For a first level refinement effort, a significant amount of information has been collected, the antenna seems to perform with and without the amplifiers as expected and the work provides a very useful base of information from which to continue the solid-state SPS development.

Obviously, the limited investigation provided under the contract was inadequate to do all the investigative things that one would like to do. It is thus appropriate, at this juncture, to attempt to list those investigative areas where future research should be focused. The recommendations are as follows:

1. Incorporation of realistic power levels of 1 to 3 watts per amplifier, with a total module power of 4-12 watts.

2. Incorporation of FET's to provide a more realistic basis for the integrated module design.

3. Conduct measurements of harmonic levels, noise levels, and phase tracking to assure that the module will perform in conformity with the overall SPS design requirements.

4. The power-combining antenna concept should be further developed to reduce losses. The Epsilam-10 should be replaced with the appropriate ceramic substrate, aluminum should be used to replace the brass cavity, and conducting epoxy for assembly should be further examined. More accurate indoor antenna range measuring capability will be available within Boeing in 1980 to supplement this work.

5. Means should be investigated to reduce the radiated cross-polarization below the 1% level. 0.1% seems an appropriate goal. Techniques to explore this include overcoating of the narrow coupling slotline with a dielectric material to minimize radiation; use of a substrate material with a higher dielectric constant; and utilizing designs where the narrow coupling slotlines are in line with the radiating slots.

6. The impact of amplifier failure on module phase error correction and antenna pattern needs to be examined.

7. The antenna modules with regard to their dc power are intended to be arrayed in series-parallel strings where voltages within the module will be substantially higher than the neutral ground plane and cavity. Means need to be developed to dc isolate the module electronics from the module ground plane. Operation of a string of modules, including phasing, needs to be demonstrated to validate both dc and rf requirements. This will include effects of slot-to-slot mutual coupling.

8. Low cost metalization of the ceramic substrate must be developed whether thick film (silk screening) or thin film (sputtering and plating) techniques are used. Before the thick film process could be selected, research needs to be conducted to determine the adequacy of the approach with regard to circuit losses and line width resolution tolerance.

7.0 APPENDIX

ANTENNA CHARACTERIZATION:

The antenna parameters which will be evaluated are the directivity, the gain and the efficiency. The directivity, D, of an antenna is defined as the ratio of the peak radiated power to the total power radiated by the antenna. The gain, G, is defined as the ratio of the peak power radiated by the antenna to that which would be radiated by an ideal isotropic radiator. Since the ideal isotropic radiator does not exist, the gain is measured by comparing the peak radiation intensity of the antenna in question to that of another antenna, or as described below, to that of other antennas. The efficiency, η, is simply the ratio of the power radiated by the antenna, to the power put into the antenna.

For an ideal antenna, the gain and directivity are clearly identical. However, for a given input power, all real antennas will radiate less peak power, and hence, will exhibit less gain than expected from the directivity. Because this discrepancy is due to loss within the antenna, the efficiency of the antenna is related to the measured parameters G and D by

$$\eta = \frac{G}{D} , \qquad (1)$$

Of the three parameters, η, G, and D, G and η bear directly on the SPS performance. The gain is of importance in the power transmission beam efficiency. The significance of η is obvious. The measurement of D has no intrinsic utility except that, with G, it can be used to determine η. Of course, there are other methods of determining η, such as measuring radiation into a surrounding cavity, or radiometric/calorimetric techniques. While these are quite promising, they are less mature, and will not be further considered at this time.

The following text describes the intended procedures for the measurement of the gain, directivity, and hence, efficiency, of the SPS solid state module. The anticipated errors in each measurement are identified, and their magnitudes are estimated. With the gain measurement, the overall 3σ root-sum-square (RSS) uncertainty is estimated to be $\pm$ 0.33 dB. In the

C-2

determination of D, a maximum RSS error of $\pm$ 0.41 dB is expected. Combined in quadrature, these lead to an expected uncertainty in η of $\pm$ 0.53 dB.

GAIN MEASUREMENT:

Three Antenna Method:

The gain of the SPS solid state antenna module will be determined using the three antenna method which involves measurements of the insertion loss between three antennas, including the SPS module, taken in pairs. The insertion loss, I, between a pair of antennas is defined as

$$I = \frac{P_R}{P_T} \quad , \tag{2}$$

where P_R is the power out of the receiving antenna, and P_T is the power into the transmitting antenna. Ideally, the insertion loss is related to the gains of the two antennas by

$$\frac{P_R}{P_T} = G_T \, G_R \, \left(\frac{\lambda}{4\pi S}\right)^2, \tag{3}$$

where G_R and G_T are the gains of the receiving and transmitting antennas, respectively, λ is the wavelength and S is the antenna separation. Equation (3) can be readily inverted to yield the product of the gains of the two antennas, $\mathcal{G}_{ij} = G_i \, G_j$ in terms of the measured insertion loss, wavelength, and separation. Thus, measurement of the insertion loss for three pairs made from three antennas gives three independent equations from which can be found the gain of any of the three antennas, according to the relationship

$$G_i^2 = \frac{\mathcal{G}_{ij}\mathcal{G}_{ki}}{\mathcal{G}_{jk}} \quad . \tag{4}$$

This is more conveniently expressed by taking the log of both sides, to give

$$2 \log G_i = \log \mathcal{G}_{ij} + \log \mathcal{G}_{ki} - \log \mathcal{G}_{jk} \quad . \tag{5}$$

The Measurement System:

The antenna gain measurement system is diagrammed in Figure 9. The generator section consists of an oscillator which drives the transmitting antenna through an isolator. The oscillator frequency and power are monitored by the frequency counter and the power meter. Should frequency stabilization and/or leveling be required, these capabilities can be incorporated in the frequency and/or power monitoring arms. The receiving antenna is coupled to the load, which consists of a mixer, a precision receiver, and an SWR meter employed to indicate the receiver output. A precision variable attenuator is placed in front of the mixer, to allow the receiver to operate at the same level for all inputs, thereby eliminating errors arising from non-linearity in the receiver.

The two antennas are positioned on the antenna range, as shown in Figure 10. The transmitting antenna is fixed to the balcony of the building which contains the measuring equipment. The receiving antenna is located on a tower which can be rolled away from the building. The maximum separation, S, which can be achieved is 50 m, which is of the order of 50 D^2/λ for the largest antenna likely to be employed in this measurement, where D is the aperture dimension and λ is the wavelength. Both antennas are placed at a height of 13 M above the ground.

Uncertainty in the Gain Measurement:

Equation (3), and hence Equations (4) and (5), are based upon the following assumptions:

1. Antenna range - infinite antenna separation, free-space conditions.

2. Equipment - ideal waveguide leads and connectors; stable generator and receiver; single sinusoidal frequency; and single waveguide mode.

3. Antennas - reciprocal, polarization parameters matched and boresights aligned.

4. Transmitting medium - linear, lossless, reciprocal and isotropic.

It is reasonable to assume that condition (4) will be adequately satisfied. Unfortunately, the same cannot be asserted a priori with respect to the other three conditions. Condition (1) will be violated by the fact that the antennas may not be placed truly in each other's far fields and by the inevitability of multiple transmission reflections. Condition (2) is primarily affected by the existence of imperfect impedance matches throughout the system. Finally, antenna alignment cannot be effected to arbitrary accuracy (Condition 3). To explicitly account for these realities, Equation (3) can be rewritten as [1].

$$G_T G_R = \left(\frac{MN}{DR}\right) \left(\frac{4\pi S}{\lambda}\right)^2 \left(\frac{P_{R_O}}{P_T}\right) , \qquad (6)$$

where M is an impedance mismatch factor, N is a near-field correction factor, D is a pointing error correction, R is a correction for polarization mismatch, and P_{R_O} is the received power, P_R, corrected for multiple reflections.

By proper conduct of the measurement, N, D, and R can be taken as unity, with very small or negligible error. In the case of the near-field correction, N, this entails separation of the antennas by more than $10D/\lambda$ [1], which is easily accomplished, as noted above, on the selected antenna range. Assuming sufficient coincidence between the electrical and mechanical boresights, the pointing error represented by D can be reduced by careful antenna

alignment, to a negligible value compared with other errors. This is especially true in the case of the relatively low-gain antennas of interest here. Because, for small polarization errors, R does not vary rapidly with polarization, R also can be considered as unity, to a negligible uncertainty.

The separation, S, and the wavelength, λ, can be measured to accuracies which justify their neglect in the error budget. The separation can be measured to better than 0.1%, with a laser distance meter. The frequency drift characteristics of the generator and the receiver, are also negligible over the duration required of the gain measurement.

The significant probable uncertainties in the measurement of $\mathcal{G}_{ij}$ are those arising from mismatches and those in the determination of P_{Ro}/P_T.

The factor, M, represents the combined effect of four different impedance mismatches. As shown in Figure 9, these include Γ_G, the reflection coefficient looking into the generator output; Γ_T, the reflection coefficient looking into the transmitting antenna input, Γ_R, the reflection coefficient looking into the receiving antenna input, and Γ_L the reflection coefficient looking into the load. In terms of the four reflection coefficients, the factor M is well approximated by[1]

$$M \cong (1 + |\Gamma_T|^2 + |\Gamma_R|^2)$$

$$\pm 2\,((|\Gamma_G|\,|\Gamma_T|) + (|\Gamma_R|\,|\Gamma_L|) + (|\Gamma_G|\,|\Gamma_L|)) \qquad (7)$$

where the second term represents the limits of uncertainty in M due to uncertainty with regard to the relative phases of the various Γ factors. For the components of the anticipated test configuration, the reflection coefficients are estimated to be $|\Gamma_G|$, $|\Gamma_L| \leq 0.11$ and $|\Gamma_T||\Gamma_R| \leq 0.06$. When these values are incorporated into Eq. (5) via Eqs. (6) and (7), with the individual uncertainty terms combined in quadrature, the uncertainty due to M will be no greater than $\pm$ 0.07 dB.

Uncertainty in the measurement of the insertion loss, P_{Ro}/P_T, arises from uncertainty in the calibration of the attenuator, and from multipath errors. The uncertainty in calibration of the attenuator is $\pm$ 0.1 dB.

Multipath effects are apparent as variations in insertion loss, with either antenna separation or measurement frequency. As such, they represent an uncertainty in the gain, equal to the peak-to-peak value of this variation. These variations are due to the change in relative phase of the direct-path and scattered voltage components at the receiving antenna. Where a single stray path predominates, the variation in received signal should be nearly sinusoidal, and the average value of received signal should be the same as the received signal without multipath. Thus, in principle, multipath errors can be eliminated by measuring the received power as a function of separation over several wavelengths, and then by taking the average of the received power, (P_R), as the free space received power, P_{Ro}.

To estimate the magnitude of the multipath error, the insertion loss between the antennas to be measured was observed as frequency and separation were varied on a range set up in the laboratory, with S = 3m and h = 1.5m. In these measurements, the maximum ripple was found to be 2.5 dB peak-to-peak. Because the geometry and scattering potential of the outdoor range are significantly more favorable than those of the laboratory range, the ripple encountered in the actual measurement may well be smaller than this. If the error in averaging these variations is conservatively estimated at 20%, the uncertainty in P_{Ro} due to multipath errors will be no greater than $\pm$ 0.25 dB.

The estimates of the various errors are listed in Table 1.

Source of Uncertainty	Positioning	Near Field	Mismatch	Multipath	Attenuator	Freq. Drift	RSS
Magnitude of Uncertainty	---	---	± 0.07	± 0.25	± 0.1	± 0.1	± 0.33

Table 1: Summary of Maximum Anticipated Uncertainties in the Three-Antenna Measurement of the Gain of the SPS Solid State Antenna Module. All Values Are in dB.

Their RSS value indicates an expected overall uncertainty in measured gain of ± 0.32 dB. It should be restated at this juncture, that the values listed in Table 1, represent conservative estimates of uncertainties likely to be encountered in the gain measurement. The uncertainties encountered in the actual measurement may be somewhat less than these.

DIRECTIVITY MEASUREMENT:

Antenna directivity has been previously defined as the ratio of the peak radiated power to the total radiated power. Mathematically, this is expressed by:

$$D = \frac{4\pi\, U_{pk}}{\iint U(\theta, \phi)\, d\Omega} \quad . \tag{8}$$

where U is the power and $d\Omega$ is the differential unit of solid angle. Therefore, the measurement of directivity simply implies performing the indicated integration.

The system for measuring and integrating the radiated intensity over the antenna pattern is depicted in Figure 11. It is, in many respects,

similar to the gain measuring system of Figure 10. A stable generator, through a transmitting antenna, is used to illuminate the antenna under test. These two antennas are located respectively on the range building, and the range tower, as in the gain measurement. Also, as before, the output of the test antenna is fed to a stable receiver. Beyond this, however, the gain and directivity systems differ in that the receiver output in the measurement of D is digitized and fed to a digital computer for subsequent integration.

The integration of the pattern is accomplished by first determining the received intensity at a large number of discrete points over the sphere of 4π sterradians. To accomplish this, the antenna is rotated about the vertical axis which passes through its phase center. For each degree of this rotation, the antenna is revolved around its boresight to yield 360 data points which are separated by one degree. Upon completion of the pattern scan, the data are numerically integrated to yield the directivity.

There are three sources of error which are likely to predominate in the directivity measurement. These are a "quantization" error induced by the resolution of the digital encoder, an error due to the non-linearity of the receiver, and an error due to component drift. the encoder rounds off input intensities to the nearest 0.25 dB, which can produce an error of at worst $\pm$ 0.125 dB. Because of the substantial dynamic range required of the receiver, a linearity error will also be incurred. For the SA-1742 receiver used here, this error is specified at $\pm$ 0.25 dB. Finally, because of the duration of this measurement, the long term stability of the various components must be considered. From observation of the operation of this equipment over a representative period, the drift uncertainty is estimated at $\pm$ 0.3 dB. Combined in quadrature, these three errors lead to a total 3σ uncertainty of $\pm$ 0.41 dB. The anticipated standard deviation associated with this error is $\pm$ 0.14 dB.

EFFICIENCY CALCULATION:

As noted, once the gain and directivity have been measured, the efficiency can be determined according to Equation (1). The uncertainty in the efficiency so derived, is determined by the uncertainties in G and D. Since these are independent, it is appropriate to consider their RSS value. For uncertainties in G and D of $\pm$ 0.33 and $\pm$ 0.41 dB, respectively, the uncertainty in η is expected to be no greater than $\pm$ 0.53 dB.

BIBLIOGRAPHY:

1. R. R. Bowman, NBS Technical Report #RADC-TR-68-349, November 1968.

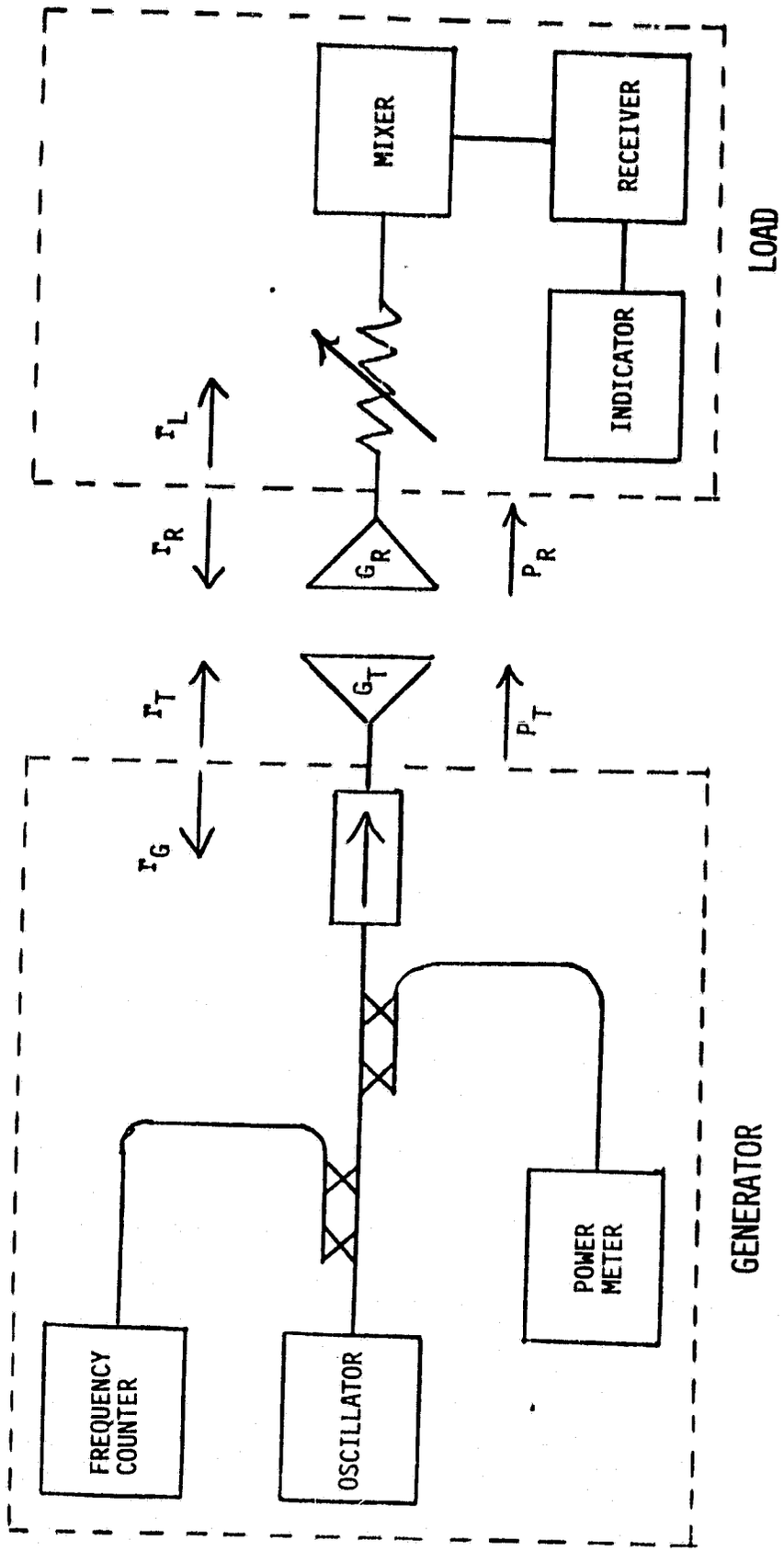

FIGURE 7.1 ARRANGEMENT OF TEST EQUIPMENT FOR THE MEASUREMENT OF ANTENNA GAIN.

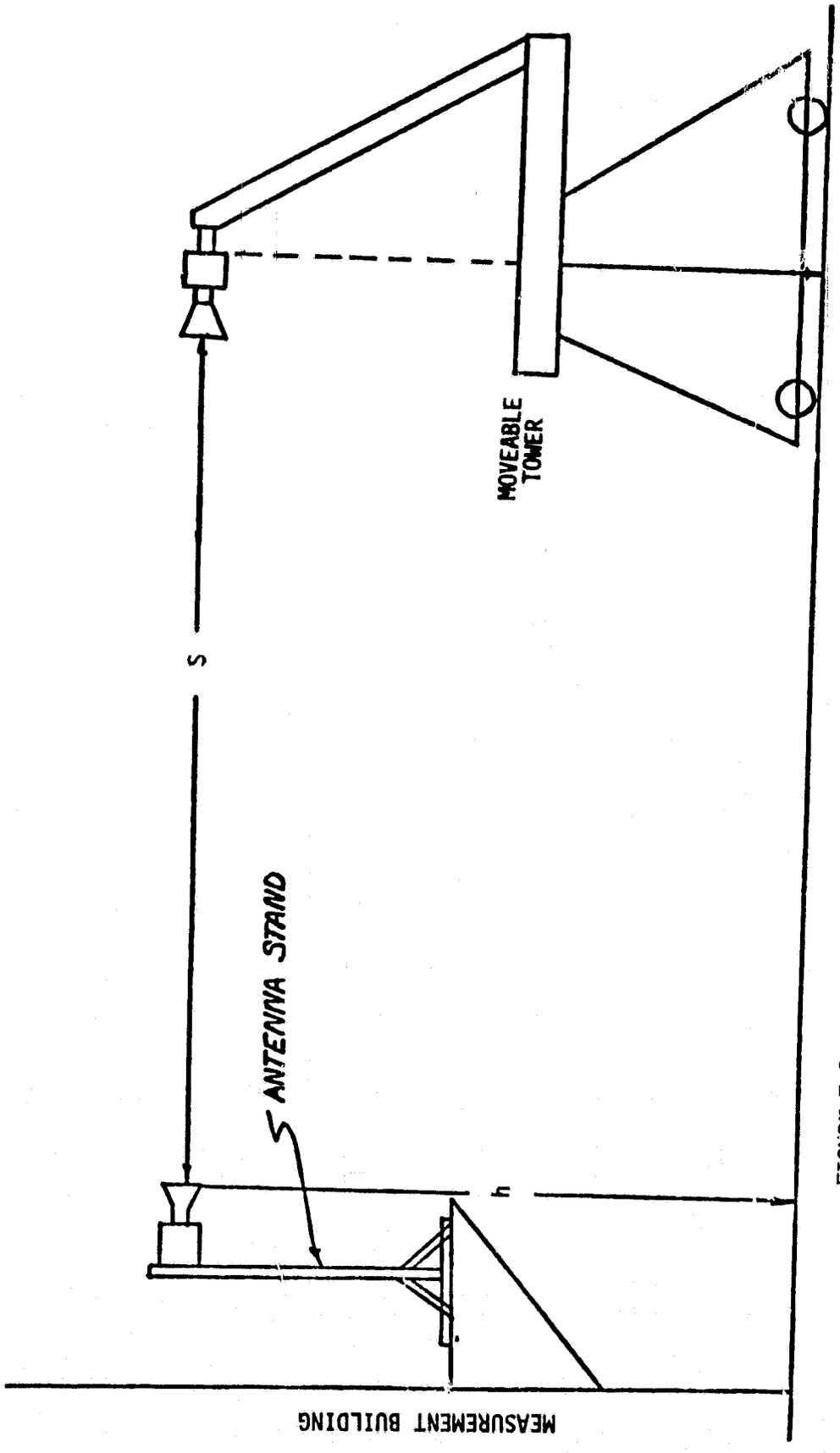

FIGURE 7.2 OUTDOOR ANTENNA RANGE TO BE USED FOR THE MEASUREMENT OF THE GAIN AND DIRECTIVITY OF THE SPS SOLID STATE ANTENNA MODULE. THE ANTENNA HEIGHT IS 13M, AND THE SEPARATION IS VARIABLE FROM 0-50M.

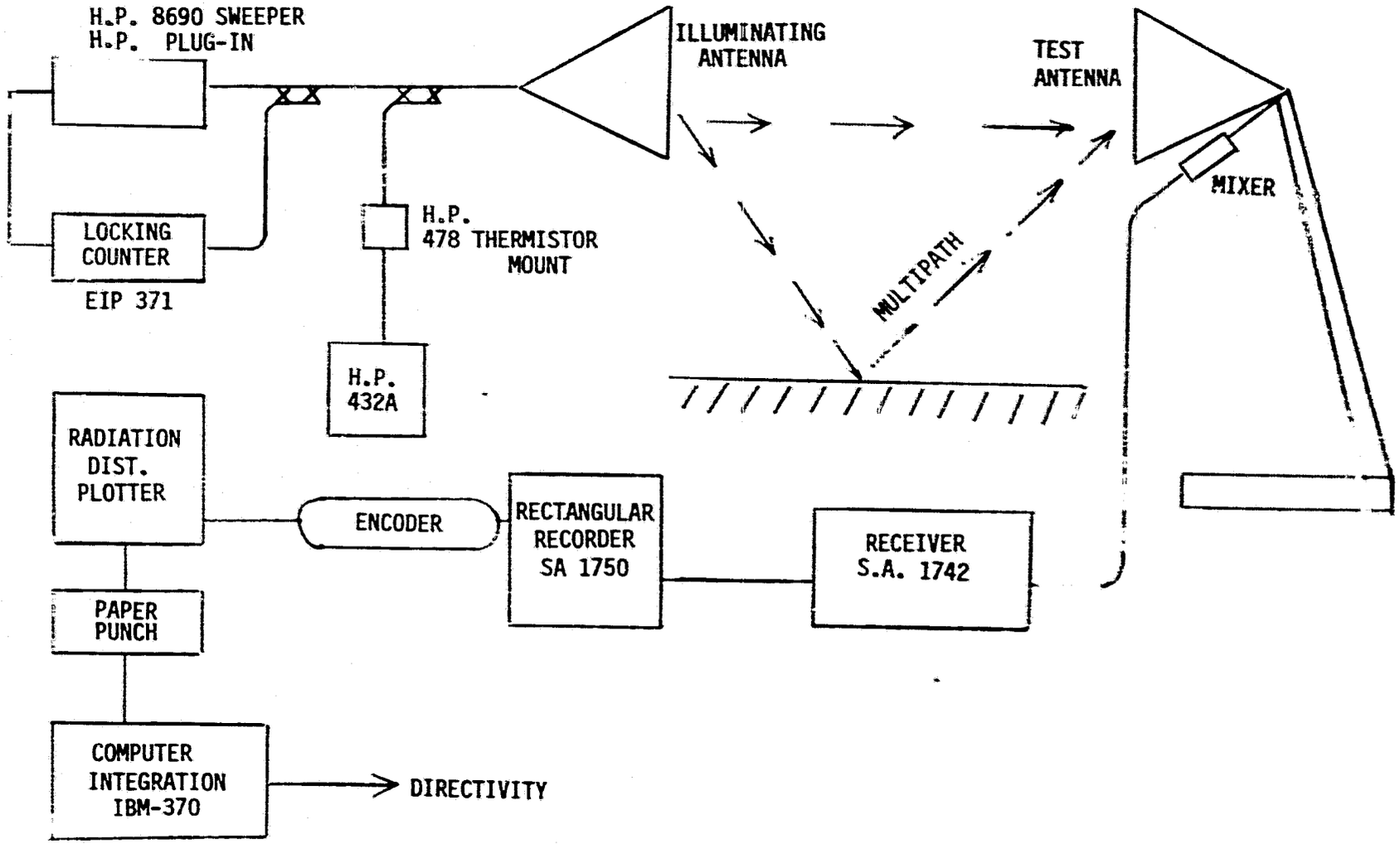

FIGURE 7.3 DIAGRAM OF THE DIRECTIVITY MEASUREMENT SYSTEM